SOURCE AND EFFECT OF ACID ROCK DRAINAGE IN THE SNAKE RIVER

WATERSHED, SUMMIT COUNTY, COLORADO

by

Laura Belanger

B.A., University of Massachusetts, 1991

A thesis submitted to the

Faculty of the Graduate School of the

University of Colorado in partial fulfillment

of the requirements for the degree of

Master of Science

Department of Civil, Environmental and Architectural Engineering

2002

This thesis entitled:

Source and Effect of Acid Rock Drainage in the Snake River Watershed,
Summit County, Colorado

written by Laura Belanger

has been approved for the Department of Civil, Environmental and Architectural

Engineering

Diane M. McKnight, Chair

Edith A. Zagona

Joann Silverstein

Date 4/17/02

The final copy of this thesis has been examined by the signatories, and we find that

both the content and the form meet acceptable presentation standards of scholarly

work in the above mentioned discipline.

ABSTRACT

Belanger, Laura (M.S., Civil, Environmental and Architectural Engineering)

Source and Effect of Acid Rock Drainage in the Snake River Watershed, Summit County, Colorado

Thesis directed by Dr. Diane M. McKnight

The Snake River Watershed in Summit County, Colorado has both anthropogenic (historical mining) and natural (the weathering of disseminated pyrite) sources of acid rock drainage (ARD). Stream waters in this system are typically acidic with elevated metal concentrations, streambeds are coated in hydrous metal oxides and aquatic biota is severely limited. The natural source of ARD was found to be the weathering of pyrite disseminated throughout the eastern side of the upper Snake River basin. The predominant anthropogenic source was the Pennsylvania Mine and its vicinity on Peru Creek (a major tributary of the Snake River). Surface waters and lateral inflows were both significant sources of ARD, with lateral flows providing the majority of mass loading at points along the stream reach. Tributary waters often had very different chemistry from lateral inflows as a result of varying exposure to rock, soils, organic matter and other solutes. Temporal variations in lateral inflows were apparent, with greater lateral flows resulting from a period of increased precipitation. Confluences were critical to the transport of metals and acidity as tributary waters and the majority of lateral inflows entered the stream in

these regions. Additionally, much of the reactive chemistry of metals occurs in confluence zones where waters of differing chemistry mix.

Samples collected in the upper Snake River revealed diel variations in iron (Fe) and copper (Cu) concentrations that were most likely the result of oxide formation, co-precipitation and iron photochemistry. Toxic concentration levels were present at several sites for Fe and Cu during only portions of the day.

Metal oxides were present at all sampling sites in the watershed with the most significant deposition occurring in confluence zones. Periphyton communities were shown to be severely stressed throughout the watershed with only minimal biomass present at all sampling sites. Concentration data along the Snake River and Peru Creek revealed that both natural and anthropogenic sources of ARD led to the presence of toxic levels of dissolved metals and metal oxide deposition in the watershed.

CONTENTS

TABLES

CHAPTER I

INTRODUCTION

Throughout their history, humans have transformed the ecosystems in which they live, both purposefully and through unintended consequences. With a human population of more than six billion, unprecedented competition for natural resources now exists around the globe. As a result many natural patterns of species distributions and interactions that have taken millions of years to develop have been altered.

This work attempts to characterize the extent of environmental degradation due to acid rock drainage resulting from both natural and anthropogenic (historical mining) sources in a region experiencing increased competition for limited water resources. Effective restoration and preservation of stream ecosystems and associated organisms requires the integration of ecosystem science and more social disciplines like economics and political science (Meyer, 1997). It is human activities that affect ecosystems and human attitudes and institutions that determine what actions will be taken to maintain their health (Meyer, 1997). The ecological integrity of the aquatic environment is of interest in terms of its structure and function as well as goods and services provided. Freshwater ecosystems, as in this study, provide direct and indirect social benefits (Wilson and Carpenter, 1999) including less easily

quantifiable services like soil and water conservation, nutrient cycling and recreational opportunities as well as more concrete products such as water for downstream use, timber and fish. Maintaining functional diversity is pivotal in supporting the flow of ecosystem goods and services as alterations to one organism may reverberate throughout the ecosystem.

1.1 - Colorado's Mining Legacy

Large-scale settlement in Colorado began in the 1860's after the discovery of gold and silver in Rocky Mountain streams (Gilliland, 1999). Initially valuable metals were extracted from easily accessible surface waters and soils. Once these ores were exhausted more invasive mining procedures took over. Miles of tunnels were excavated and waste rock from this and the ore removal process was dumped in large hillside mounds. As veins were exhausted, these more extensive extraction processes became unprofitable and miners moved on leaving ghost towns in place of once spirited settlements. There are an estimated 23,000 abandoned mines in Colorado (Colorado Mining Water Quality Task Force, 1997).

Colorado's mining history has left a legacy of environmental degradation in the form of acid rock drainage (ARD). The water quality of streams receiving ARD is typically acidic with high concentrations of dissolved metals such as aluminum (Al), cadmium (Cd), copper (Cu), iron (Fe), manganese (Mn) and zinc (Zn). ARD streambeds are characterized by bright orange and white colored deposits that indicate iron oxide and aluminum oxide deposition, respectively (Fig. 1.1). High metal ion concentrations, low pH and oxide deposition limit stream biota, including microbes, algae, invertebrates and fish, for many kilometers of streams in Colorado

(McKnight and Feder, 1984; Niyogi, 1999). Typically, fish are unable to survive and

populations of algae, microbes and invertebrates at lower trophic levels are restricted

to species that can tolerate these extreme chemical conditions. Further degradation

can occur as a result of contemporary human developments, including road and

housing construction, as well as increased water withdrawal, which place additional

stress on stream biota.

FIGURE 1.1: Fe and Al oxide deposition. Orange colored Fe oxides can be seen coating the streambed towards the bottom of the figure with bright white Al oxides towards the top.

Acid rock drainage has been referred to as the greatest water quality problem

facing the Western United States (Da Rosa and Lyon, 1997) and is a common feature

of the Rocky Mountains, eastern United States, Canada and many other parts of the

world. Cost, technology and liability concerns all contribute to make ARD

remediation a daunting issue. The Mineral Policy Center has estimated that there are

approximately 560,000 mine sites on public and private lands and that the total cleanup of all abandoned sites within the United States will cost between 33 and 72 billion dollars (Lyon et al., 1993). The U.S. Department of the Interior's Office of Inspector General estimated that it would cost approximately $11 billion to reclaim the "known universe" of all abandoned noncoal mine sites (Department of the Interior, 1991). In Colorado alone, there are an estimated 1,283 miles of stream, out of a total of 14,655 miles, affected by heavy metals and acid rock drainage (Colorado Mining Water Quality Task Force, 1997).

Mining began in the Snake River watershed with the discovery of silver in the 1860's and remained the principal industry, with a series of booms and busts, through the 1950's. Since that time the ski industry has replaced mining as the dominant economic base in the basin. The legacy of mining remains in the form of ARD.

1.2 - Purpose of this Study

This study is part of a watershed-based attempt to gain insight into the source and effect of acid rock drainage in the Snake River Watershed with the goal of providing a scientific framework to guide future development of remediation and restoration strategies.

Instream acidity and metal concentrations are driven by watershed and instream processes that may be chemical, physical or biological in nature (McKnight and Bencala, 1990). The complex nature of ARD systems can lead to substantial spatial, seasonal and diel variations in concentrations. Knowledge of the processes that control variations in metals concentrations is important for assessing the sources, storage and mobility of metals. In the process of identifying the origin and magnitude

of instream solutes, subsurface and groundwater contributions can be as, or more, important than those of surface water inflows.

Downstream concentration profiles vary as inflows influence instream chemistry (Bencala and McKnight, 1987). Characterization of instream metal loading, or mass-flow, from acid rock drainage includes identification of inflow location, discharge and solute concentrations. Inflow concentrations are important, but incoming mass-flow (calculated by multiplying concentration by discharge) has the greatest impact on downstream concentrations (Kimball et al., in press). A tributary with high concentrations but low discharge will have low mass-flow and a minimal downstream effect. Alternatively, an inflow with lower concentrations but high discharge may have larger mass-flow and a greater influence on downstream concentrations.

Subsurface and groundwater inflows can be important sources of metals and acidity. Kimball et al. (in press), for example, found subsurface inflows accounted for nearly 50% of daily Zn load in the ARD affected Cement Creek, San Juan County, Colorado and that both mined and unmined areas were sources. The relative ease with which surface water samples are collected leads to a general reliance upon these data for most water quality information. To fully understand the nature and source of incoming water, it must be acknowledged that these traditional sampling methods can neglect significant inflows entering streams through soils (Bencala and Ortiz, 1999; Kimball et al., in press). Figure 1.2 illustrates that water may flow into streams overland, through the subsurface and as groundwater.
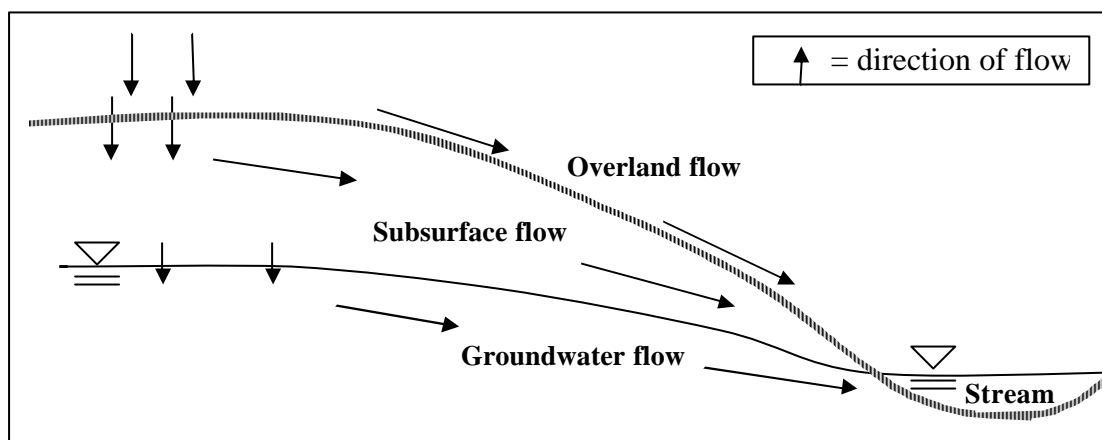
FIGURE 1.2: Possible flow paths of stream source water. Water may flow overland, through the subsurface or from groundwater into streams and lakes.

By combining discharge and chemistry a detailed profile of mass-flow can be produced for a watershed. Mass-balance methods cannot identify exact sources but can distinguish differences between sites with an increase in mass-flow indicating a source. Correspondingly, a mass-flow decrease between sites signifies a loss resulting from physical, biological and/or chemical processes.

The objective of this study is to develop a watershed-based characterization of acidity, metal concentrations and mass-flows resulting from both the natural weathering of disseminated pyrite and anthropogenic point source mines. To quantify the location and importance of sources, contributions from both surface and lateral inflows were considered, a methodology that has not commonly been taken in the past. Several quantitative stream scale approaches were used in analyzing field data collected in the Snake River Watershed in 1998 and 2000. These approaches included examining the spatial and temporal variability of instream concentrations, mass-flows and oxide deposition; determining surface and lateral inflows in

confluence and non-confluence zones; and evaluating the ecological effects of oxide

deposition and instream chemical conditions on benthic algae communities.

CHAPTER II

ACID ROCK DRAINAGE AND ITS EFFECTS

2.1 - Formation of Acid Rock Drainage

Colorado's mining history has left a legacy of environmental degradation in the form of acid rock drainage (ARD). ARD occurs naturally, but in the Rocky Mountains the most severe degradation is predominantly anthropogenic in nature. When rocks containing pyrite (FeS_2), and other sulphidic minerals, are exposed to oxygen and water they begin to weather, initiating a cycle that creates surface waters high in acidity and metals. The by-products of mining (tailings piles, waste rock, and mine workings) greatly increase the surface area of pyrite, stimulating the production of ARD. As pyrite weathers, Fe^{2+}, SO_4^{2-} and H^+ are released in to waters, as well as other trace metals that are present in surrounding rock.

The reactions involved in the weathering of pyrite are numerous and the overall process may proceed by several paths. The individual reactions have rates that vary greatly. Generally, the weathering and oxidation of pyrite occurs in three steps, with the reaction becoming autocatalytic, or self-generating, in nature. The following reactions typically occur (Singer and Stumm, 1970; Nordstrom and Alpers, 1999; McKnight and Bencala, 1990).

The first step of pyrite oxidation is a slow, abiotic reaction in which O_2 acts as the electron acceptor (Eqn. 2.1).

Equation 2.1: $FeS_2 + 3\frac{1}{2} O_2 + H_2O = Fe^{2+} + 2 SO_4^{2-} + 2 H^+$
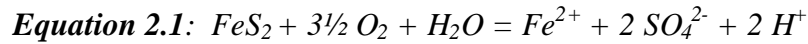
(slow, abiotic, initiator reaction)

In the next step of pyrite weathering (the rate-limited step in the reaction series), ferrous iron generated in equation 2.1 is oxidized quickly by microorganisms, generally from the genus *Thiobacillus* spp. (Nordstrom and Southam, 1997).

Equation 2.2: $Fe^{2+} + \frac{1}{4} O_2 + H^+ = Fe^{3+} + \frac{1}{2} H_2O$

(faster, biotic)

Equation 2.2 may occur abiotically, but in low pH systems, such as those resulting from ARD, the abiotic oxidation occurs at a negligible rate.

In the final abiotic reaction (Eqn. 2.3), ferric iron acts as an electron acceptor in the weathering of pyrite. Because ferric iron is insoluble at circumneutral pH, the following reaction predominates only in acidic waters.

Equation 2.3: $FeS_2 + 14 Fe^{3+} + 8 H_2O = 15 Fe^{2+} + 2 SO_4^{2-} + 16 H^+$
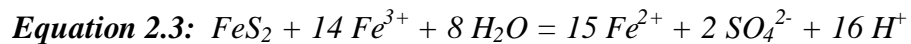
(fast, abiotic)

2.2 - Instream Concentrations

The controls on instream solute concentrations in ARD environments are complex. Solutes are derived from a variety of sources in the watershed. SO_4, H^+, Fe, Zn, Cu and Mn all have the weathering of pyrite and other sulphidic minerals as

their source. Al is mobilized when resulting acidic water weathers nearby country rock. Solutes such as Mg, Ca, Cl and Na weather from sources throughout the watershed. Once mobilized, solutes may behave either conservatively or reactively depending on the circumstance. Solutes may react chemically with other solutes, metal oxyhydroxides, soils and organic matter. Reactions can occur throughout the basin including in the subsurface, tributaries, hyporheic zone and stream column. This leads to spatial and temporal differences in solute concentrations.

2.2.1 - Watershed Controls

In the Snake River watershed, large variations in dissolved metal concentrations occur on a seasonal scale, driven primarily by the region's hydrology. The majority of yearly precipitation falls as snow. The annual hydrograph (Fig. 2.1) is characterized by low flow in winter during snowfall, a large pulse of spring snowmelt runoff which lasts several months, and a period of low flow with short episodic rainstorms in late summer and early fall. On an annual timescale, trace metal concentrations tend to decrease during high flows as unmineralized snowmelt dilutes stream water and then tend to increase during lower flows (Sullivan and Drever, 2001a; Boyer et al., 1999; McKnight and Bencala, 1990; Moran and Wentz, 1974). On a diel timescale, sampling in Peru Creek has shown that changes for many solutes (SO_4, Mn, Zn, Si, Mg, K and Ca) are driven by hydrology and are a result of daily fluctuations in snowmelt (Sullivan et al., 1998). Sullivan et al. (1998) also found that these variations decrease on the falling limb of the hydrograph as much of the snowpack has already melted.
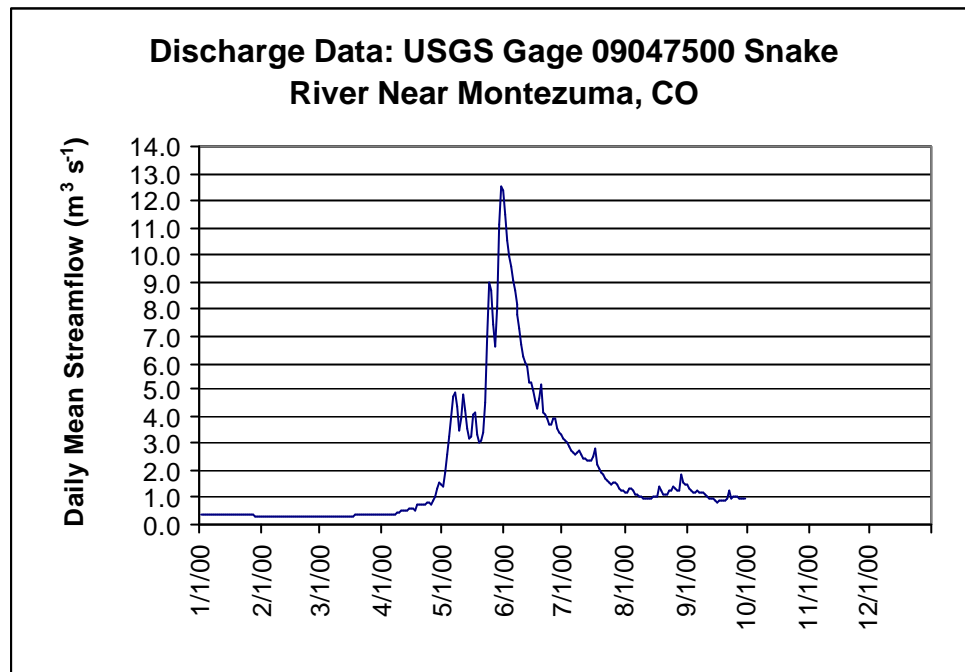
FIGURE 2.1: Snake River 2000 hydrograph. Graph compiled using data from U.S. Geological Survey stream gage 09047500 located at Keystone Ski Resort.

Differences in solute behavior may occur between those with disseminated pyrite as a source and those with sources in discrete mines (Brooks et al., 2001). Additionally, depending on the path taken, the chemical composition of incoming waters can vary greatly (Bencala and McKnight, 1987). Interaction with sediments, solids and organic matter in the subsurface and hyporheic zone may affect trace metal concentrations (Bencala 1984; Bencala et al. 1990, Lottermoser et al. 1999).

A significant exchange of water occurs between the stream column and hyporheic zone in low order mountain streams (McKnight and Bencala, 1990; Harvey and Bencala, 1993). Hyporheic zone flow occurs along the length of a steam reach as water moves in and out of the sediment on a timescale that can be considered fast, though downstream transport is less than in the main stream column. Flow through transient storage zones and stream bed sediment can play an important part in solute

transport, as solutes may be retained in these zones and in contact with reactive

sediment surfaces for substantial amounts of time (Bencala et al., 1990 and 1984;

Lottermoser et al., 1999).

2.2.2 - Instream Controls

In ARD affected streams, many of the reactions that occur are pH dependent.

Most metals are very soluble in the low pH environments that are typical of acid rock

drainage streams, and become less soluble at higher pH. Much of the reactive

chemistry of metals occurs in confluence zones where waters of differing chemistry

mix (McKnight and Bencala, 1990). Several of the metals that have high

concentrations in ARD streams, such as Al, Fe and Mn, can form hydroxides (with

concurrent decreases in instream concentrations) when inflows of more neutral waters

raise stream pH (Kimball et al., 1994; McKnight and Bencala, 1990; Broshears et al.,

1996). For Fe, when the pH rises above 4, the following reaction occurs (Eqn. 2.4),

creating precipitates that coat the streambed.

Equation 2.4: $Fe^{3+} + 3\ H_2O = Fe(OH)_3 + 2\ H^+$
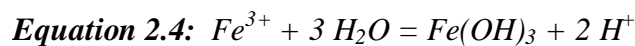
The precipitation of free aluminum ion as aluminum hydroxide becomes an important

reaction above pH 5 and follows a reaction similar to that shown for ferric iron in

equation 2.4. The composition of oxide deposition changes with distance

downstream with upstream locations having the most Fe (McKnight et al., 1992)

followed by Al. Hydrous oxides may exist as suspended colloids or as deposits on

the streambed.

Instream Fe chemistry is complex as it is also affected by photochemistry. This generates significant diel fluctuations in instream concentrations. Photoreduction of suspended particles and Fe oxyhydroxides on the streambed leads to mid-day increases in Fe^{2+} and FeT concentrations (McKnight et al., 1988 and 2001; McKnight and Bencala, 1989; Runkel et al., 1996).

The presence of metal oxide precipitates has been found to affect the chemistry of other metals by adsorption, co-precipitation and photochemical reactions (Runkel et al., 1999; Williams and Smith, 2000; McKnight et al., 1992; Sullivan and Drever, 2001b, Munk et al., 2002). The importance of these reactions varies. Theobald et al. (1963) found Mg, Pb, Cu and Cr in Al precipitates in the Upper Snake River, but at low levels. In St. Kevins Gulch, a drainage impacted by acid mine drainage near Leadville, Colorado, concentrations of As, Cd, Cu, Fe, Mn Pb and Zn in Fe-rich suspended particulates were higher than those reported in soils (Kimball et al., 1992). Johnson (1986) found that Cu and Zn concentrations in an ARD impacted river were driven by co-precipitation reactions. Many metals are more soluble than Al and Fe at neutral pH and will be transported further downstream with concentrations decreasing predominantly due to pristine inflows.

In the process of pyrite weathering SO_4 is mobilized in proportion to Fe^{2+} and H^+ in ARD environments. However, it is also present in gypsum and barite which are found in association with ore minerals (Bove et. al., 2000). SO_4 is generally present in high concentrations in ARD streams and behaves conservatively in these acidic environments (Sullivan and Drever, 2001a) though minor losses have been documented in the formation of iron oxides (Theobald et al., 1963; Kimball

et al., 1994). SO_4 can be useful as a nominally conservative ambient tracer (Bencala et al., 1987) though this usefulness is system dependent. In St. Kevins Gulch, Lake County, Colorado, Kimball et al. (1994) found that while SO_4 and Mn tended to behave conservatively, reactive behavior was documented in the subreaches most affected by ARD.

2.3 - Influences of Water and Substrate Quality on Periphyton

The effects of ARD on aquatic organisms are complex and can be both direct and indirect. Multiple stressors include acidity, high concentrations of dissolved metals, metal oxide deposition and changes in species interactions (Niyogi et al., 2001; Clements, 1999). Stream communities may be influenced by a complex set of pressures making it difficult to quantify and predict the impact of ARD (Gray, 1997). This also complicates attempts at remediation. For example, oxide deposition may limit the ecological recovery of streams despite improvements in water chemistry (Niyogi et al., 1999).

Individual species have adapted to ARD environments leading to biotically distinct streams that are found in the Rocky Mountains and in geochemically similar locations around the world (McKnight and Feder, 1984; Clements, 1994; Mulholland et al., 1992). Secondary impacts of ARD may be felt by species due to changes in competition, predation or grazing. Decreases in grazing pressure from invertebrates, which are often more sensitive to changes in water chemistry, has been found to stabilize or increase the biomass of algal communities (Elwood and Mulholland, 1989).

Studies of stream biota in the headwaters of the Snake River and Deer Creek have shown that the species composition of algae and benthic invertebrates are much different in the Snake River compared to Deer Creek, which has species typical of pristine Rocky Mountain streams (McKnight and Feder, 1984). Periphyton in the Snake River above the confluence is typical of those in acid mine drainage streams and much less abundant than in Deer Creek. Below the confluence, where the streambed is coated in Al precipitates, periphyton were very sparse (McKnight and Feder, 1984).

In ARD environments, metal oxide deposition has been found to have more detrimental effects on stream biota and ecological processes than low pH or high concentrations of dissolved metals (McKnight and Feder, 1984; Niyogi et al., 1999). Oxide deposition limits stream biota, including microbes, algae, invertebrates and even fish, for many kilometers of streams in Colorado. Niyogi et al. (1999) also found that metal oxides may vary by type in their effects on stream biota, with aluminum precipitates being more detrimental than iron.

CHAPTER III

SITE DESCRIPTION

<u>3.1 - Background on Study Area</u>

3.1.1 – Economy

Mining began in the Snake River watershed with Colorado's first silver strike
in 1863 (Gilliland, 1999). Lead, silver and zinc were the primary metals mined
though minor amounts of gold, copper and bismuth have also been noted (Moran and
Wentz, 1974). Large scale mining continued through the 1950's with a series of
booms and busts produced by fluctuations in silver prices as well as natural disasters
(Gilliland, 1999). In recent decades, the ski industry has replaced mining as the
dominant economic base of the region with the development of Arapahoe Basin,
Breckenridge, Copper and Keystone ski areas in Summit County, Colorado. The
growth of this industry has driven a second population boom. From 1970 to 1980
Summit County was the fastest growing county in the nation, experiencing a 232%
increase (Summit County, 2001). From 1970 to 1998, county population increased by
720% (Summit County, 2001).

Land uses in the Snake River watershed are varied and include extensive U.S.
Forest Service lands, Keystone Resort and Arapahoe Basin ski areas, the small town

of Montezuma, dispersed residential development in unincorporated areas and numerous historic mining sites. Keystone Resort has been making snow with water from the main stem of the Snake River for several years and is quickly developing prime riverfront real estate. Arapahoe Basin is currently seeking approval to extend its ski season by making snow with water from the unpolluted North Fork of the Snake River.

3.1.1 - Geography and Geology

The Snake River Watershed is bordered by the Continental Divide to the north, east and south and terminates in Dillon Reservoir (a primary drinking water source for the Denver metropolitan area) on the west (Fig. 3.1). The catchment is mountainous, ranging in elevation from 2749 m to 4188 m, with its headwaters above tree line. This study concerns the 150 km^2 of the watershed located upstream of USGS stream gage #09047500 located at Keystone Ski Resort. Geology of the study region is characterized by Precambrian Swandyke Hornblende Gneiss and Idaho Springs Formation, Cretaceous Hornfels, Tertiary Porphyritic Quartz Monzonite and Aplite, and Quaternary surficial deposits along its waterways (Neuerburg and Botinelly, 1972).

The headwaters of the Snake River drain a region of disseminated pyrite before running through a naturally occurring iron bog (Fig. 3.2). Natural weathering of pyrite produces waters in the upper Snake River that are acidic (pH 4.0) and have high concentrations of heavy metals (Bencala et al., 1987). The presence of this natural source of metals and acidity complicates remediation efforts, as background conditions may be sufficient to severely stress aquatic ecosystem along large sections

of stream reach. Below this source, the Snake River meets with Deer Creek which has relatively pristine water quality and approximately equal flow. An estimated 4.5 km from the Deer Creek confluence, Peru Creek flows into the Snake River increasing metal and acidity loads. Seven kilometers further downstream, in the vicinity of Keystone Resort, the Snake River is joined by its North Fork just above USGS stream gage #09047500.

Peru Creek is the Snake River's largest tributary. It flows by several smaller mines before receiving acidic and metal laden runoff from the Pennsylvania Mine which has extensive mine workings and large tailings piles. This mine is believed to be the primary source of anthropogenic contamination, though numerous abandoned (and several, small active) mines are scattered throughout the watershed (Wilson and LaRock, 1992). Several remediation attempts in the basin have focused on the Pennsylvania Mine drainage but have either failed or been stifled due to liability concerns associated with the Clean Water Act. As a result, much of the mine's drainage is collected into a holding pond (Fig. 3.3) and released into a trench (Fig. 3.4) which empties into Peru Creek. Three kilometers below the Pennsylvania Mine, the pristine Chihuahua Gulch tributary joins Peru Creek, diluting its waters and causing the formation of metal precipitates (McKnight and Bencala, 1990). Several kilometers further downstream, Peru Creek meets the Snake River.

FIGURE 3.1: Snake River Watershed to Dillon Reservoir. Map adapted from the Arapahoe Basin Master Development Plan (Dillon Ranger District, 1999)
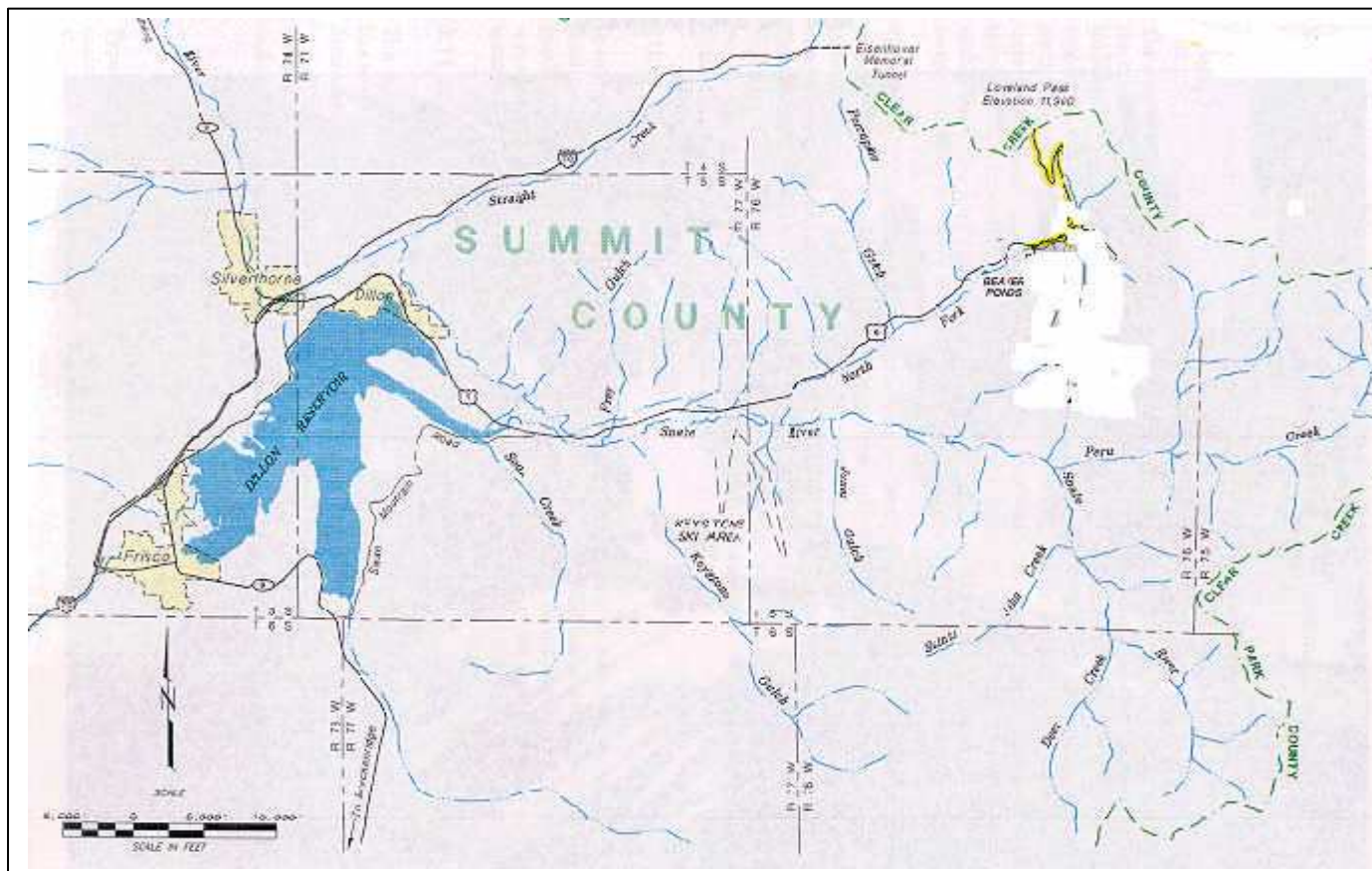
FIGURE 3.2: Geology of the upper Snake River

Geology by T.S. Lovering (1935)
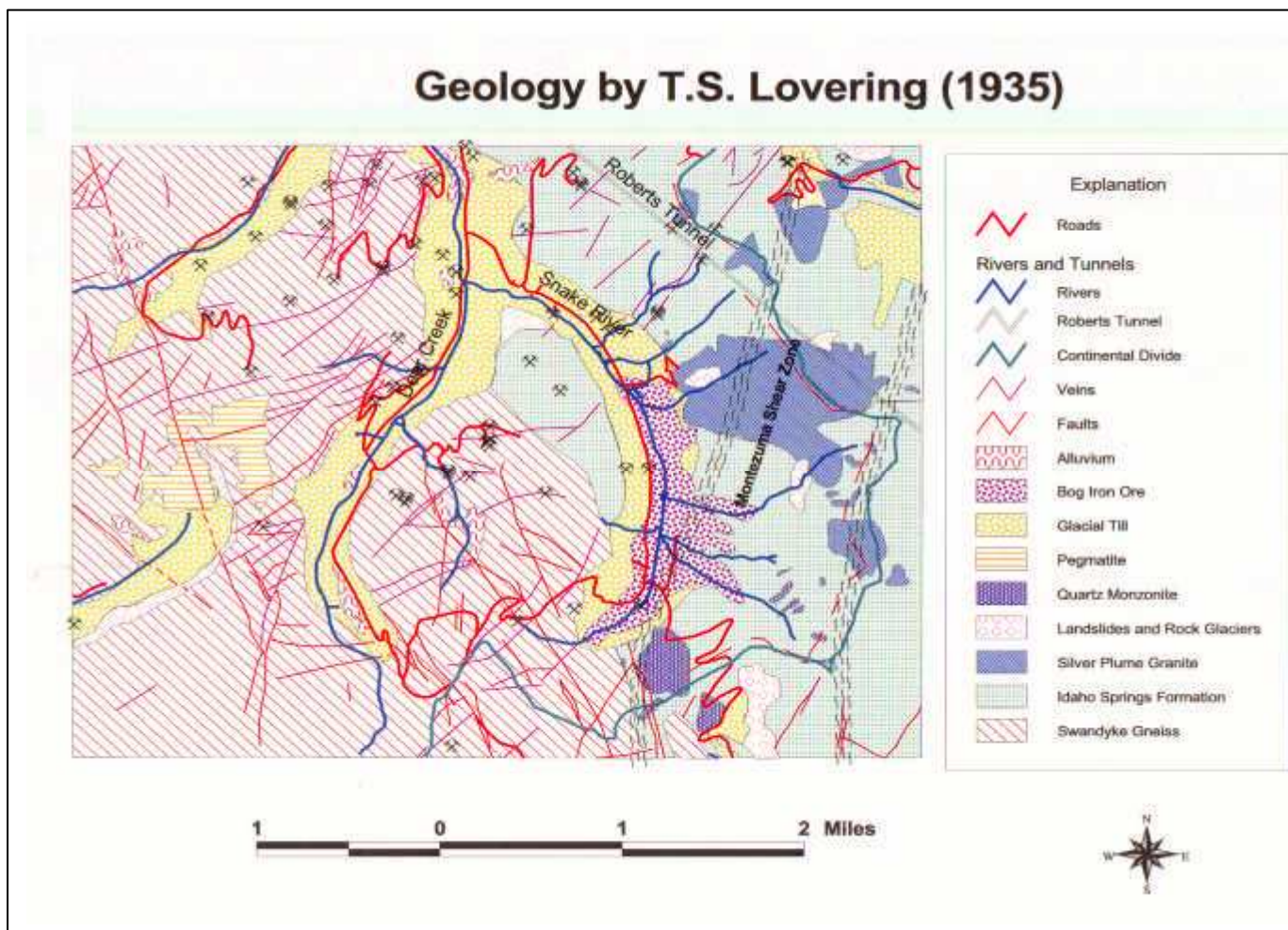
FIGURE 3.3: Holding pond at the Pennsylvania Mine. Runoff was collected and routed through this pond, which quickly saturated, in a failed remediation attempt.
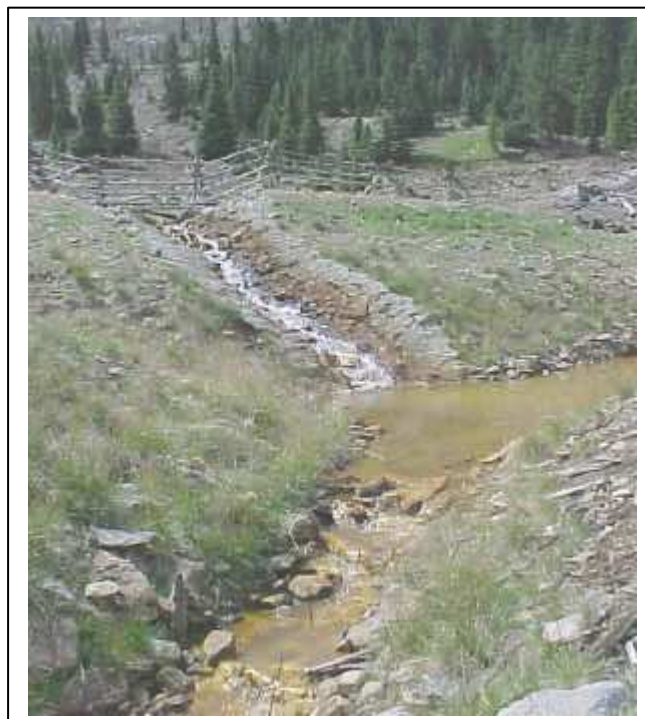
FIGURE 3.4: Runoff from the holding pond at the Pennsylvania Mine enters the drainage and eventually drains into Peru Creek. The orange colored deposits in the drainage trench are Fe oxides.

The stream length of the Snake River is affected by acid rock drainage of both natural and anthropogenic sources. Large sections of the Snake River and Peru Creek have stream water with elevated metals concentrations and low pH. Streambeds are coated in Fe and Al oxides. Both the Snake River and Peru Creek are identified on Colorado's 1998 303 (d) list of impaired water bodies due to high concentrations of Zn, Cd, Cu, Pb and Mn.

3.1.2 - Watershed-based Remediation Efforts

The effects of ARD are complex and may occur on a variety of scales. Rather than examining each source individually, decisions about remediation require an understanding of all the sources in a watershed, their relative importance in the basin and the impact on the aquatic environment. A watershed-based approach is a useful and efficient means of unifying interested agencies and disciplines in identifying the sources and effects of ARD and in developing remediation alternatives (Kimball et al. 1999).

In April of 1999, the Snake River Watershed Task Force formed with a mission *"to improve water quality in the Snake River watershed...focusing in particular on identifying, evaluating, and implementing opportunities to reduce heavy metal concentrations of concern"* (Snake River Watershed Task Force, 1999). This volunteer stakeholders group embraces public participation in water pollution control activities by bringing together multiple parties in a watershed based approach and includes representatives from citizens groups, government agencies, ski areas, and environmental groups as well as concerned individuals and research scientists. Since its inception, this diverse group has been compiling available data and identifying

gaps with the goal of developing projects that help establish reasonable standards and which prevent, reduce or eliminate pollution from the various sources within the basin. The task force itself, and its use of the broad knowledge base and levels of expertise provided by its members, is an innovative means of addressing the unique problem of ARD from abandoned mines and natural causes. This research was designed in collaboration with task force members and funded in part through the group. As the task force works to fulfill its mission, relationships with research institutions, such as the University of Colorado, have proven mutually beneficial. A complete list of task force members and interested parties are presented in the appendices in tables A.13 and A.14, respectively.

3.2 - Study Sites

Two sets of data were collected and analyzed for this research providing resolution at the watershed- and smaller sub basin-scale (Fig. 3.5). Samples were obtained during lower-flow, open water conditions in July and August. These samples are satisfactory for indicating major differences among sites, but are not representative of all seasons.

3.2.1 - Upper Snake River Diel Study

The upper Snake River diel study was designed to examine the effects of acid rock drainage caused by the natural weathering of disseminated pyrite in the headwaters of the upper Snake River. Discharge, pH and conductivity were measured in the field. Stream samples were collected and analyzed for dissolved metals, cations, anions and dissolved organic carbon (DOC). Additionally, calculations were

made to estimate lateral inflows, mass-flows and concentrations. Measurements were made and samples collected throughout the day to determine if diel changes were evident.

Eleven stream and four tributary sites (three draining the eastern side of the basin, one draining the western side) were selected covering approximately 2.25 km of headwater stream (Fig. 3.6). The first and uppermost site was located just above the road crossing to Webster Pass (0 m) with sites continuing downstream to the next road crossing (2250 m). Downstream sites were named according to the approximate distance downstream from the uppermost site. In confluence zones, sites were selected to allow for complete mixing with tributaries. Upstream confluence sites were located approximately 10 meters above inflows and downstream sites 25 meters below inflows. Additional reaches between confluences were sampled to distinguish longitudinal changes on the scale of hundreds of meters.

3.2.2 - Snake River Watershed Synoptic Study

The Snake River watershed synoptic study was designed to examine the effects of acid rock drainage on a watershed-wide basis, including both the natural weathering of pyrite in the upper Snake River and weathering occurring in abandoned mines scattered throughout the basin, with a special emphasis on Peru Creek. Discharge, pH and conductivity were measured in the field. Samples were collected and analyzed for dissolved metals, cations, anions, DOC, Fe and Al oxide deposition and periphyton biomass. Additionally, calculations were made to estimate lateral inflows, mass-flows and concentrations.

Ten stream and five tributary sites were chosen to target areas of interest (Fig. 3.7). The five Peru Creek sites began just upstream of the Pennsylvania Mine drainage (PR1) and ended just above the confluence with the Snake River (PR5). In addition, Pennsylvania Mine drainage (PN1 – sampled in the drainage trench below the holding pond) and Chihuahua Gulch (CH1 - a high flow, neutral pH tributary) were sampled. On the Snake River, sites began above the Deer Creek confluence on the Snake River (SN1) and ended below the confluence with the Snake River's North Fork at Keystone Resort (SN8). Tributaries that were sampled included the pristine Deer Creek tributary (DC1) and the North Fork (NF1) which is not impacted by acid rock drainage. In confluence zones, sampling sites were selected 5 to 20 meters upstream or downstream from inflows. A detailed analysis of the North Fork and Snake River confluence is not presented in this paper. Sampling data for the North Fork can be found in the appendices in tables A.6 – A.12.

The area covered by the Snake River synoptic study is larger and more geochemically heterogeneous than the watershed area of the upper Snake River diel study necessitating greater distances between sampling sites. As a result longitudinal variations are distinguishable over a scale of kilometers rather than meters, making some processes that can control mass-flow more difficult to ascertain. Data were collected only for select tributaries as logistics made it unrealistic to sample every visible inflow. This necessitated that an unknown number of visible inflows were not sampled and that their contributions were included in lateral contributions. Additionally, July discharge data was not collected for PR1, PR2, PR3, PR4 and PN1 making certain calculations for these sites impractical.
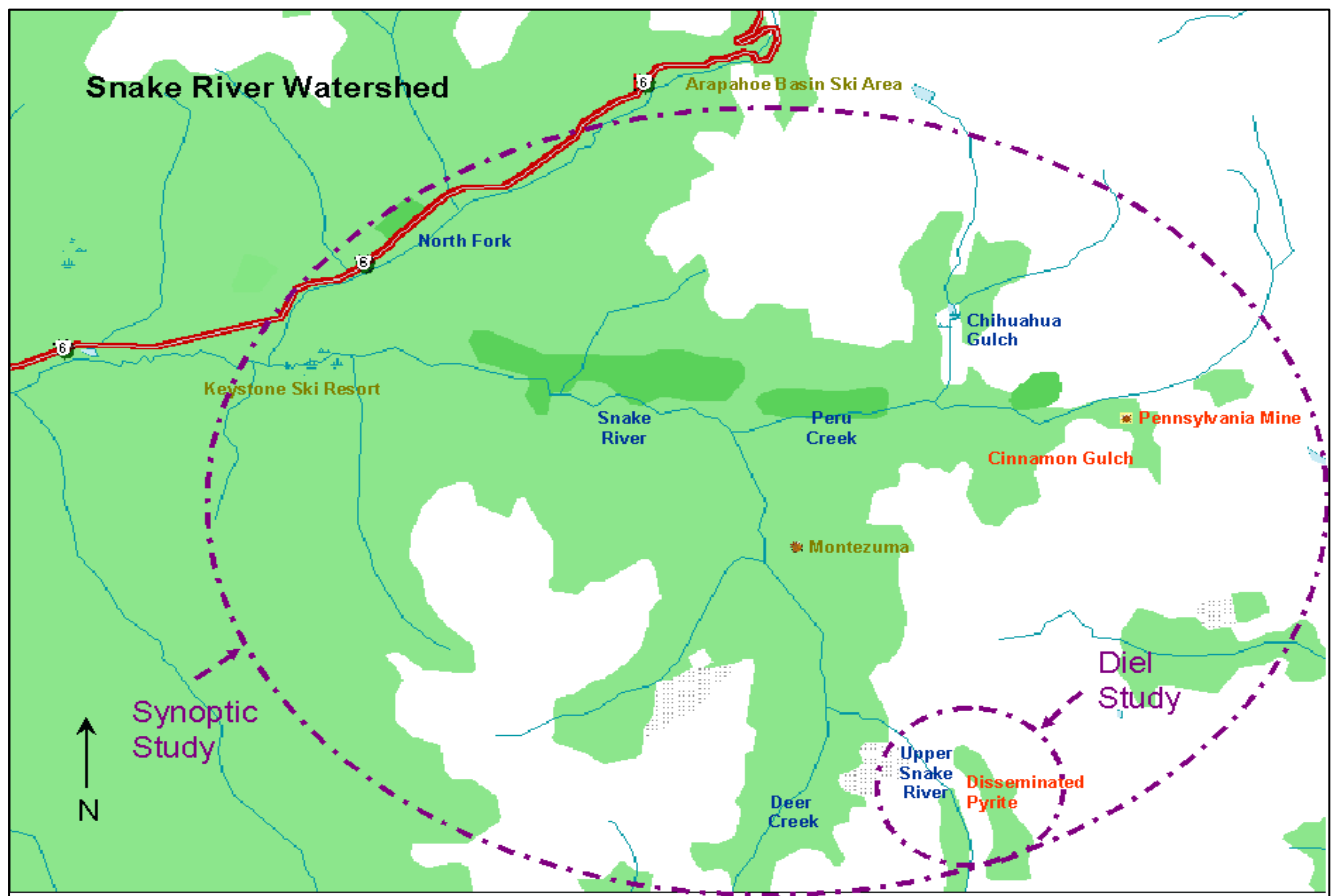
FIGURE 3.5: Study regions. Area covered by the Snake River Watershed synoptic study and the upper Snake
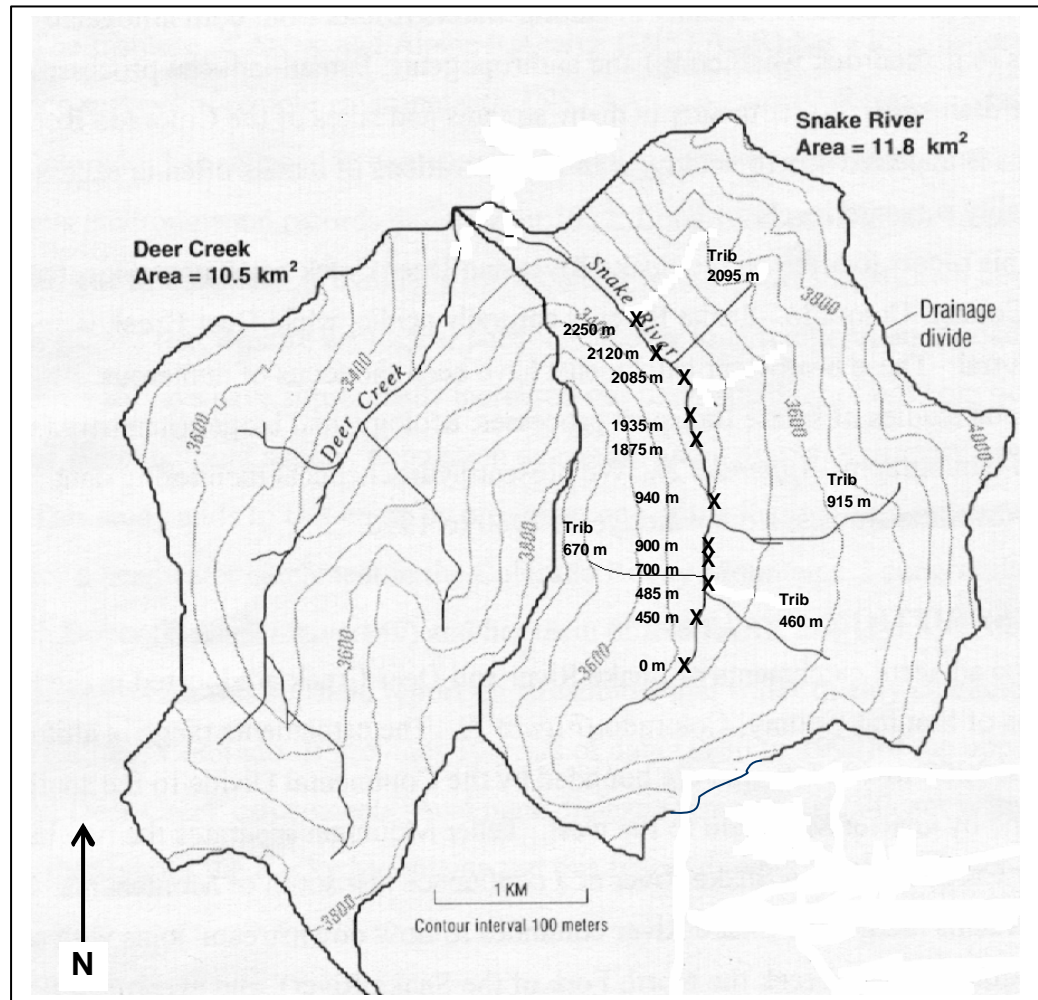
FIGURE 3.6: Upper Snake River diel study sampling sites. (Adapted from Boyer et al., 1999)
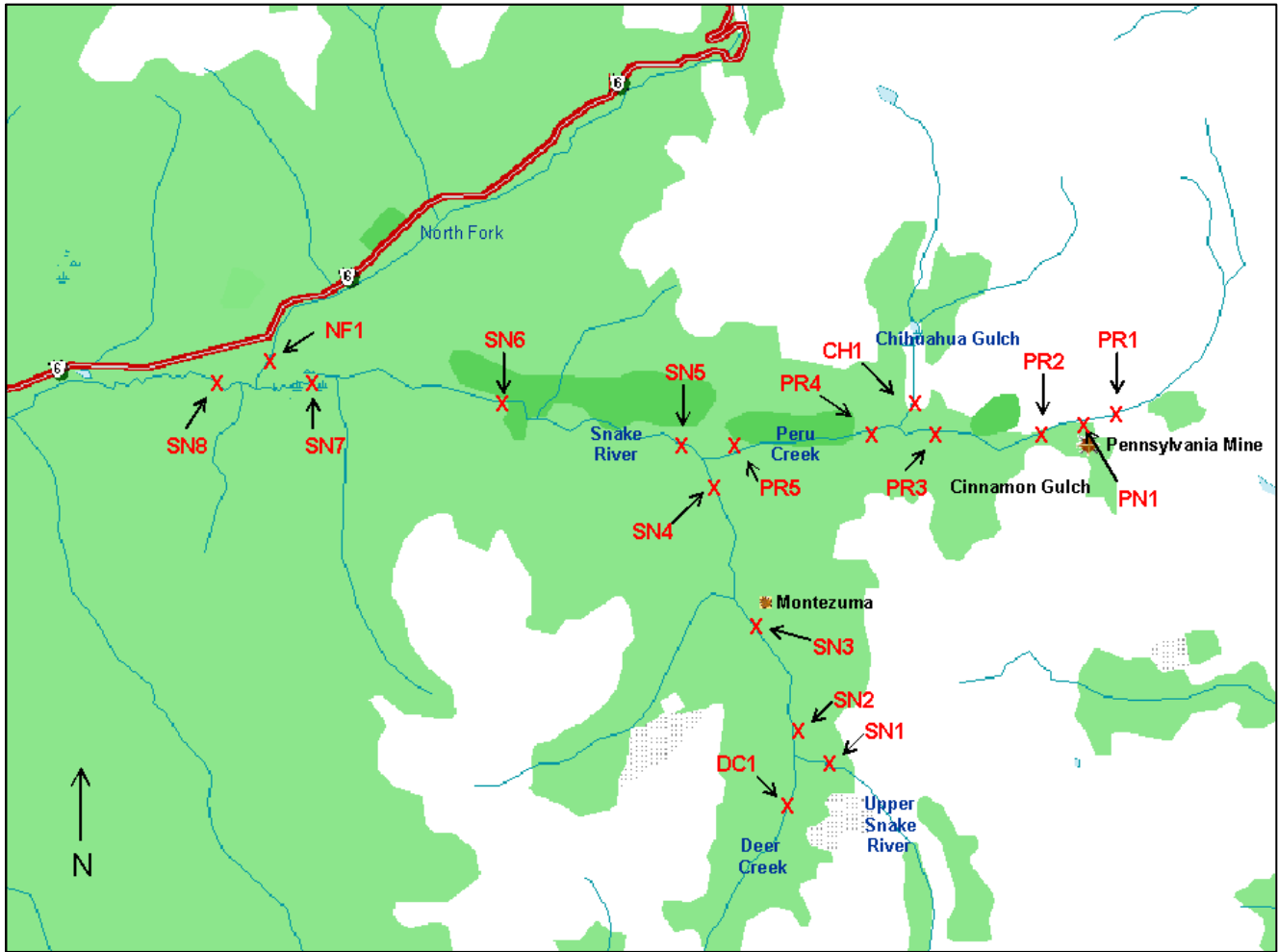
FIGURE 3.7: Snake River Watershed synoptic study sampling sites

3.3 - Methods

3.3.1 - Upper Snake River Diel Study

Diel samples were collected in the headwaters of the Snake River on July 28, 1998 from 0930 to 1500 hours. At the majority of sites, samples were collected thrice during the day at approximately 0930, 1200 and 1500 hours. Samples were collected once every hour at the upper- and lower-most site.

Discharge, pH and Conductivity

Discharge was measured at each site once during the day using a pygmy meter, with measurements beginning at site 2250m at 0912 hours and working upstream. pH and conductivity were measured in the field with an ion-specific electrode and probe, respectively.

Dissolved Metals, Cations and Anions

Samples for dissolved species were filtered through 0.1 µm nitrocellulose filters. Samples for metals and cations were acidified in the field with Ultrex nitric acid. Samples for analysis of Fe^{2+} and readily soluble Fe were analyzed using the 2,2'-bipyridine colorimetric method (Brown et al., 1970) with reagents added immediately after filtration in the field and spectrophotometric analysis within 24 hours. Total Fe (FeT), Zn, Al and Mn were analyzed in the laboratory by inductively coupled plasma atomic emission spectrometry (ICP-AES) and Cu, Ca and Na by flame atomic absorption spectroscopy (AA). Anion samples were analyzed by ion chromatography (IC).

Soluble iron concentrations analyzed immediately after sampled collection tended to be lower than FeT samples analyzed using the ICP spectrometer several months later. For this reason, the term readily soluble Fe has been applied to the samples analyzed colorimetrically and reflects the dissolved ferrous iron (Fe^{2+}) plus that portion of the dissolved ferric iron (Fe^{3+}) which was rapidly reduced by adding hydroxyl amine to the filtered sample. FeT measure by ICP was slightly greater because any colloidal Fe^{3+} not reduced in the colorimetric analysis was detected under the conditions of the ICP method involving a high temperature plasma.

Dissolved Organic Carbon

Dissolved organic carbon (DOC) samples were filtered through pre-combusted Whatman glass fiber filters into pre-combusted amber bottles and analyzed using a Dorhman DC-190 Carbon Analyzer.

3.3.2 - Snake River Watershed Synoptic Study

Synoptic samples were collected during two field efforts on July 26 – 28 and August 24 and 25, 2000. Samples were collected to obtain a "snapshot" of the system though logistics required that samples be collected over several days. This type of sampling is appropriate for streams in which most variations occur in the longitudinal direction but may not be for larger streams where significant chemical variations may occur within a given cross-section (Kimball et al., in press).

Discharge, pH and Conductivity

Discharge was measured with a pygmy meter, except at site SN8 where data was taken from a USGS stream gage (#09047500). pH and conductivity were measured in the field with an ion-specific electrode and probe, respectively.

Dissolved Metal, Cations and Anions

Samples for dissolved metals, cations and anions were filtered through 1.0 µm Pall Gelman glass microfiber filters (type A/E). Dissolved metals and cation samples were then acidified with Fisher trace metal nitric acid and stored in acid rinsed bottles and analyzed in the laboratory by ICP-AES. Anion samples were analyzed by IC.

Dissolved Organic Carbon

DOC samples were filtered through pre-combusted Whatman 4.7cm glass fiber filters into pre-combusted amber bottles and analyzed using a Shimadzu Model 5050A Organic Carbon Analyzer.

Fe and Al Metal Oxides

Two rocks were collected from each site for analysis of Fe and Al metal oxide deposition. The rocks were scraped clean in the laboratory and rinsed with de-ionized water (DI) into pre-weighed aluminum boats. Samples were dried, weighed and rehydrated in glass beakers with 0.01N HNO_3. Digestion followed a procedure modified from Makos and Hrncir (1995). 1.0 ml each of concentrated H_2SO_4 and HNO_3 was added to each sample and the mixture heated to reduce volume approximately by half. An additional 1 ml each of H_2SO_4 and HNO_3 was added and samples left to sit covered for 48 hours. Samples were reheated and reduced to

approximately half volume. The solution of the extracted metals was filtered through a 0.1 μm membrane, brought up to a known volume and analyzed by ICP-AES. During the initial sampling trip, two additional rocks were brushed clean of precipitates at each site and placed back in the stream. In August the same rocks were recovered, the oxides scraped from them and analyzed and a rate of oxide deposition determined.

Periphyton Biomass

Two rocks from the riffle zone were scraped clean of algae into separate containers and diluted to a known volume with DI water. Samples were then partitioned for ash free dry mass (AFDM) and chlorophyll *a*. AFDM samples were filtered onto precombusted 47mm Whatman GF/C filters and analyzed according to the methods described in Steinman and Lamberti (1996). Chlorophyll *a* samples were filtered onto 47mm Whatman GF/C glass microfiber filters and analyzed spectrophotometrically following hot ethanol extraction (Morris and Lewis, 1988). During the initial sampling trip, two rocks (in addition to those cleaned for oxide deposition) were brushed clean and placed back into the stream at each site. They were recovered in August, the periphyton removed and analyzed and a rate of algal colonization calculated.

Surface Area

Surface area was estimated for rocks from which metal oxide and periphyton samples were collected based upon the mass of aluminum foil required to cover the surface of the rock (Steinman and Lamberti, 1996).

3.3.3 - Lateral Inflow, Concentration and Mass-Flow

Lateral contributions were calculated throughout the study region and include both groundwater and subsurface water inflows. Lateral inflows, concentrations and mass-flows were calculated using conservation of mass equations (Bencala and Ortiz, 1999; Bencala and McKnight, 1990; Kimball et al., in press). Calculations to estimate lateral concentrations and mass-flow assume conservative solute behavior. Though some solutes are chemically reactive to some extent in ARD environments, these calculations are useful in identifying sources and pathways. Figure 3.8 depicts an idealized stream reach with a downstream sampling site B, an upstream site A, a measurable tributary T, and possible lateral inflows which may have groundwater or subsurface seeps as their origin.
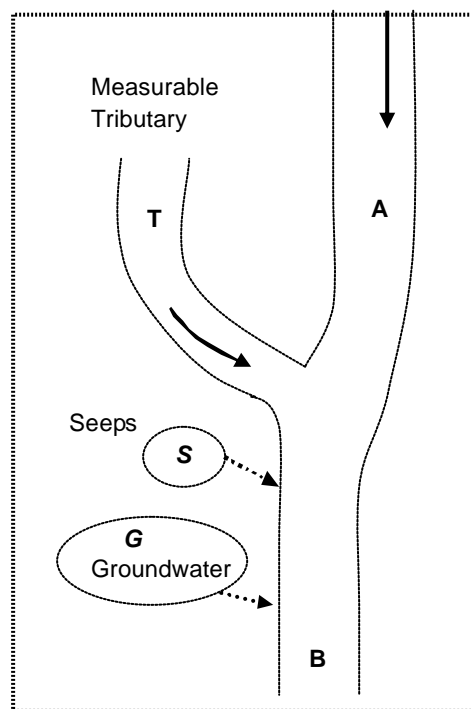
FIGURE 3.8: Idealized stream reach with inflows. Water flows past upstream point A, may receive inflow from a visible tributary T, and possible inflows from subsurface and groundwater inflows before passing downstream point B. (Adapted from Bencala and Ortiz, 1999)

Lateral discharge is the sum of seeps and groundwater inflows (Eqn. 3.1).

Equation 3.1: $Q_L = Q_S + Q_G$

Where:

Q_L = estimated lateral discharge (Units: volume/time)

Q_S = discharge entering through seeps

Q_G = discharge entering through groundwater

It is impractical to measure Q_S and Q_G so lateral discharge entering a stream reach between two sampling points was determined using equation 3.2. Upstream and sampled tributary discharge values were subtracted from downstream discharge.

Equation 3.2: $Q_L = Q_B - Q_A - Q_T$

Where:

Q_B = measured discharge at downstream site

Q_A = measured discharge at upstream site

Q_T = measured discharge in tributary

Logistics prevented the sampling of every visible tributary in the Snake River Watershed synoptic study area. For this reason, in the synoptic study, calculated lateral inflows may include contributions of other unmeasured tributaries.

The mass-flow at a generalized sampling site X, is determined in equation 3.3.

Equation 3.3: $M_x = Q_x C_x$

Where:

M_X = mass load at point X (Units: mass/time)

Q_X = discharge at point X

C_X = instream concentration at point X (Units: mass/volume)

Lateral mass-flows were estimated (Eqn. 3.4) similarly to discharge, with a mass-balance of upstream, downstream and tributary inflows.

$$\textit{Equation 3.4: } M_L = Q_B C_B - Q_A C_A - Q_T C_T$$

Where:

M_L = lateral mass load

C_B = sampled concentration at downstream site

C_A = sampled concentration at upstream site

C_T = sampled concentration in tributary

Lateral concentrations, assuming conservative solute behavior, were estimated using equation 3.5 which is a derivation of equations 3.2 through 3.4.

$$\textit{Equation 3.5: } C_L = \frac{Q_B C_B - Q_A C_A - Q_T C_T}{Q_B - Q_A - Q_T}$$

CHAPTER IV

RESULTS

The complete results from the upper Snake River diel study and the watershed-wide synoptic study are tabulated in the Appendices (tables A.1 – A.12). Tables A.1 and A.2 present upper Snake River diel data collected at sampling sites including mass-flows. Tables A.3 – A.5 contain calculated lateral inflow data for the upper Snake River diel study including discharge, concentration and mass-flow. Sampling data for the Snake River watershed synoptic study is presented in tables A.6 – A.12. Tables A.6 – A.9 contain concentration, mass-flow, oxide deposition and periphyton data. Tables A.10 – A.12 provide the results of lateral inflow calculations including discharge, concentrations and mass-flows.

In the results below, when data from the Snake River watershed synoptic study were similar or July data incomplete, only August data is presented for reasons of simplification.

4.1 - Upper Snake River Diel Study

Discharge along the 2.25 km study reach increased six-fold from 0.04 to 0.24 $m^3 s^{-1}$ with discharge increases in the vicinity of tributaries 460 m, 915 m and 2095 m and losses near tributary 670 m (Fig. 4.1). Figure 4.2 illustrates confluence zone

inflows and highlights the significance of subsurface, or lateral, inflows on total instream flow. At confluence 450-485 m, nearly three times the amount of water entered the stream laterally than in the measurable tributary. An anomaly was seen in the vicinity of the confluence with tributary 670 m where water was lost to the subsurface. Lateral inflows accounted for more than half of inflows at the confluence with the tributary at 915 m. At the most downstream confluence, the majority of discharge entered the stream in the tributary, though lateral inflows remained significant. Lateral inflows were present throughout most of the study reach with the exception of the region near tributary 670 m and from 1875 m to 2085 m which were losing reaches. Because the distance between sampling sites varied, it is useful to determine the discharge gained from lateral inflows per longitudinal meter of stream (Fig. 4.3). Much more water flowed into the stream laterally in confluence zones than elsewhere along the study reach.
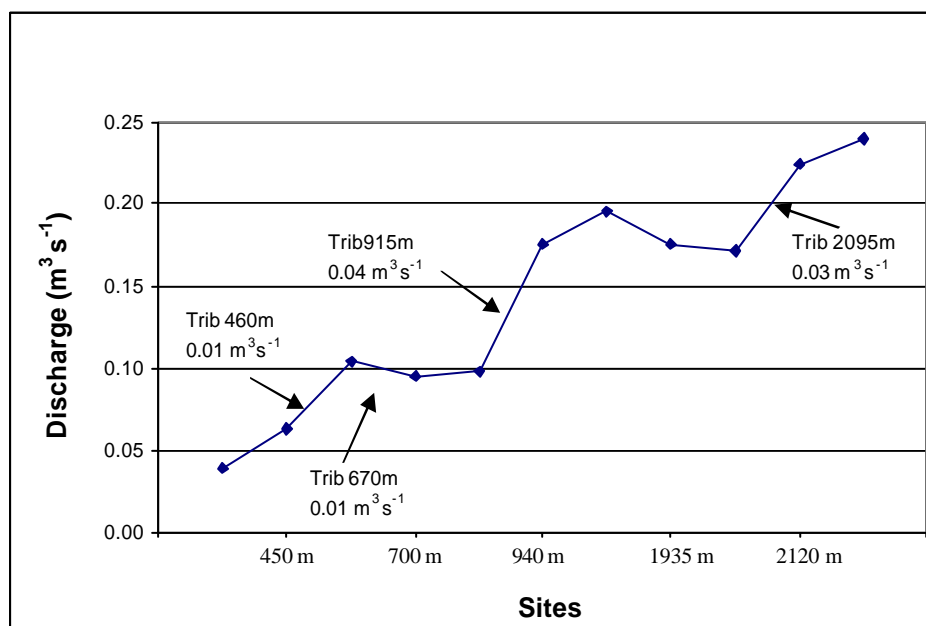
FIGURE 4.1: Snake River discharge with tributary inflows noted, upper Snake River diel study.
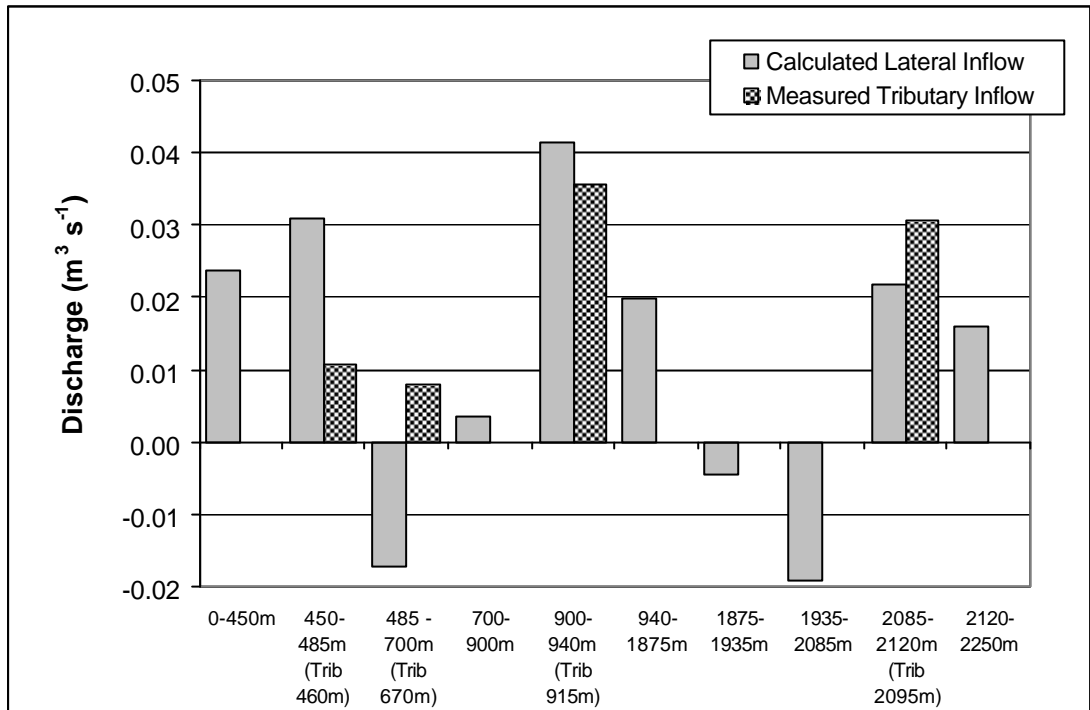
FIGURE 4.2: Confluence zone inflows including lateral and tributary inflows,upper Snake River diel study.
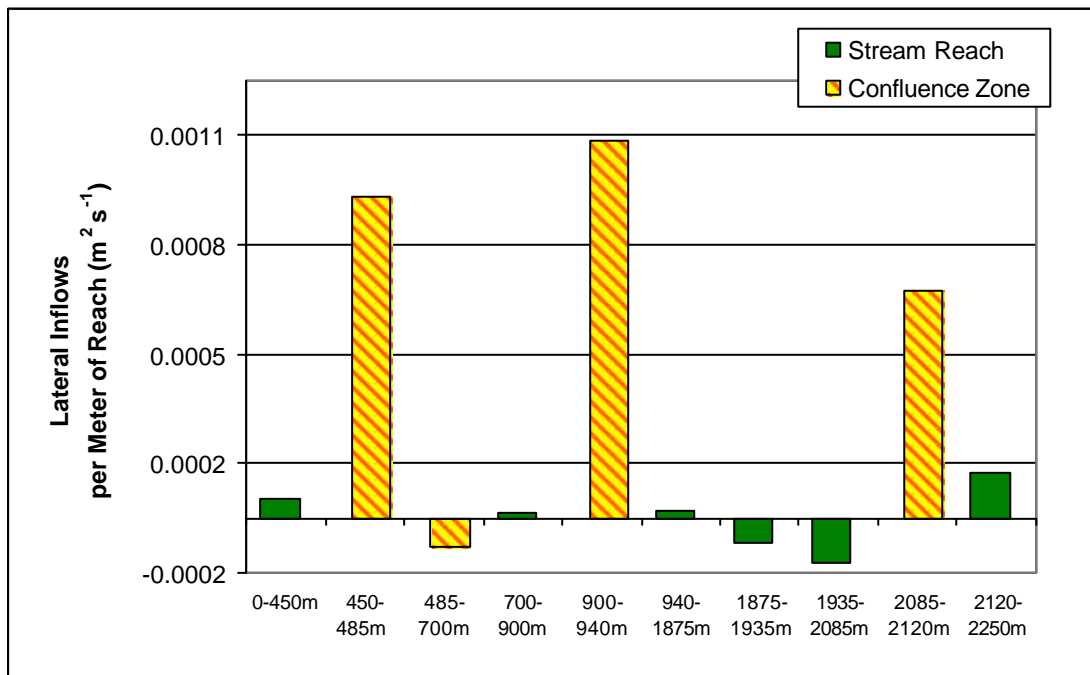
FIGURE 4.3: Lateral discharge gain per meter of stream reach, upper Snake River diel study

Figure 4.4 shows the impact of tributary inflows on stream chemistry. Elevated metal concentrations and mass loading were apparent in samples collected from tributaries 460 m, 915 m and 2095 m which drain the eastern side of the basin. Metal concentrations and mass-flows in tributary 670 m, draining the western basin, were negligible. Tributaries 460 m and 2095 m had similar concentrations of Zn and Mn, while concentrations of these metals were lower in tributary 915 m. Mass-flows of these two metals were highest in tributary 2095 m. Fe^{2+} concentrations were highest in the uppermost tributary (460 m) and decreased down to tributary 2095 m. Mass-flows for Fe^{2+} were highest in tributary 915 m. Al concentrations and mass-flows were significantly larger than for the other metals. The highest Al concentrations were found in tributary 2095 m followed by tributary 460 m. Mass-flows of Al were also highest in tributary 2095 m. Tributaries 460 m and 915 m contributed similar mass loads.
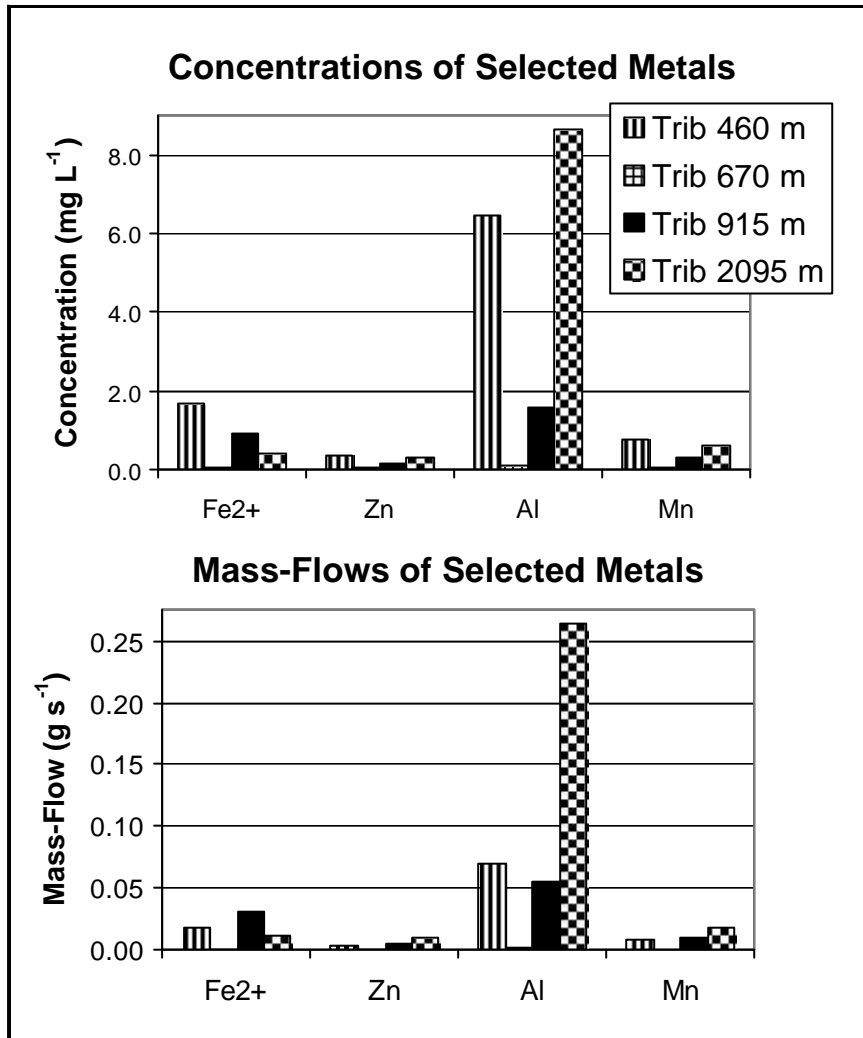
FIGURE 4.4: Tributary data, upper Snake River diel study

The pH in the upper Snake River (Fig. 4.5) was initially 5.0 at site 0 m, decreased to 4.0 by the third site (485 m), and remained constant throughout the rest of the study reach. Figure 4.6 shows longitudinal variations in solute concentrations at the eleven stream sites. Tributary data is not presented. SO_4 and Na behaved similarly to pH, increasing to stable values by the third site. Ca displayed the reverse pattern, decreasing to a somewhat less stable value by the third site. Concentration profiles for metals fluctuated in the downstream direction. Fe^{2+} and FeT concentrations increased to a maximum value at site 485 m and then began to decrease. Other metals concentrations increased and decreased with patterns that vaguely mimicked stream discharge. Overall increases in the downstream direction were seen for all metals, with the exception of Fe. For example, concentrations of Zn increased nearly three-fold, Cu four-fold and Al five-fold throughout the study reach. Figure 4.7 reveals a tight correlation ($R^2 = 0.96$) between H^+ and SO_4 concentrations.
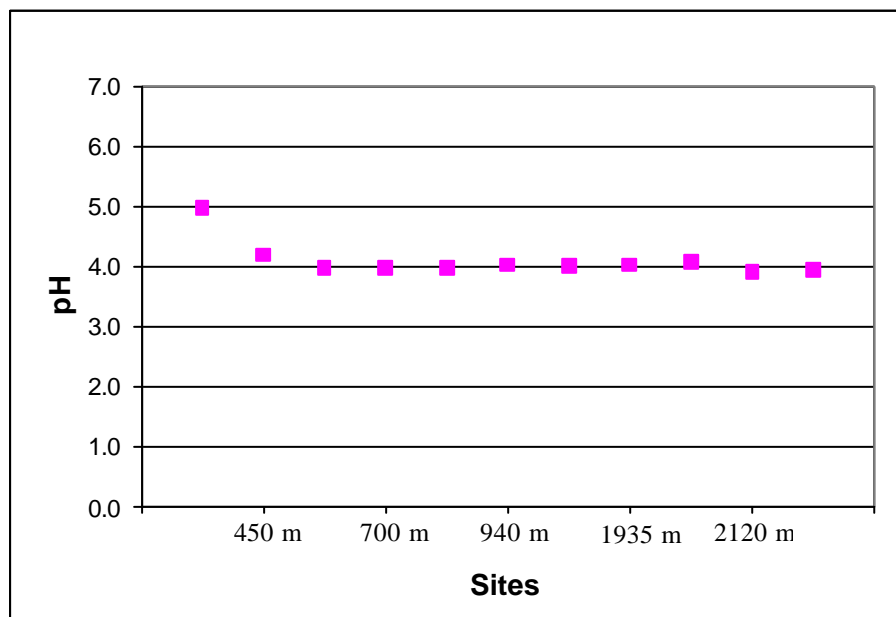
FIGURE 4.5: Mean pH, upper Snake River diel study
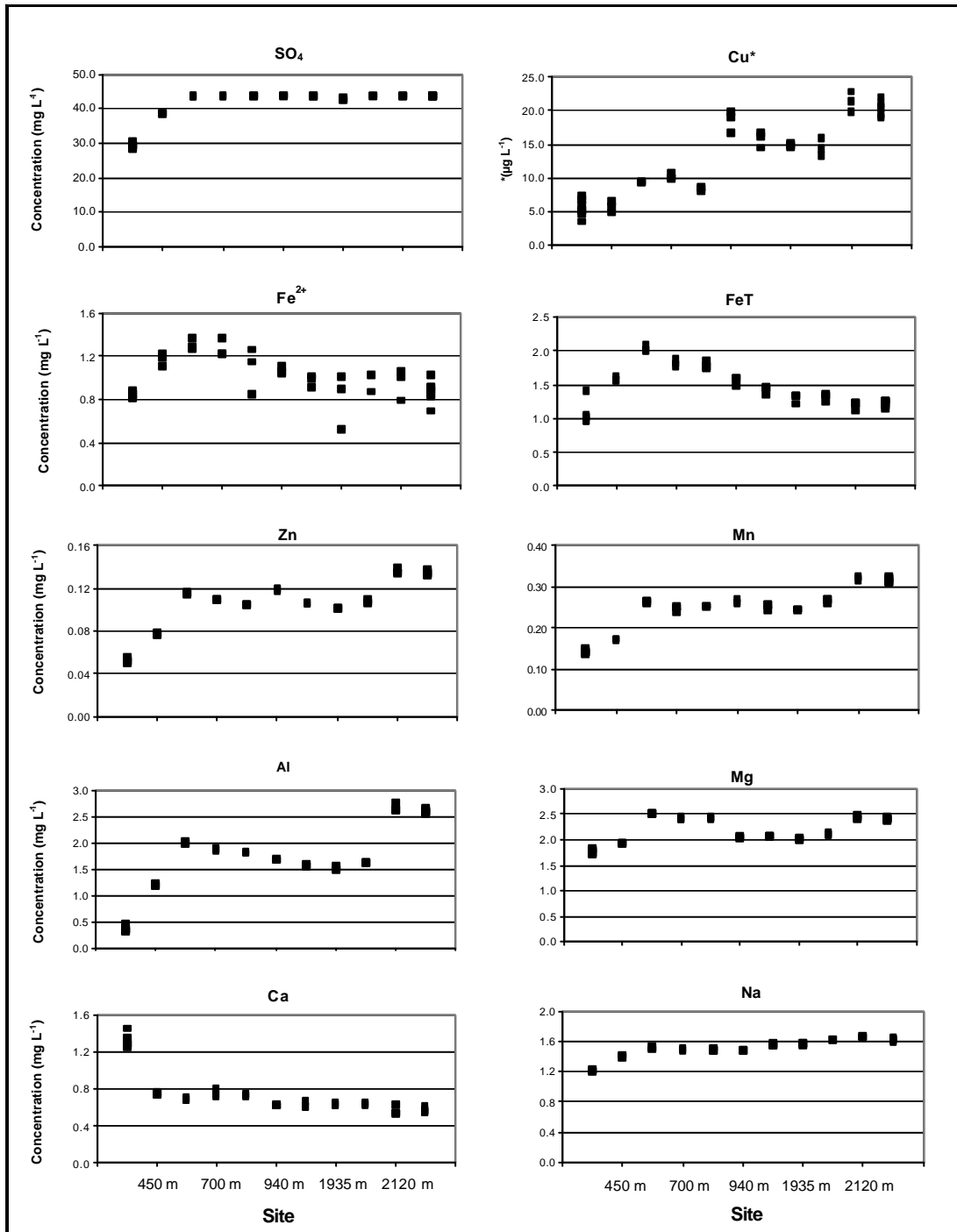
FIGURE 4.6: Instream concentrations, upper Snake River diel study. All concentrations are in mg L-1, except for Cu which is in units of µg L-1.

42

Figure 4.6 also presents the variations in concentrations during the day at each site. The concentrations of most metals remained constant throughout the sampling period. Significant diel variations were evident only for Fe^{2+} and Cu and are represented by the scattering of data points seen for each site. Very minor diel changes were observed for the other solutes. Figure 4.8 reveals a poor correlation between Fe^{2+} and Cu at most sites.

Diel and longitudinal variations in solute mass-flow are depicted in figure 4.9. In comparison with variations in concentrations, mass-flows increased for all solutes in the downstream direction. Mass-flow patterns are similar for all solutes and generally mimic downstream changes in discharge.
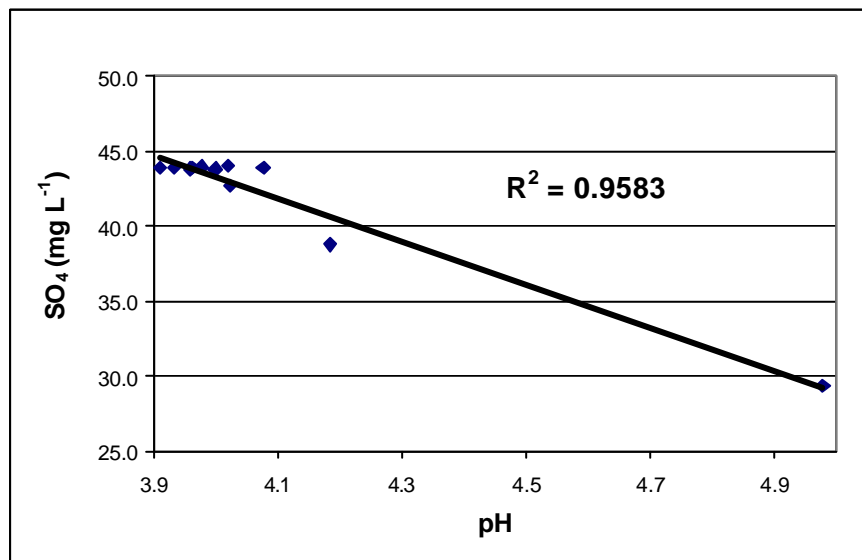
FIGURE 4.7: Relationship between pH and SO_4, upper Snake River diel study
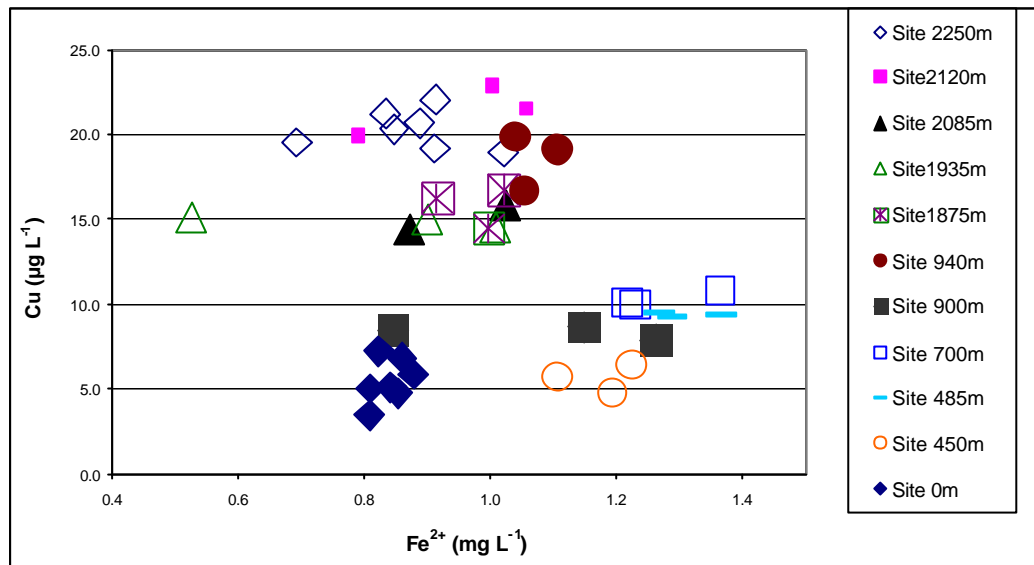
FIGURE 4.8: Relationship between Fe $^{2+}$ and Cu, upper Snake River diel study
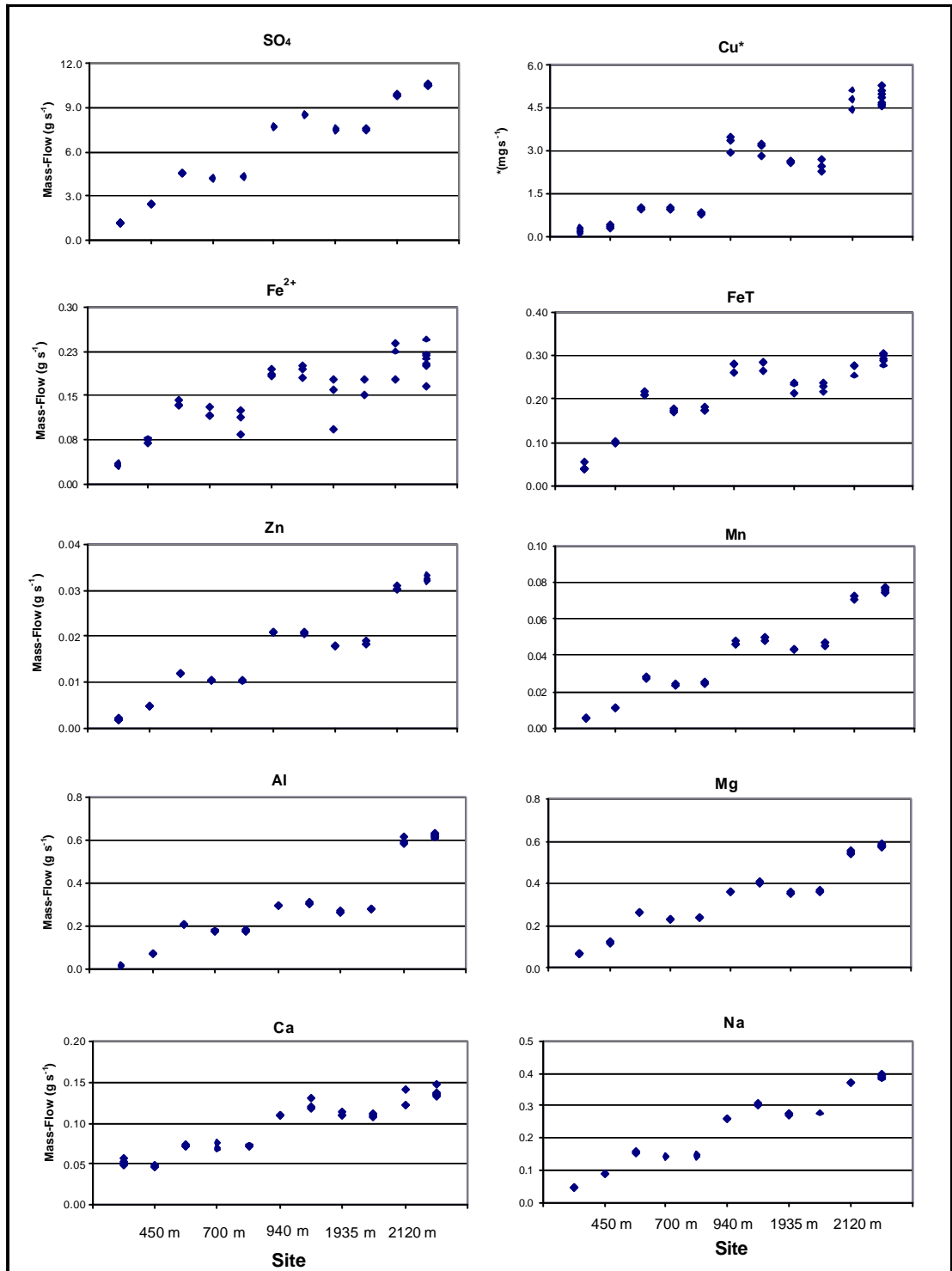
FIGURE 4.9: Mass-Flows, upper Snake River diel study. All mass-flows are in g s-1, except for Cu which is in mg s-1.

Figures 4.10 through 4.12 compare lateral and tributary mass-flows as well as estimated lateral and measured tributary concentrations for the three gaining confluences. The confluence with tributary 670 m is not included because it was a losing reach and negligible source of metals and acidity. Figure 4.10, represents the uppermost confluence where the majority of water entered the stream laterally. Nearly equal mass-flows of most metals (Zn, Al, Mn, FeT, Cu) entered through the subsurface and in tributary waters, though the tributary tended to be a slightly larger source. Lateral contributions for SO_4, Fe^{2+}, readily soluble Fe, Mg, Na and Ca were substantially higher. Inflow concentrations exhibited very different patterns. Al concentrations, for example, were estimated to be much greater in the tributary than in subsurface inflows. The same is true for most other metals, yet high lateral discharge produced nearly equal mass-flows.

The next downstream confluence is with tributary 915 m (Fig. 4.11) where the majority of mass-flow for most solutes entered the stream laterally. Lateral mass-flows for Al, Mn and FeT and Na were only slightly greater than tributary mass-flows and Zn mass-flows were equal among the two sources. Lateral mass-flows for readily soluble Fe, Fe^{2+}, SO_4, Mg, and Ca were greater than in the tributary. Cu was the only solute with higher tributary mass-flows. Lateral and tributary concentrations at this confluence were equal, or nearly so, for the majority of solutes. Concentrations of Cu in the tributary were greater than in lateral inflows while tributary concentrations were only slightly greater for Zn, Al and FeT. Higher lateral concentrations were calculated for readily soluble Fe, Fe^{2+}, SO_4, Mg and Ca. Mn and Na concentrations were effectively equal among source waters.

At the most downstream confluence (Fig. 4.12), concentrations were higher in tributary waters for all solutes with the exception of Fe^{2+}, which may be precipitating. Differences were largest for Al and Cu, which had tributary mass-flows three to five times greater than lateral mass-flows, and Fe^{2+}, which had lateral mass-flows nearly four times greater than tributary loads. Concentrations behaved similarly to mass-flows with higher tributary concentrations for the majority of solutes (Zn, Al, Mn, Cu, Mg and Na). Lateral and tributary concentrations for readily soluble Fe, FeT, SO_4 and Ca were equal or very similar and lateral concentrations were greater for Fe^{2+}.
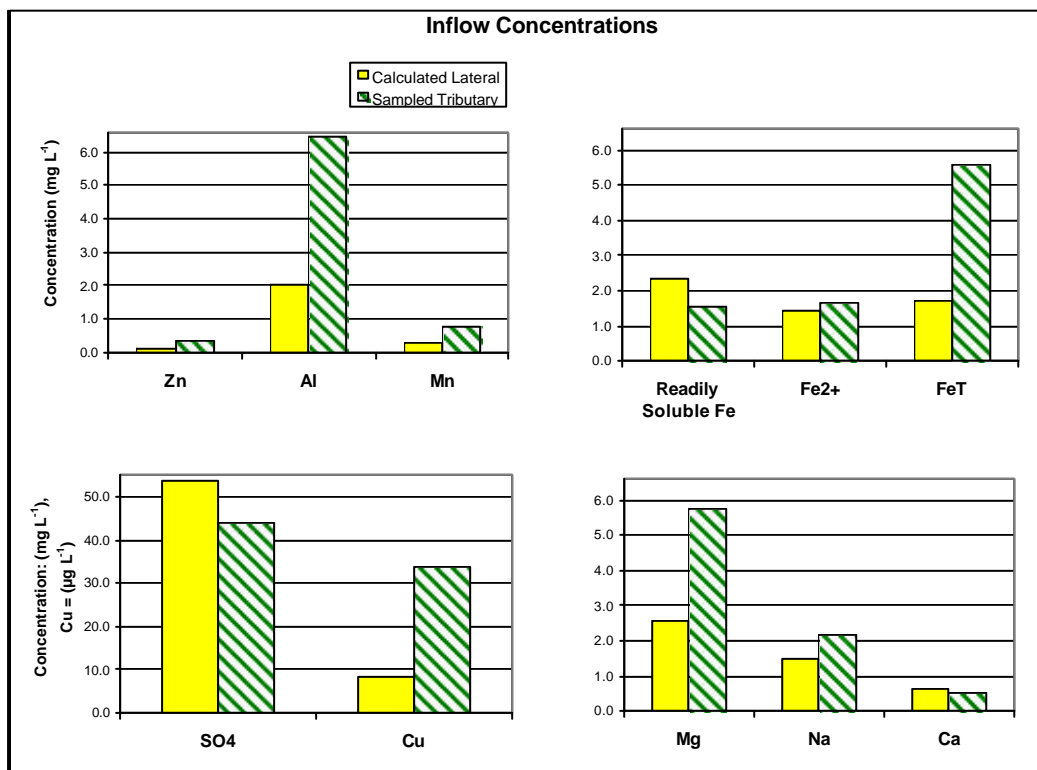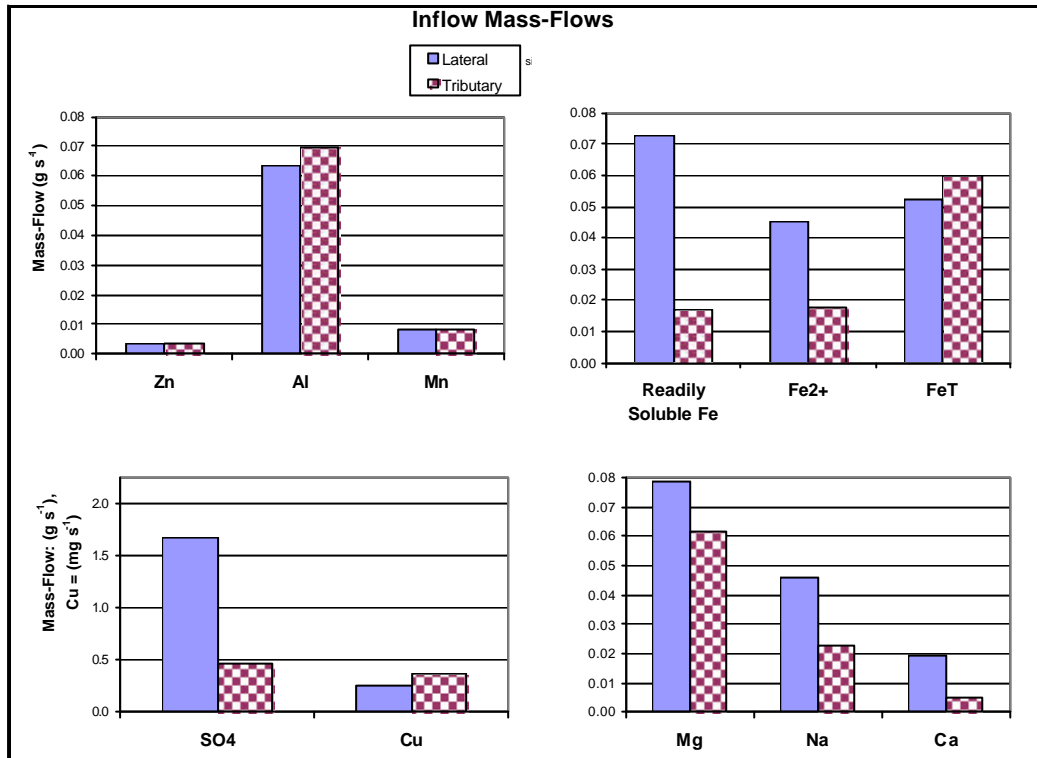
FIGURE 4.10: Inflow between sites 450 and 485 m (Trib 460 m), upper Snake River diel study
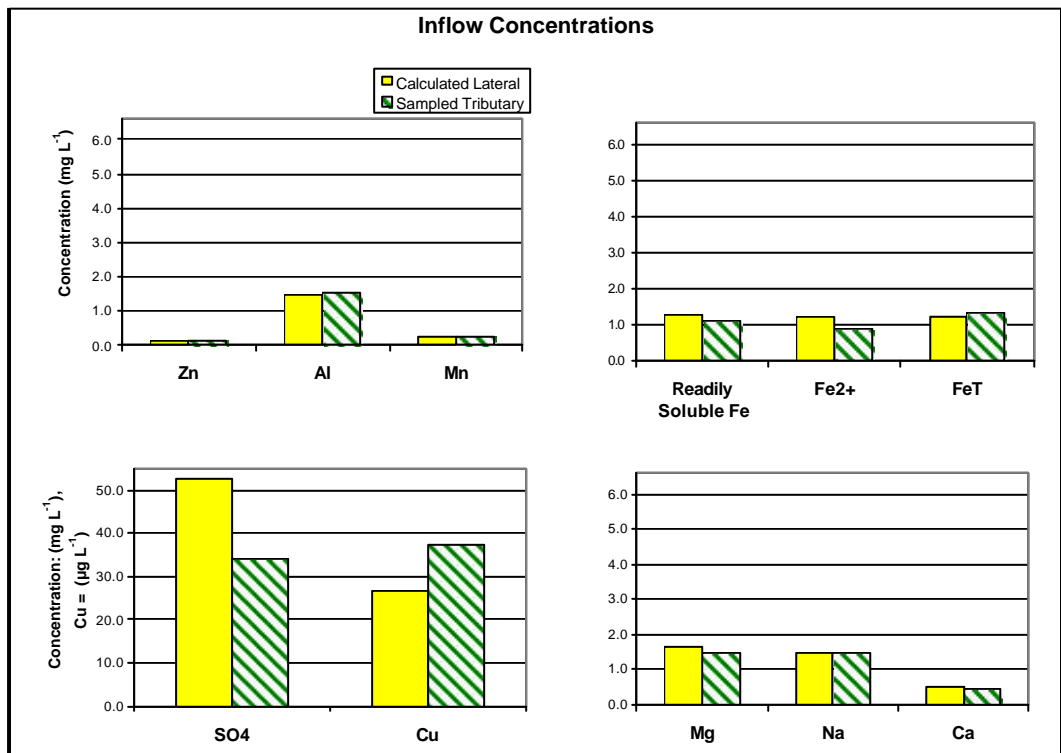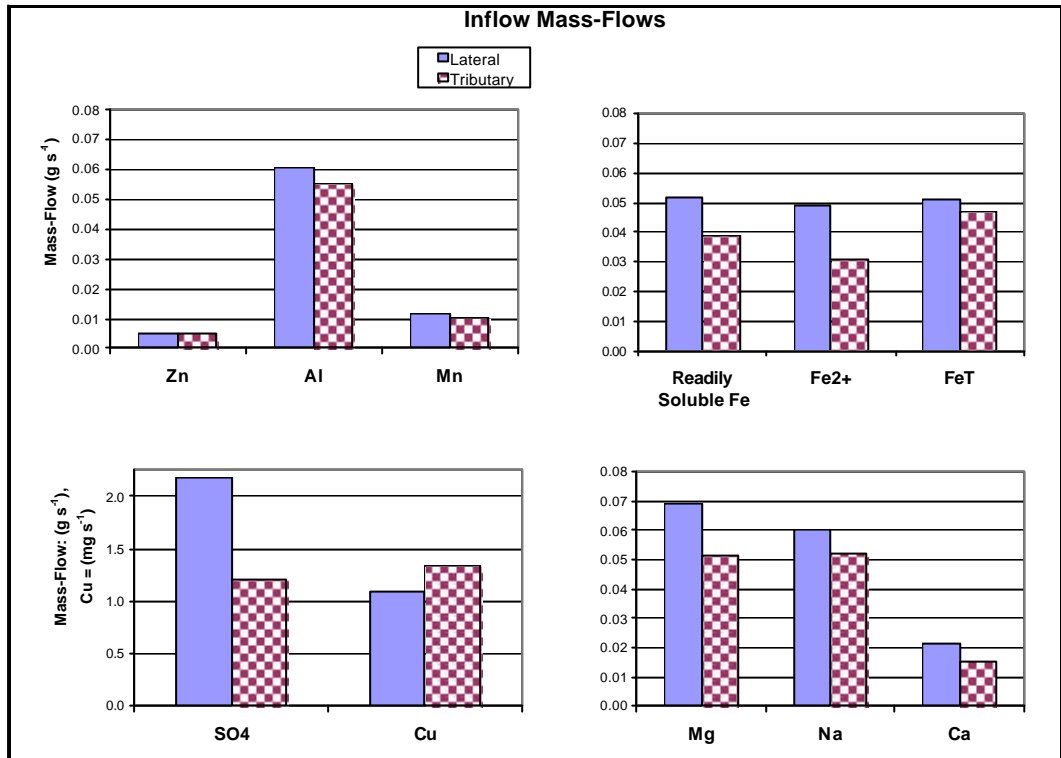
FIGURE 4.11: Inflows between sites 900 and 940 m (Trib 915 m), upper Snake River diel study
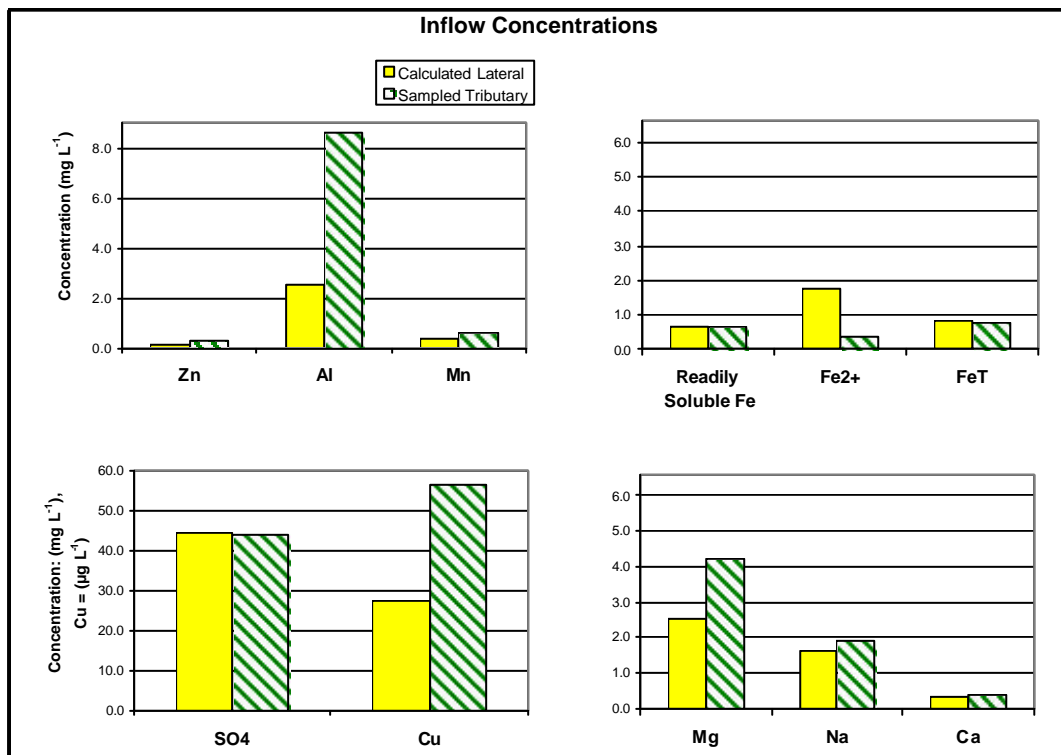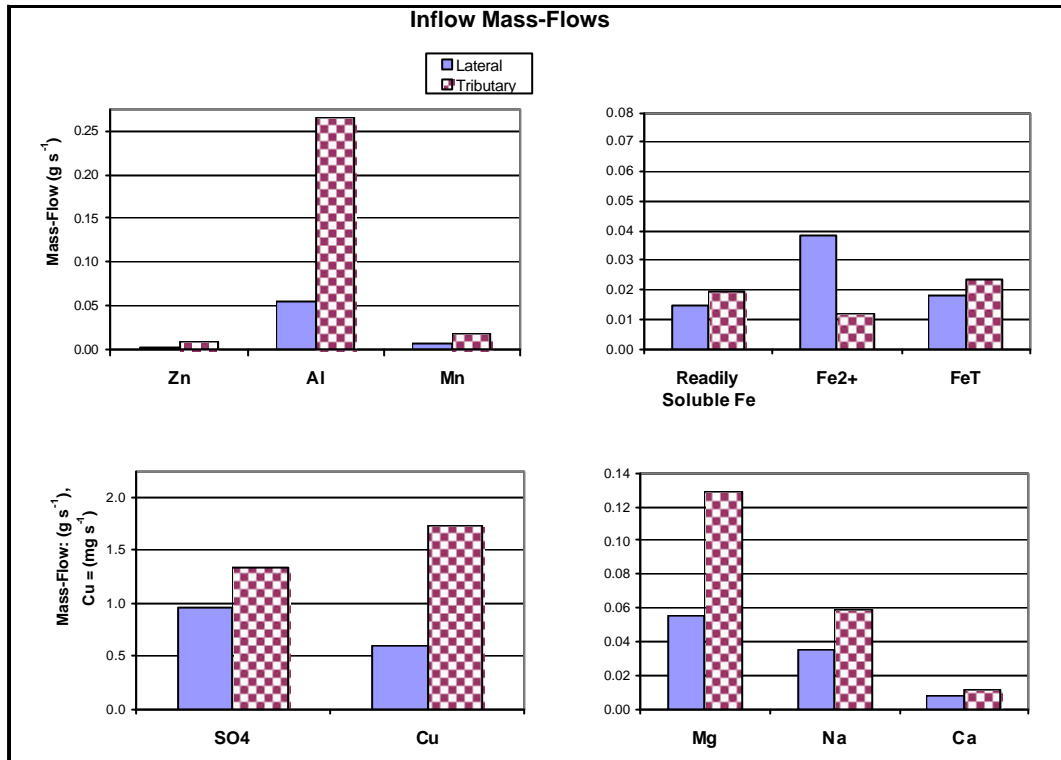
FIGURE 4.12: Inflows between sites 2085 and 2210 m (Trib 2095 m), upper Snake River diel study

4.2 - Snake River Synoptic Study

Discharge data for the study area is shown in figure 4.13. Snake River flows increased from 0.1 to 0.4 m^3 s^{-1} just before the Peru Creek confluence. A large increase to 1.4 m^3 s^{-1} occurred below the confluence followed by decreases until the river was joined by its North Fork. Flows in Peru Creek increased from 0.1 m^3 s^{-1} above the Pennsylvania Mine to a maximum value of 0.6 m^3 s^{-1} just below Chihuahua Gulch. Streamflow then decreased down to the Snake River confluence.
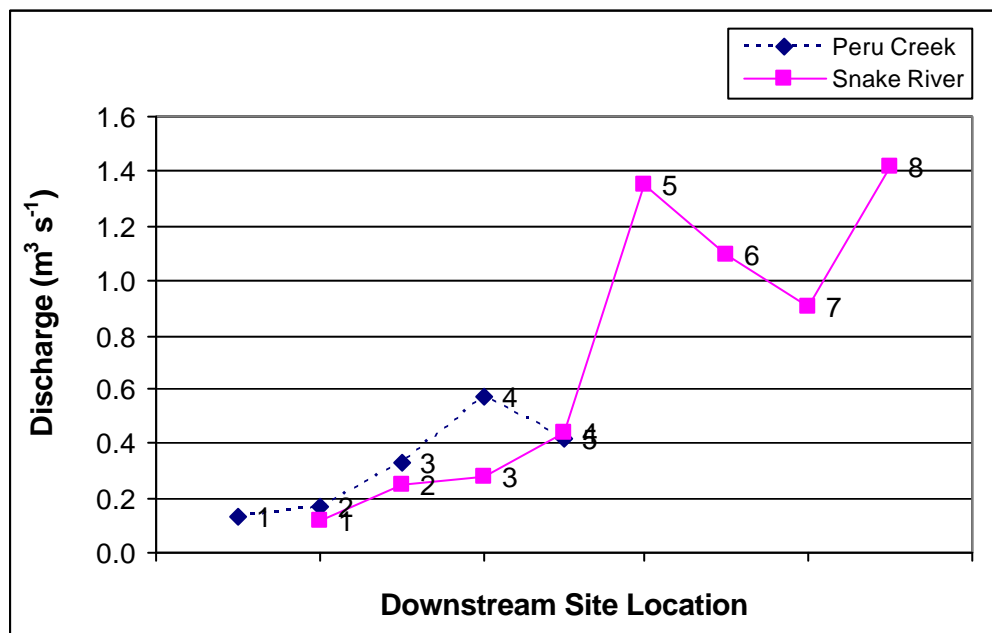
FIGURE 4.13: August discharge in the Snake River and Peru Creek, Snake River Watershed synoptic study. Site locations refer to figure 3.7.

Figure 4.14 represents incoming flows in the vicinity of the sampled confluences as well as reaches of stream where no tributaries were sampled for the months of July and August. Differences between gaining and losing reaches can be observed in the longitudinal direction as well as between months. Discharge data was

not collected at most Peru Creek sites in July. Lateral losses were observed in July in the Deer Creek confluence zone. Lateral gains were then experienced between sites SN2 and SN4. Water was lost to the subsurface in the vicinity of the Peru Creek confluence. No lateral inflows were present between sites SN5 and SN6 and lateral losses were seen between sites SN6 and SN7. Lateral gains are visible in the North Fork confluence zone. In August, nearly equal amounts of water flowed into the stream in the Pennsylvania Mine discharge as did laterally. Lateral gains continued below this confluence between sites PR2 and PR3. Losses occurred in the vicinity of Chihuahua Gulch and further downstream to PR5. On the Snake River lateral gains were experienced at the Deer Creek confluence. Lateral gains continued between sites SN2 and SN4 as well as in the Peru Creek confluence zones. Lateral loses occurred between sites SN5 and SN7 with lateral gains in the vicinity of the North Fork confluence.
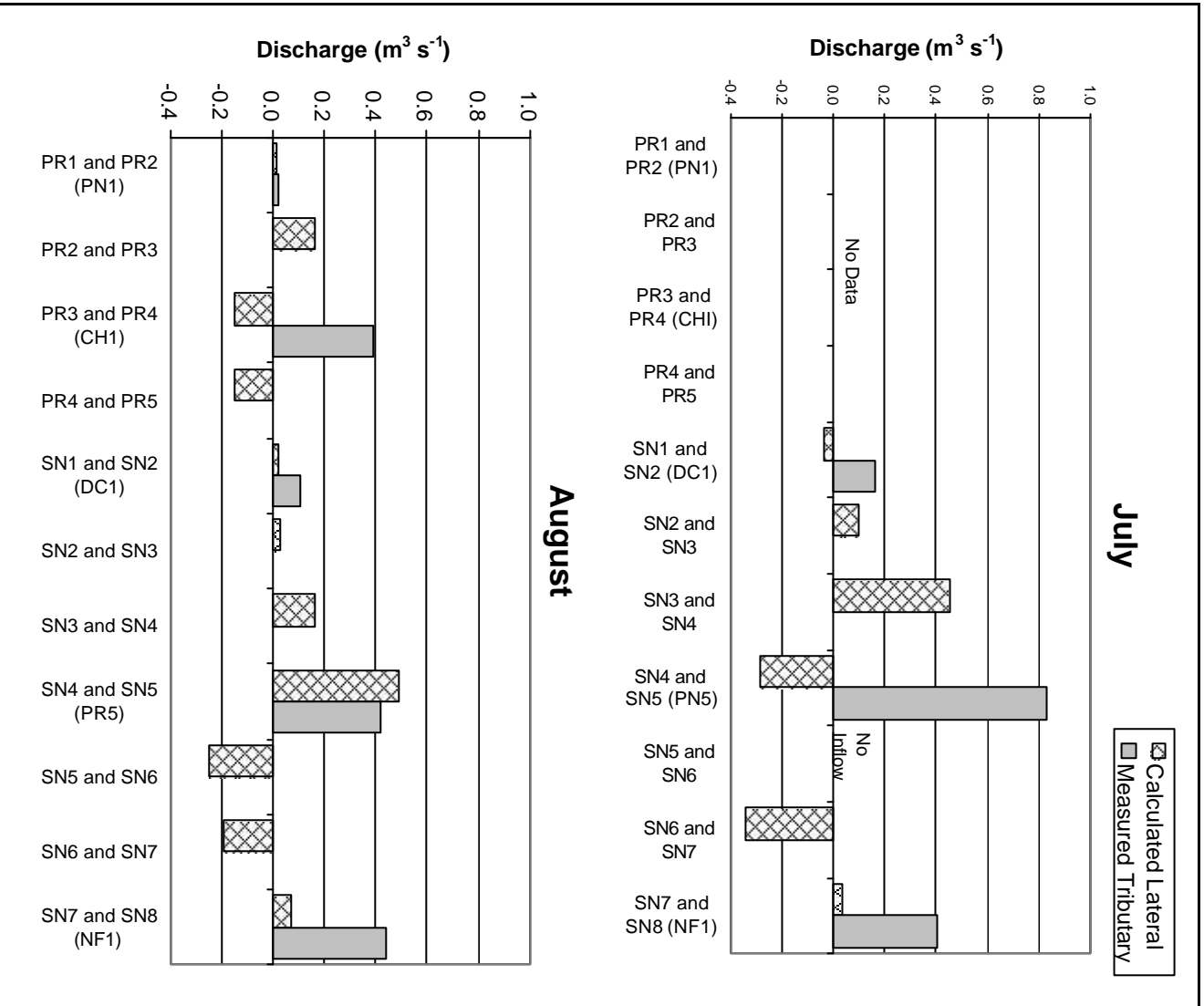
FIGURE 4.14: Lateral and tributary inflows, Snake River Watershed synoptic study

53

Because of variations in lateral inflows in July and August and the Peru Creek's importance as a source of metals and acidity to the Snake River, additional flow data for the Peru Creek and Snake River confluence was solicited from members of the Snake River Task Force and other sources. Figure 4.15 presents data from the United States Geological Survey (USGS) and the Environmental Protection Agency (EPA) for September and December of 2001. Small lateral gains were seen in the September data while small lateral losses were present in October. Figure 4.16 contains cumulative precipitation data for the months of May – October 2000 in Dillon, Colorado (where the Snake River terminates). Precipitation in August, when lateral inflows were more prevalent, was greater than in any other month.

Figure 4.17 shows selected metal concentrations and mass-flows in various tributaries and at points along the Snake River and Peru Creek. Concentrations were noticeably higher in Pennsylvania Mine drainage than at any other sampling point. The mine also had the highest mass-flows for Fe^{2+}, Zn and Mn. In contrast, Al mass-flows were highest in the upper Snake River. Interestingly, Zn and Mn mass-flows decrease only slightly between the Pennsylvania Mine and the downstream Peru Creek site while Fe^{2+} and Al concentrations decreased substantially.
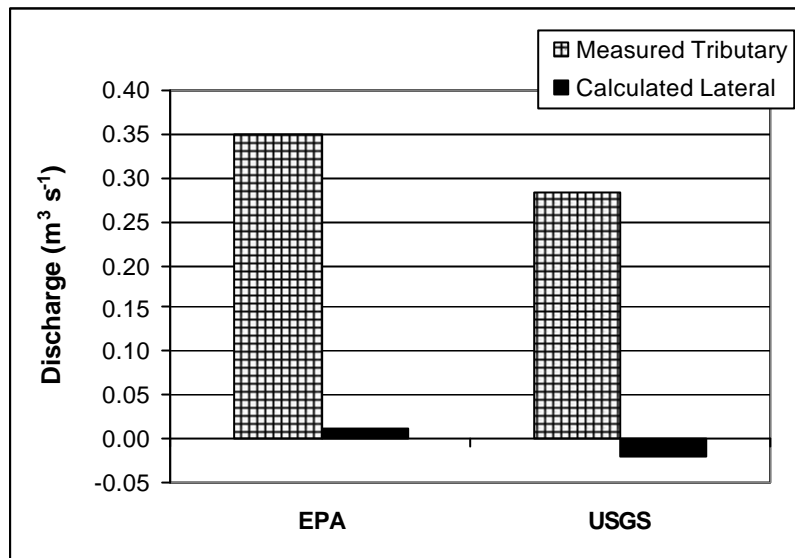
FIGURE 4.15: Additional discharge data for the Snake River and Peru Creek confluence. EPA data was collected on September 26, 2001. U.S. Geological Data was collected over two days, October 10 and 11, 2001 (USGS, 2001; EPA, 2001)
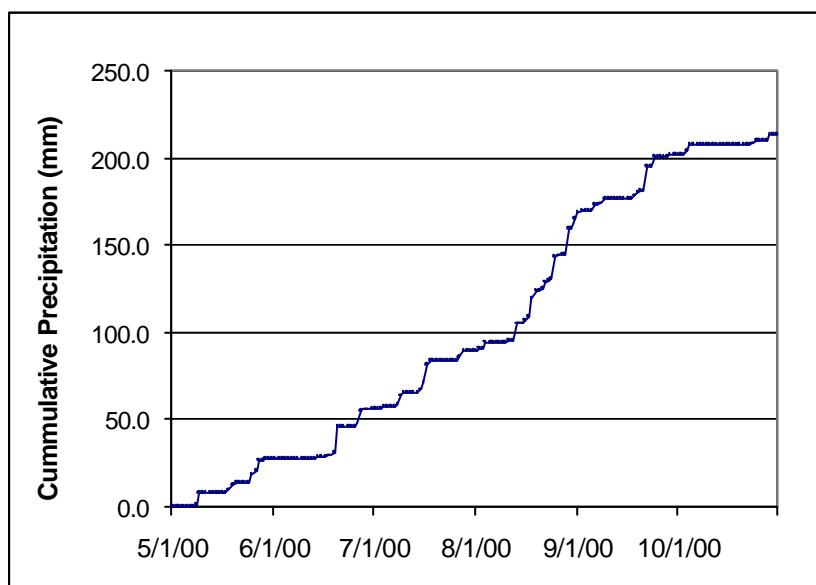
FIGURE 4.16: Cumulative precipitation from May – October 2000 for Dillon, Colorado (Colorado Climate Center, 2002)
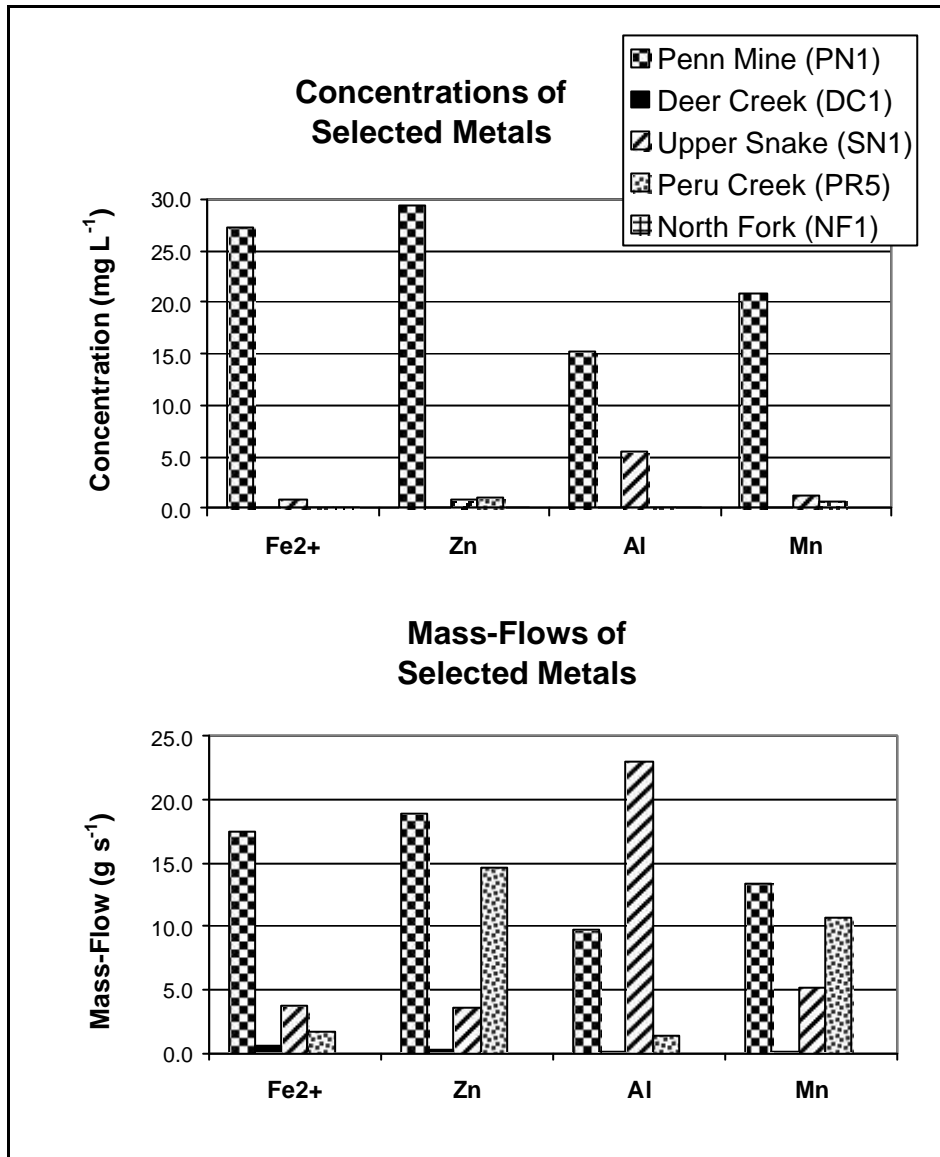
FIGURE 4.17: August selected tributary data, Snake River Watershed synoptic study

Considering stream chemistry, the pH (Fig. 4.18) in the Snake River increased in the downstream direction from an initial value of 4.1 just above the Deer Creek confluence. A decrease from 6.9 to 6.4 was apparent below the Peru Creek confluence as the slightly more acidic Peru Creek waters flowed in. Neutral values were achieved by the most downstream site. In Peru Creek, pH initially decreased as the Pennsylvania Mine drainage entered the stream. Values continued to decrease to just above the Chihuahua Gulch confluence. With this inflow, waters were diluted leading to a pH increase which continued in the downstream direction.
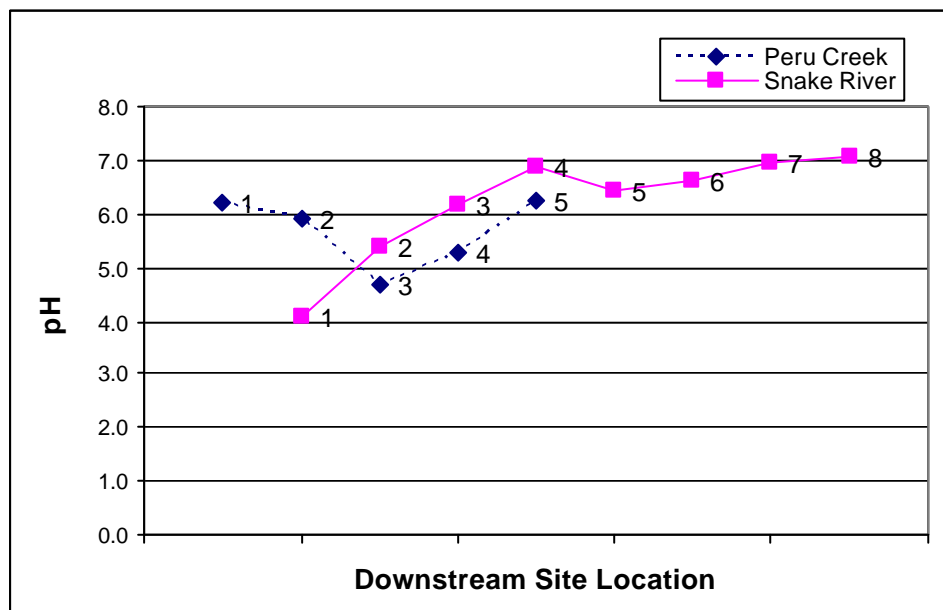
FIGURE 4.18: August pH, Snake River Watershed synoptic study

Longitudinal variations in instream solute concentrations are illustrated in figure 4.19. In general, most concentrations decreased along the Snake River until the Peru Creek inflow when an increase in solute concentrations occurred. Below this point, concentrations again began to decrease. Along Peru Creek, solute concentrations tended to increase until the Chihuahua Gulch confluence where dilution produced decreases. The magnitude of Peru Creek influence on Snake River concentrations depended on the solute. For example, Fe, Al and Mn showed only minor concentration increases below the Peru Creek confluence, while Cu, Pb and Zn concentrations increased more substantially.

It is also useful to look at mass-flows along the study area (Fig. 4.20). Variations between solutes were apparent for mass-flows. SO_4, Zn, Pb, Ca and Mg increased along the Snake River with large increases at the confluence with Peru Creek. Below this confluence, until the North Fork inflow, mass-flows for these solutes decreased. The more reactive metals, Al, Fe and Cu, behaved differently, with mass-flow decreasing along the reach upstream of the Peru Creek confluence. The North Fork appears to be a source of certain solutes, including Ca, Mg, Al, Fe and Pb. Along Peru Creek, mass-flows for most solutes increased until just below the Chihuahua Gulch confluence (PR4) at which point they began decreasing. This was different from concentration profiles which tended to reach their highest values at site PR3 which is immediately above the confluence.
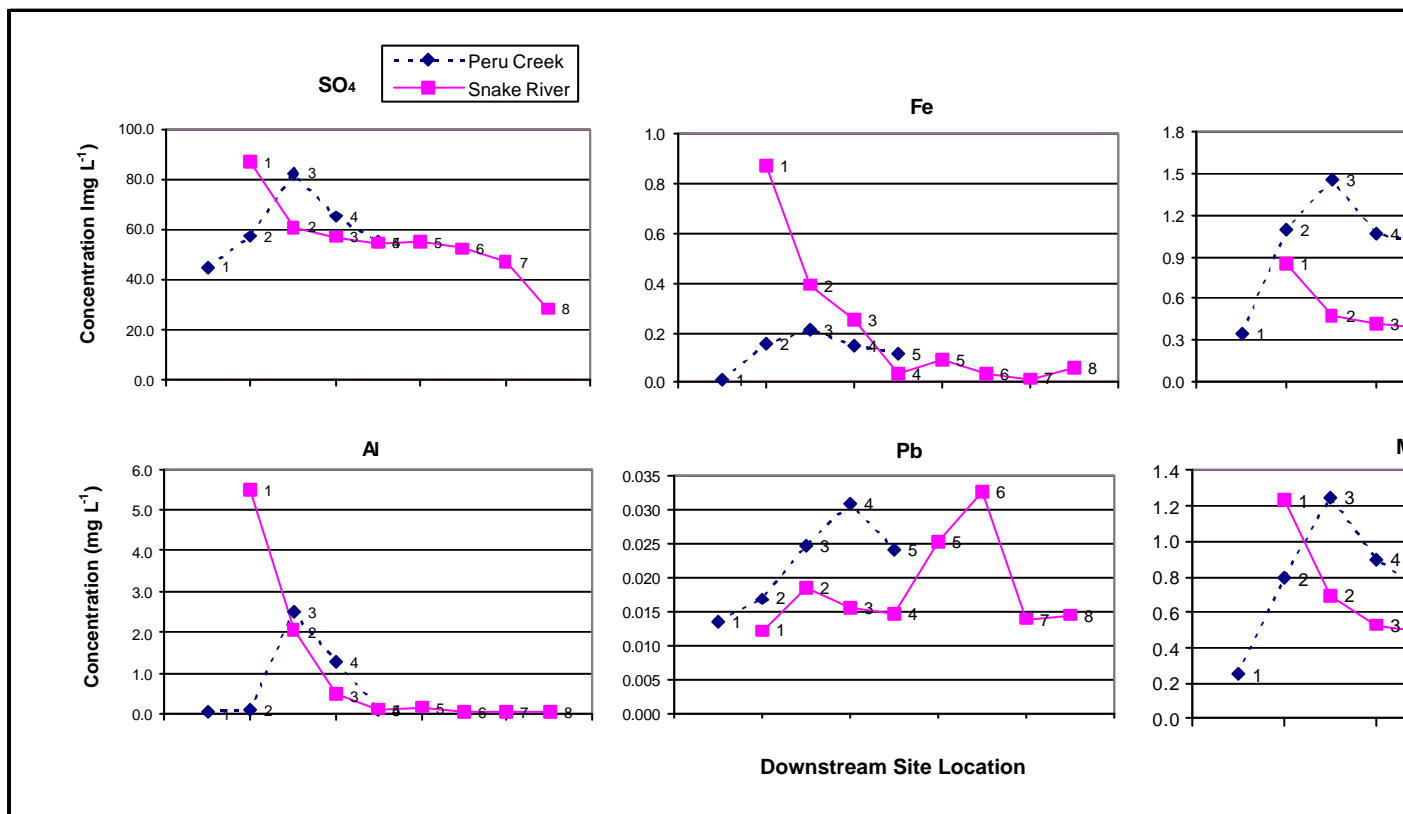
FIGURE 4.19: August instream solute concentrations, Snake River Watershed synoptic study. All concentratio[ns]... for Cu concentrations which are in units of μg L-1.
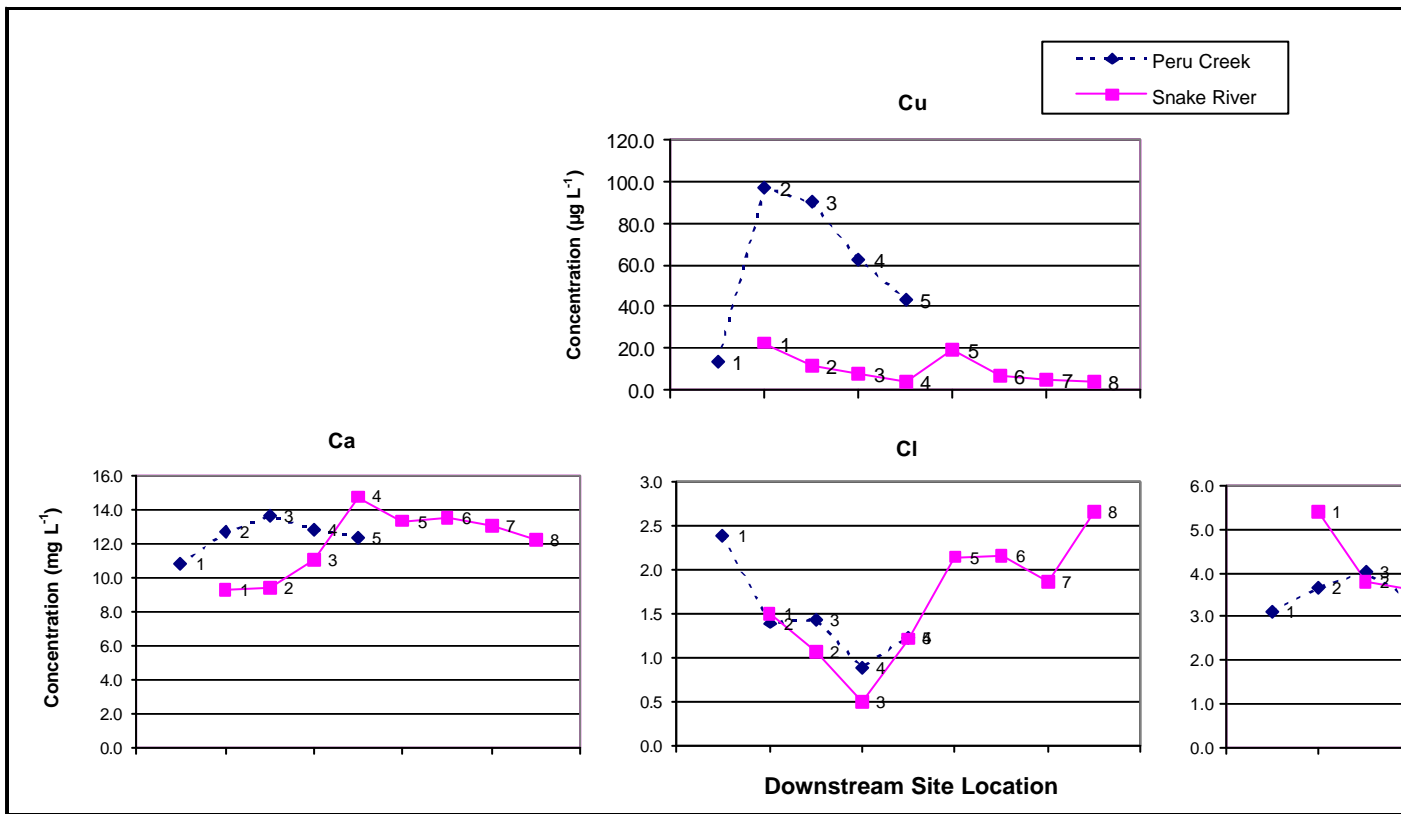
FIGURE 4.19: August instream solute concentrations, Snake River Watershed synoptic study. All concentratio
for Cu concentrations which are in units of μg L-1.
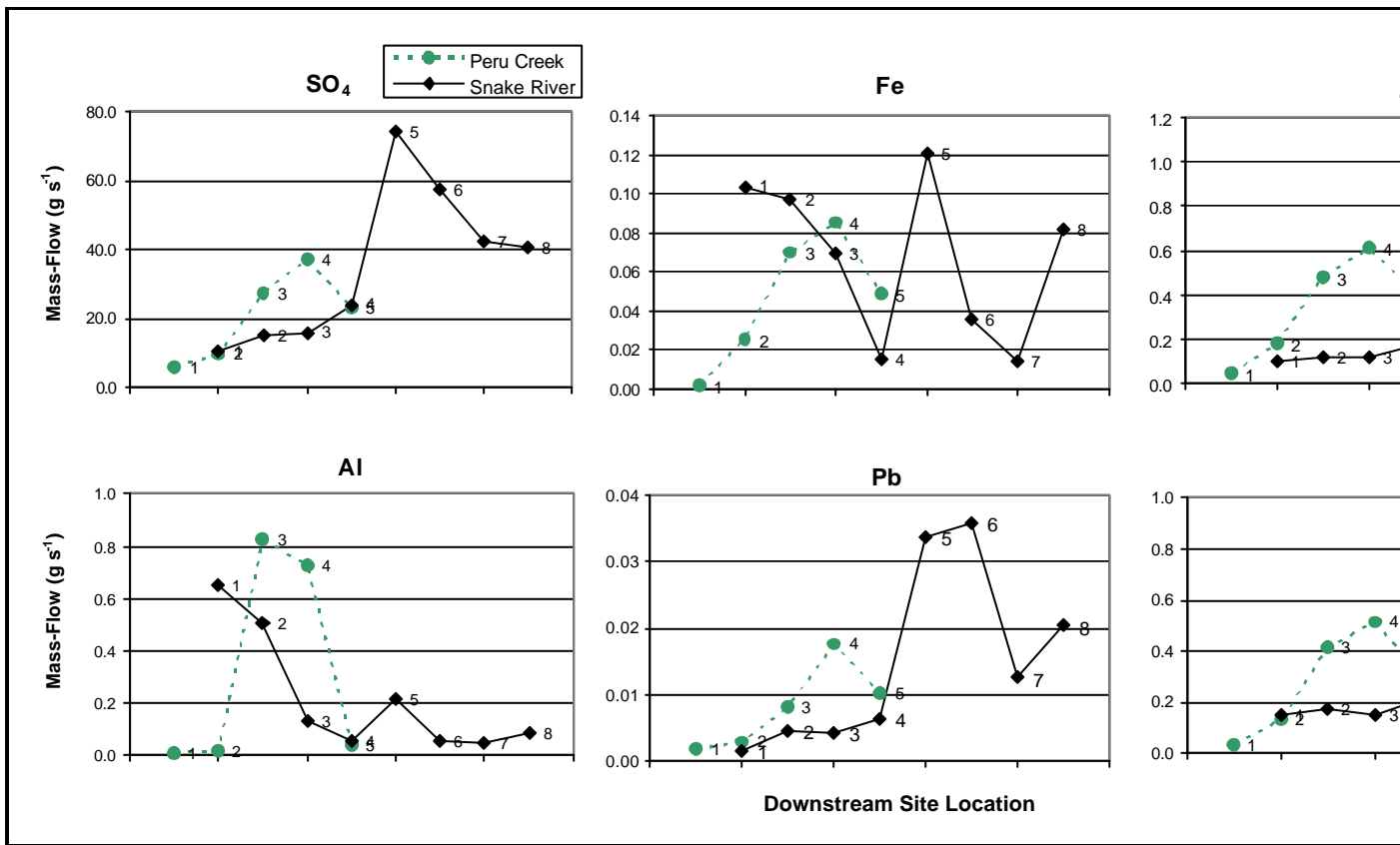
FIGURE 4.20: August instream mass-flows, Snake River Watershed synoptic study. All Mass-flows are in g s -1
mg s -1

**FIGURE 4.20: August instream mass-flows, Snake River Watershed synoptic study. All Mass-flows are in g s -1
mg s -1**

Confluence zones are reactive and can have a large influence on stream concentrations. Figures 4.21 through 4.23 present detailed concentration and mass-flow data for confluence zones. The most striking results were in Peru Creek where the Pennsylvania Mine drainage enters the stream. At this confluence (Fig. 4.21), lateral/confluence zone mass-flows were calculated to be negative for all solutes. This indicates a loss of solute occurred in the confluence zone between the two upstream sites (PR1 and PN1) and the downstream site (PR2). At the confluence of the Snake River and Deer Creek (Fig. 4.22), concentration patterns varied greatly between solutes with SO_4 showing lateral concentrations an order of magnitude greater than Deer Creek concentrations. Only Zn and Mn exhibited behavior similar to sulfate. Fe, Al and Cu to a lesser extent, showed losses (seen as negative lateral mass-flows) as the circumneutral waters of Deer Creek raised the pH from a value of 4.1 to 5.4 in a mater of meters. At the confluence of the Snake River and Peru Creek (Fig. 4.23), the chemical composition of subsurface and tributary waters was similar. Lateral mass-flows were equal or greater than tributary (Peru Creek) for most solutes as more flow was calculated to be entering the stream through the subsurface. Only Zn and Cu had higher tributary mass-flows.

Mass-Flow

Concentration
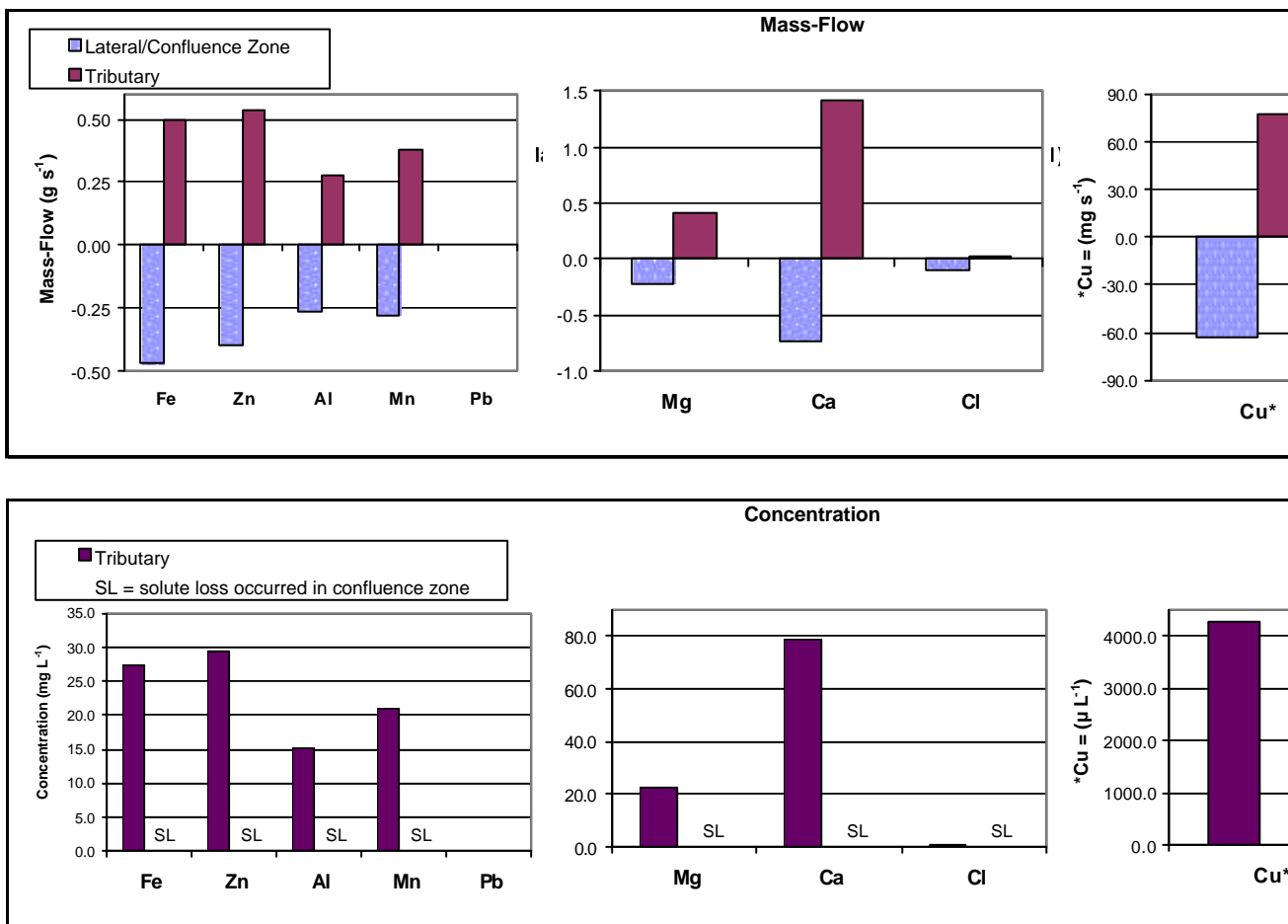
FIGURE 4.21: August inflows between sites PR1 and PR2 (Trib PN1), Snake River Watershed synoptic

Mass-Flow

- Lateral/Confluence Zone
- Tributary

Mass-Flow (g s^{-1})

-0.01	
-0.06	
-0.11	
-0.16	

Fe Zn Al Mn Pb

1.0	
0.8	
0.5	
0.3	
0.0	

Mg Ca Cl

*Cu = (mg s^{-1})

4.0
3.0
2.0
1.0
0.0
-1.0

Cu*

Concentration

- Lateral
- Tributary
- SL = solute loss occurred in confluence zone

Concentration (mg L^{-1})

1.0
0.8
0.5
0.3
0.0

SL Fe Zn SL Al Mn Pb

10.0
8.0
6.0
4.0
2.0
0.0

Mg Ca Cl

*Cu = (µ L-1)

160.0
120.0
80.0
40.0
0.0

SL

Cu*
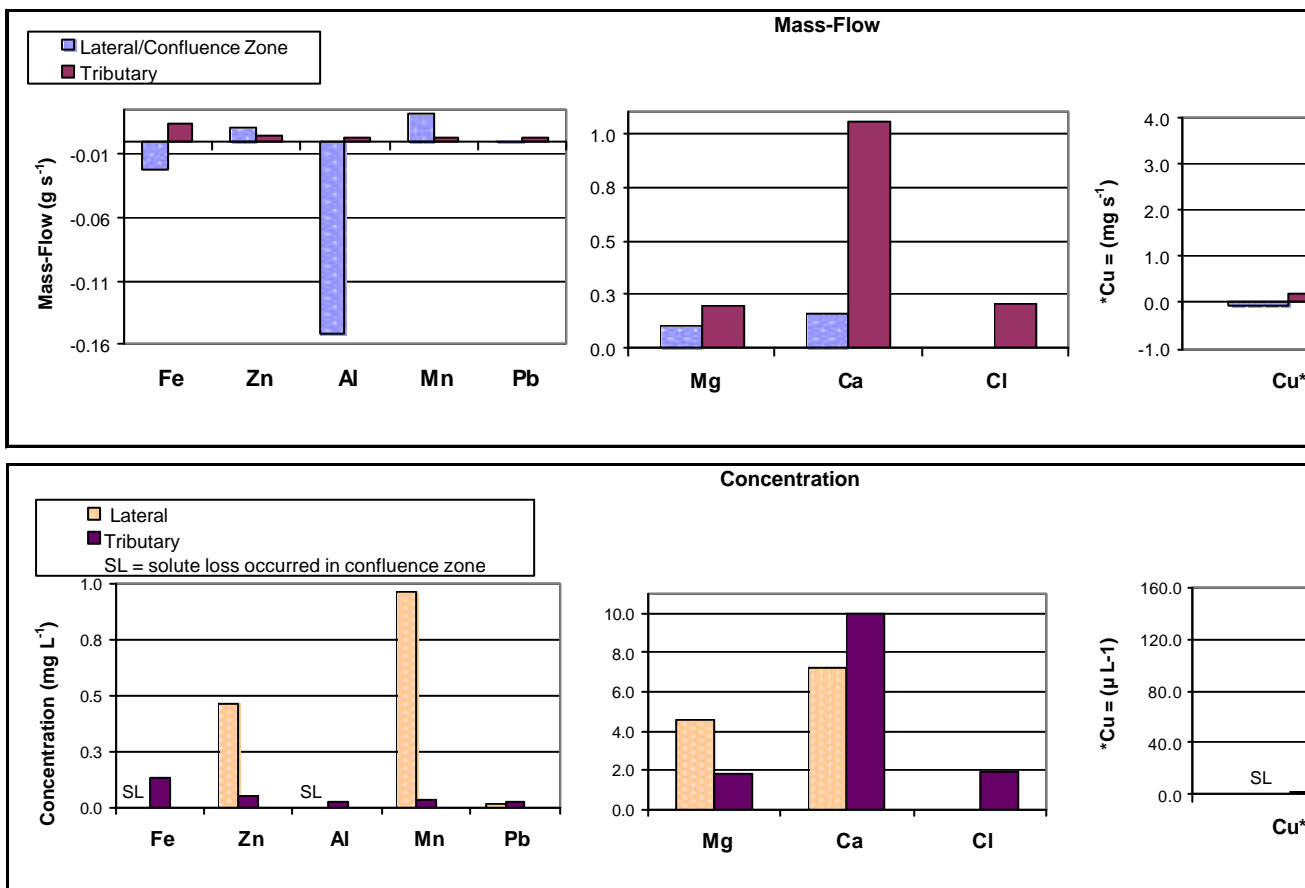
FIGURE 4.22: August inflows between sites SN1 and SN2 (Trib DC1), Snake River Watershed synoptic

Mass-Flow

Concentration
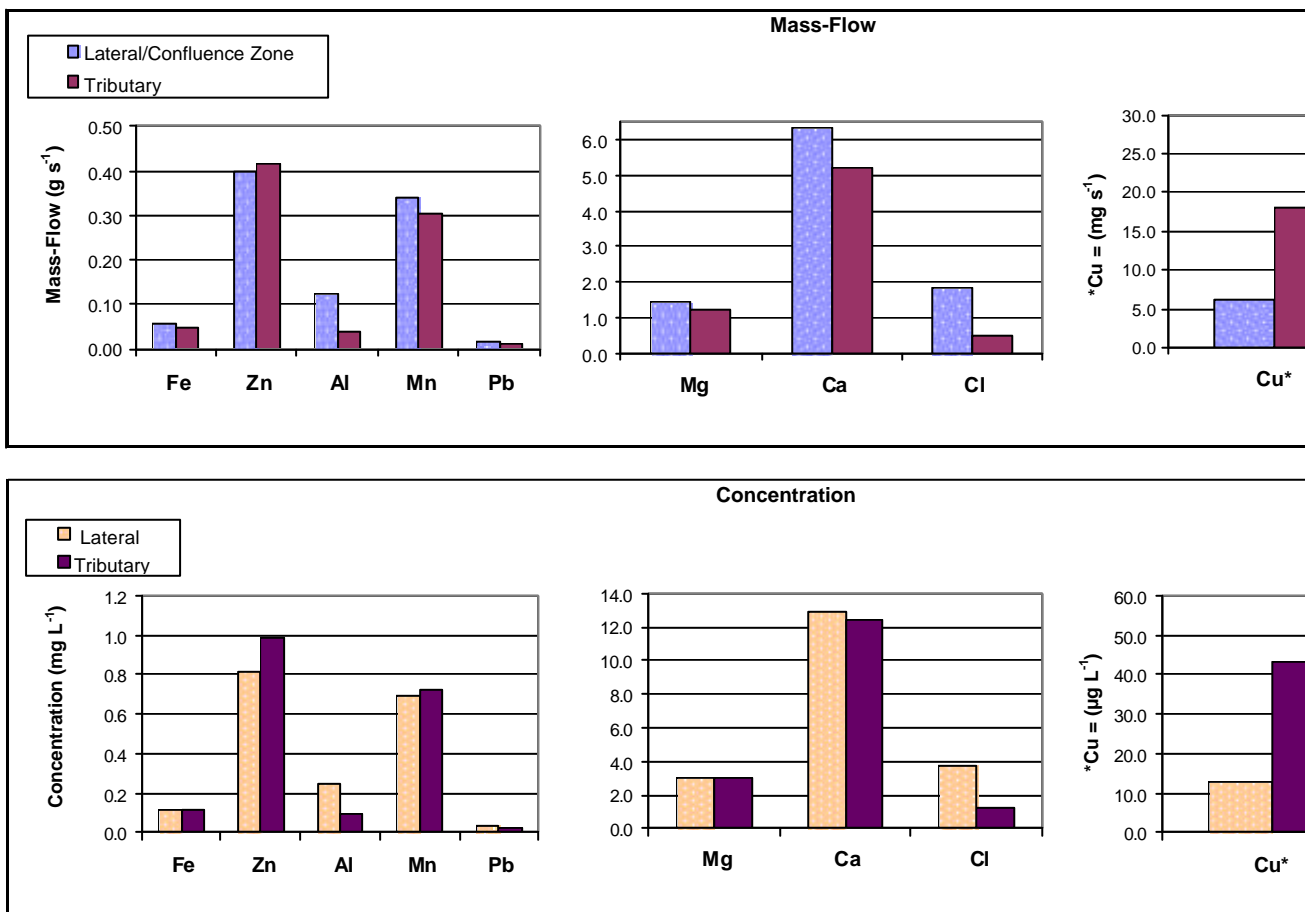
FIGURE 4.23: August inflows between sites SN4 and SN5 (Trib PR5), Snake River Watershed synoptic s

In addition to confluence zones, lateral mass-flows were calculated for the reaches of stream where no tributaries were measured. Mass-flows were not calculated for losing reaches. Results (Fig. 4.24) show that Al, Fe and Cu (and Mn to a lesser extent) were lost from the stream water column for several kilometers below the Deer Creek confluence (from sites SN2 to SN4). Other solutes showed positive lateral mass-flows along the same reach. On Peru Creek, metals continued to enter the stream laterally downstream of the mine inflow and above Chihuahua Gulch as evidenced by positive mass-flows for all solutes.
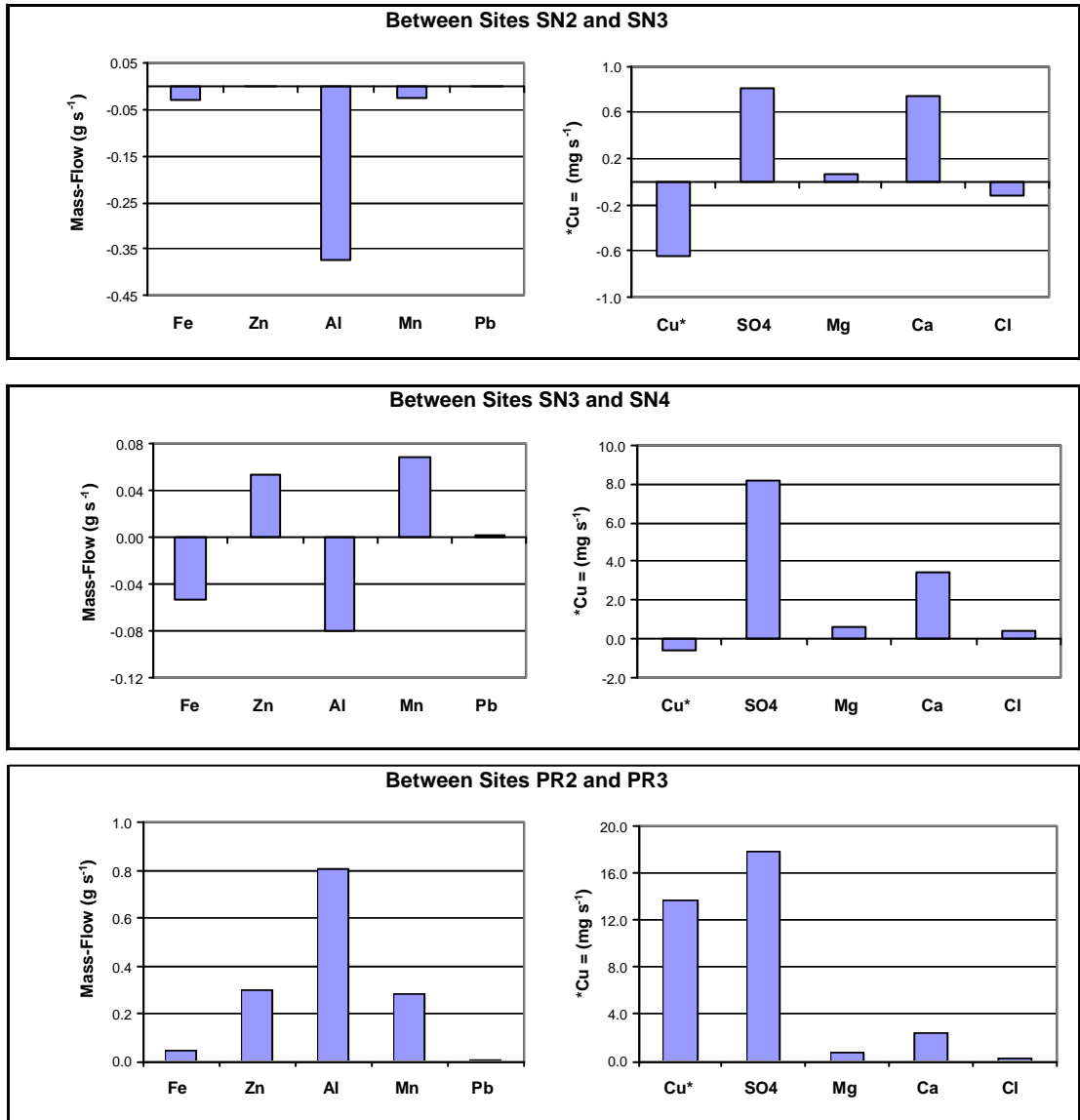
FIGURE 4.24: August stream reach lateral mass-flows, Snake River Watershed synoptic study

4.2.1 - Composition and Extent of Metal Oxide Deposition

Oxide deposition was prevalent throughout the Snake River Watershed. Figure 4.25 presents Fe and Al oxide data for July and August and reveals the presence of oxides at all stream sampling sites. Looking at Fe values, the formation of Fe oxides for July in Peru Creek began at the most upstream site, increased below the Pennsylvania Mine drainage and peaked above the Chihuahua Gulch inflow before tapering off. In the Snake River, July Fe deposition was nominal in the vicinity of the Deer Creek confluence. Deposition increased at site SN3 before gradually decreasing at sites SN4 and SN5. Another zone of significant Fe oxide deposition occurred in July at site SN6. Deposition decreased downstream of this site. August values represent one month of deposition so tended to be smaller than in July. Fe oxide deposition in August was similar in Peru Creek to July, with a peak at site PR3 above the Chihuahua Gulch confluence and decreases downstream. The profile of Fe oxides in the Snake River showed more precipitation of Fe at upstream sites (above and below the Deer Creek confluence) with less deposition downstream than in July. Again, site SN6 was a second area of increased deposition. In both months, the greatest Fe deposition was found in Peru Creek at site PR3.

Examining Al oxide data, deposition in July in Peru Creek began at the uppermost site, increased immediately below the Pennsylvania Mine drainage, and decreased greatly at site PR3. A second significant zone of Al oxide deposition was just below the Chihuahua Gulch inflow. Much less Al oxide deposition was sampled downstream at site PR5. In the Snake River, July Al deposition was minimal above Deer Creek with the greatest area of deposition just below the Deer Creek confluence.

Al oxides decreased to site SN4 and began increasing at sites SN5 and SN6. The two lowest sites had much less deposition. A similar profile for Al oxides was observed in August. In Peru Creek deposition was present above the Pennsylvania Mine drainage and increased below this point. Deposition was much less immediately above the Chihuahua Gulch confluence and a large increase occurred below this inflow. At site PR5 Al deposition was present but in lesser amounts. In the Snake River deposition was greatest below the Deer Creek confluence with significant decreases below this point. Increased deposition was present at sites SN5 and SN6. In both months, Site PR4 immediately below the Chihuahua Gulch confluence was the region of the greatest Al oxide deposition followed by SN2 just below the Deer Creek inflow.
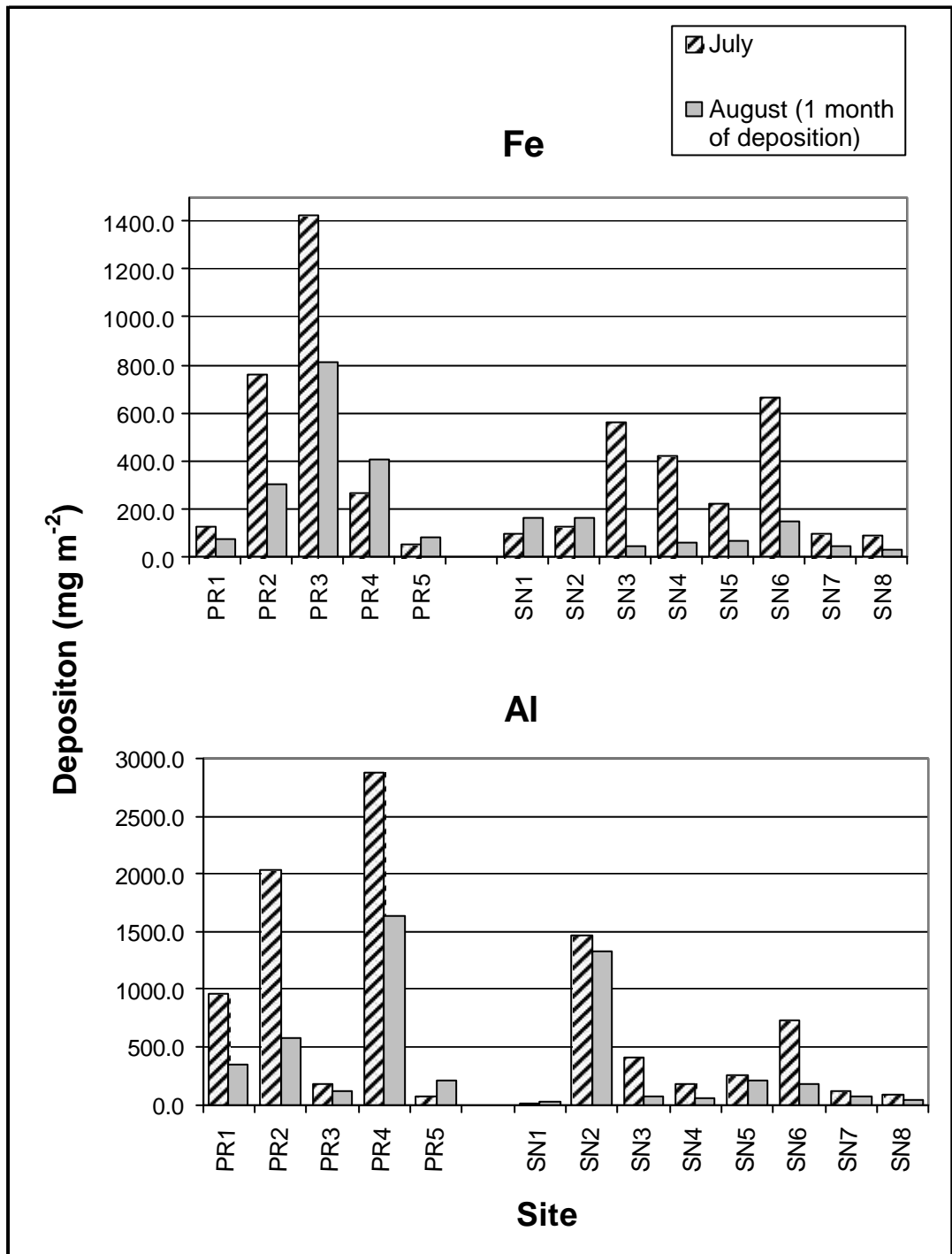
Figure 4.25: Fe and Al oxide deposition, Snake River Watershed synoptic study

4.2.2 - Periphyton Presence and Biomass

Biologic samples were collected for periphyton. Data revealed sparse populations throughout the entire study area (table 4.1). It is interesting to compare periphyton biomass in the Snake River to biomass in other Rocky Mountain streams. Table 4.2 (Niyogi, 1999) presents data from approximately 45 streams. The lowest median biomass by far, 0.3 mg chl a m^{-2}, was found in sites with a preponderance of Al oxides. Most other sites had values more than one to two orders of magnitude greater. Values at all sites in Watershed were 0.36 mg chl a m^{-2} or less.

Table 4.1: Periphyton biomass, Snake River Watershed synoptic study

	Range chl a (mg m^{-2})
JULY	
Peru	0.01 - 0.25
Snake	0.00 - 0.36
AUGUST	
Peru	0.00 - 0.24
Snake	0.00 - 0.25

Table 4.2: Biomass and common taxa of primary producers at five classes of sites. Table from Effects of stress from mine drainage on ecosystem functions in Rocky Mountain streams, Dev Kumar Niyogi, 1999, PhD thesis, University of Colorado.

Site Description	Median Biomass chl a (mg m^{-2})	Range chl a (mg m^{-2})
Pristine sites	27	6 – 119
Sites with only high Zn	75	4 – 94
Sites with low pH, high Zn, low metal oxide deposition	85	12 – 145
Sites with iron oxide deposition	17	0.1 – 110
Sites with aluminum oxide deposition	0.3	0.1 – 6.2

Figure 4.26 illustrates longitudinal periphyton variations for July and August. On Peru Creek, a decrease occurred below the mine drainage in both months with a rebound in biomass in the region above Chihuahua Gulch. Biomass decreased sharply immediately below the Chihuahua Gulch confluence. In July increases were seen between sites PR4 and PR5 while decreases were present in August. On the Snake River differences between months occurred throughout the system. In July, for example, biomass increased below the Deer Creek confluence while a stark decrease occurred in August. Attempts were made to determine the effects of water chemistry and oxide deposition on periphyton communities but very low biomass made these calculations problematic. Numerous relationships were plotted with only one displaying an acceptable level of correlation ($R^2 = 0.39$). In figure 4.27, a negative relationship is seen between chlorophyll *a* and the percentage of Al by mass in deposited oxides.
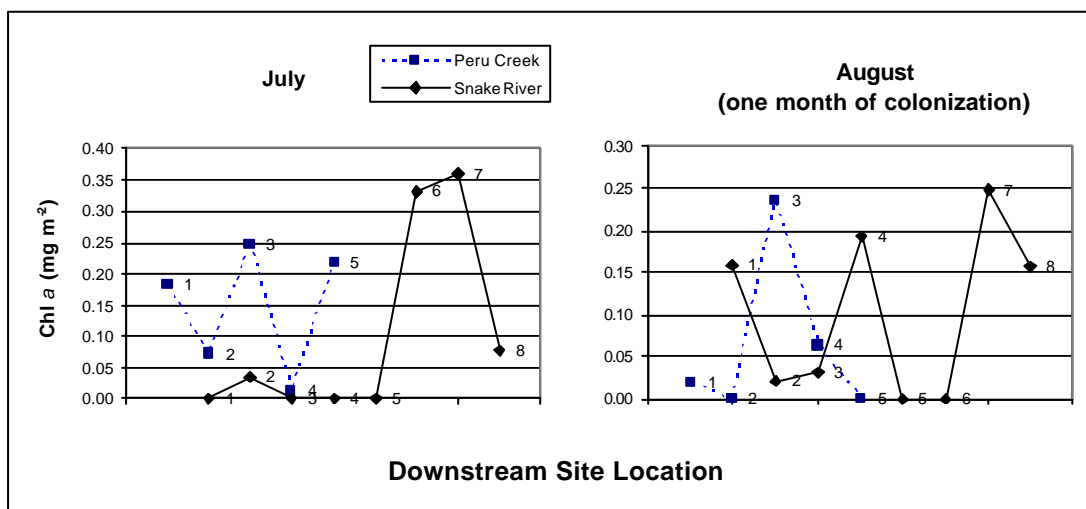
FIGURE 4.6: Periphyton biomass, Snake River Watershed synoptic study
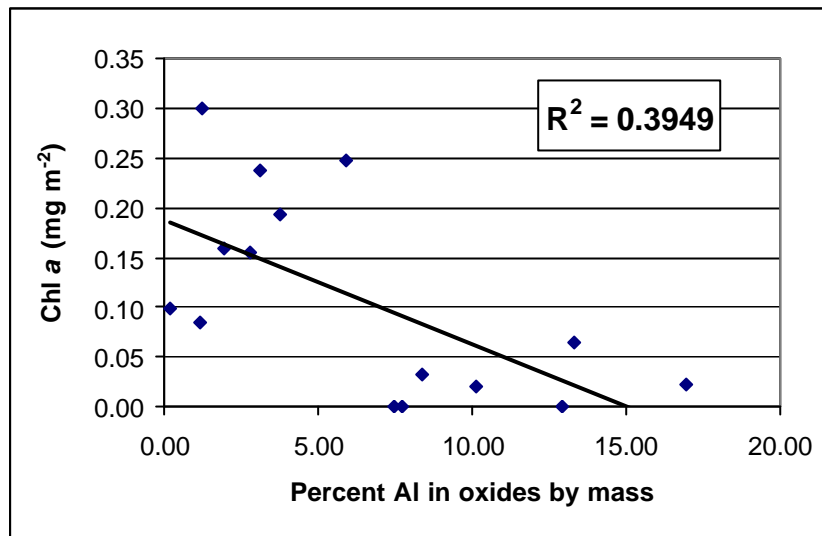
FIGURE 4.27: Relationship between chlorophyll *a* and Al oxides, Snake River Watershed synoptic study

Rates of oxide deposition were determined (Fig. 4.28) using August oxide data which represents one month of deposition. Looking at the sites with the most deposition (PR3 for Fe and PR4 for Al), approximately half the mass that was present on the rocks in July had accumulated in one month. Rates of Fe oxide deposition ranged from 1.2 to 27.9 mg m^{-2} d^{-1}, depending on the site. Rates of Al oxide deposition ranged from 1.1 to 56.5 mg m^{-2} d^{-1}. The rapid deposition of a large mass of Al oxides at numerous sites throughout the basin is of concern as the presence of Al oxides appears to be extremely detrimental to periphyton communities.
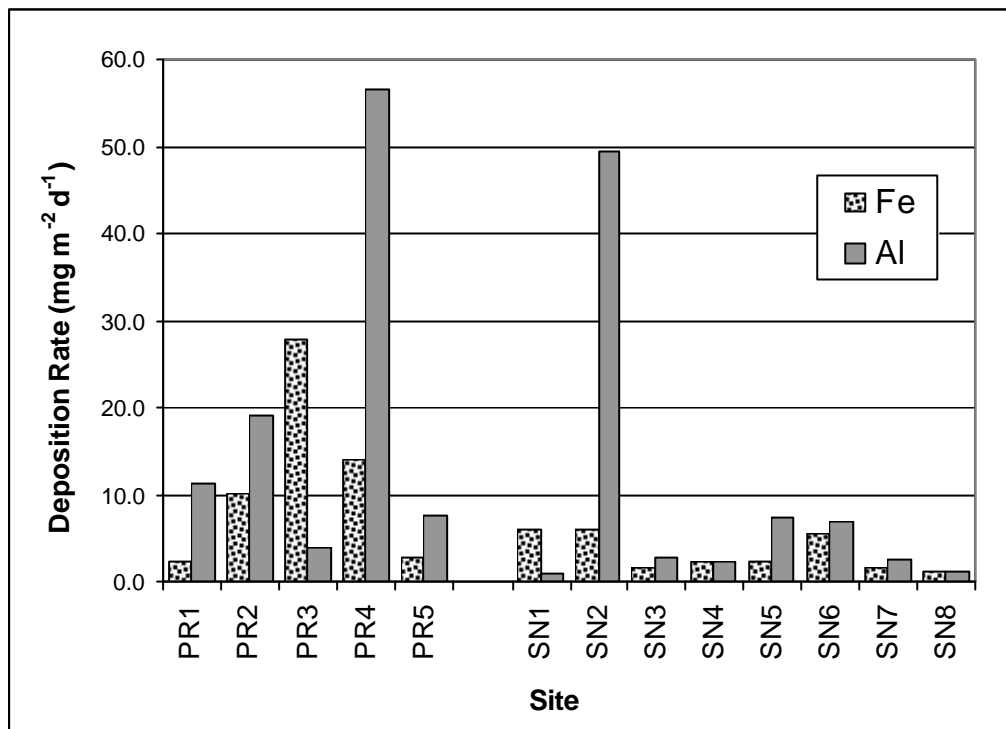
FIGURE 4.28: Oxide deposition rates from one month of deposition, Snake River Watershed synoptic study

CHAPTER V

DISCUSSION

5.1 - Upper Snake River Diel Study

Upper Snake River diel study results provide a glimpse of the sources and effects of the natural weathering of disseminated pyrite in this headwater basin. Tributary concentrations and mass-flows reveal that the eastern basin is the primary source of metals and acidity to the upper Snake River. This result is significant as the few mines that are present are located along the western basin (Wilson and LaRock, 1992). The low pH and high metal concentrations in the upper Snake River have a natural, not anthropogenic, source. The region's geology (Fig. 3.2) supports this finding. A bog iron ore deposit, an indication of pyrite weathering under a previous hydrologic regime, extends upland from the riparian zone in the eastern side of the basin. The Idaho Springs Formation to the east of this deposit is the source of ARD.

The flow paths that water takes before arriving in the stream are of great interest because of the disseminated nature of ARD in the upper Snake River. The weathering of pyrite occurs throughout the eastern basin, rather than at specific abandoned mine sites. Accordingly, as water flows through soils there is increased contact with source rock and subsequent weathering. Results show lateral inflows to be a significant source of solutes along most of the study area. Several stretches of

losing reach were also present. The majority of lateral flow entered the stream in the vicinity of eastern confluence zones with subsurface flows being focused in a narrow zone similarly to surface waters. Confluence zones in the upper Snake River are therefore critical in the conveyance of metals and acidity to streams with a large percent of their flow entering unseen through the subsurface. Lateral inflows comprised the majority of flow at the most upstream confluence and decreased in importance in the downstream direction.

Lateral inflows were important sources of metals and acidity to the Snake River, accounting for more than half of mass-flows at several confluences. Discharge appeared to be a predominant factor in determining whether lateral or tributary inflows were the primary source of metals to the stream. For several metals, subsurface concentrations were estimated to be lower than tributary concentrations, but high lateral discharge generated greater mass-flows. At the middle confluence, lateral flows were slightly greater as were lateral mass-flows, though concentrations were approximately equal for most solutes. At the most downstream confluence more water and mass-flow entered the stream through the tributary. This tight relationship between mass-flow and discharge is likely a result of the constant, distributed nature of pyrite in the upper Snake River basin.

The chemical composition of tributary water was often very different from that of subsurface water. This result indicates that the sampling of surface water only can be misleading, overlooking a potentially large and varied source of ARD as solutes in subsurface waters have the opportunity to react more intensely with rock,

soils, sediments and other solutes. Metal loading calculations must take lateral discharge as well as solute concentration into consideration.

Examining instream chemistry, longitudinal results revealed that SO_4 concentrations and pH achieved constant values by the third stream site. In the process of pyrite weathering, H^+ and SO_4 are released in proportion to one another. This relationship was maintained throughout the study reach suggesting that sulfate was behaving relatively conservatively and could be useful as an ambient tracer in these headwaters. Concentrations of all metals, with the exception of Fe, increased in the downstream direction. Decreasing Fe concentrations were most likely evidence of the formation of iron oxides. Equilibrium controls may prevent Fe^{2+} from accumulating at concentrations above 1.4 mg L^{-1} (Runkel et al., 1996).

Diel variations were apparent only for Fe and Cu, the probable result of iron oxide formation and photochemistry. Fe reactions may drive Cu concentrations through co-precipitation and sorption to oxides and suspended colloids and release during mid-day photoreduction. It is important to consider how concentrations may fluctuate during the day when sampling. For example, Fe^{2+} and Cu concentrations exceeded aquatic life toxicity standards during only part of the day at several sites (table 5.2). Neglecting these variations could lead to a mischaracterization of stream waters regarding their impact on stream biota. Brick and Moore (1996) found evidence of diel cycles in an ARD affected stream in dissolved Mn and Zn and particulate Al, Fe, Mn, Cu and Zn. Variations were related to several factors including changes in pH and dissolved oxygen, redox reactions in sediments, an influx of hyporheic waters, and a general increase in total suspended matter seen

during nighttime hours. Brick and Moore (1996) noted the importance of these variations to monitoring and assessment. Sullivan and Drever (2001a) also report diel variations in solutes related to seasonal variations in snowmelt, with most solute concentrations increasing as snowmelt diminished, as well as instream processes. Sullivan and Drever (2001a) found hydrologic, photochemical and biological processes to be important on the diel timescale, producing daily concentration variations of up to 40%.

5.2 - Snake River Watershed Synoptic Study

Discharge data revealed gaining and losing reaches on both the Snake River and Peru Creek with variations seen between months at the Deer Creek and Peru Creek confluences. This is of interest particularly at the Peru Creek confluence which showed large differences in lateral flows between months and is a primary source of ARD to the Snake River. Additional data secured from the EPA and USGS also revealed differences in lateral flows, with the confluence losing in October and gaining in September. In both these studies the amount of lateral flow was minimal as flows were in or approaching base flow conditions. This data suggests that lateral inflows fluctuate in importance throughout the year at this confluence and other locations in the basin. The Snake River synoptic study captured a late season pulse of lateral discharge resulting from a month of above average precipitation, as seen in figure 4.16. Increased runoff is also apparent in the small, secondary peak in discharge visible in the 2000 hydrograph (Fig. 2.1) for late August. To better understand the timing, magnitude and chemical composition of lateral flows in this

region, more monitoring of the confluence and upstream areas is suggested, especially as remediation options and their impacts are considered.

Lateral inflows are also of great interest in the vicinity of the Pennsylvania Mine on Peru Creek. In August, mine drainage discharge was only slightly greater than calculated lateral inflows between sites PR1 and PR2 with additional lateral inflows calculated downstream. A visible inspection of the Pennsylvania Mine and Cinnamon Gulch region provides evidence of the extent of lateral inflows with visible seeps present along much of the reach. Figure 5.1, shows the region downstream of the Pennsylvania Mine inflow. Water can be seen dripping from the stream bank and Fe and Al oxides coat the streambed.
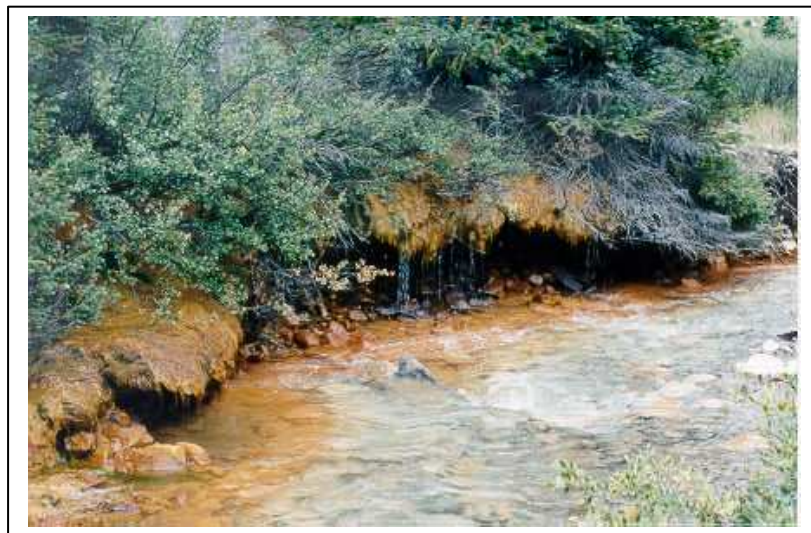
FIGURE 5.1: Peru Creek downstream of the Pennsylvania Mine drainage inflow. Water can be seen dripping from the eroded bank. Fe oxides coat the bank and the edge of the streambed. Al oxide precipitates are present towards the center of the stream.

A second area of interest along Peru Creek is the Chihuahua Gulch confluence zone, calculated to lose some water to the subsurface in August. This is significant as

the two stream waters that meet at this confluence have very different chemistries. Downstream chemistry could be affected depending on what water is lost to the subsurface and if or where it reemerges into the stream.

Figure 4.17 presented concentration and mass-flow data for various tributaries. The Pennsylvania Mine drainage had the highest concentrations and mass-flows for most metals. Al mass-flows were highest at the upper Snake River site, most likely the result of the greater extent of weathering of country rock by acidic subsurface water. In the upper Snake River pyrite weathering and lateral flows occur throughout the eastern basin. Al is a secondary product of pyrite weathering, mobilized as resulting acid interacts with surrounding rocks. The disseminated nature of ARD in the upper Snake allows for more weathering of Al than would be expected to occur at a localized abandoned mine sites.

The formation of oxides and concurrent removal of Fe and Al from the stream column is documented in the large differences between Pennsylvania Mine and downstream Peru Creek mass-flows. Assuming the Pennsylvania Mine is the primary source of ARD to Peru Creek, it is interesting to compare mass-flows in the Pennsylvania Mine drainage to mass-flows at site PR5 further downstream. Zn and Mn mass-flows decreased slightly between these two sites as would be expected for metals behaving relatively conservatively due dilution from pristine inflows including Chihuahua Gulch. In contrast, the difference between Pennsylvania Mine drainage mass-flows and PR5 mass-flows for Fe^{2+} and Al was great. Only a small percentage of original mass-flow remained in the stream column, evidence of loss during upstream oxide formation.

Longitudinal pH and concentration profiles also provide useful information as to the sources and effects of ARD throughout the basin. In general, these results show that the weathering of disseminated pyrite and associated rock in the upper Snake River was a major source of acidity, Al, Fe, Zn, Cu, Mn, SO_4 and Mg to the Snake River. Below this source pH increased and concentrations decreased. Peru Creek was also a major source of metals and acidity to the Snake River, though its importance varied by metal. Zn, Cu and Pb concentrations in the Snake River all increased substantially below this confluence while other metals displayed only slight concentration increases.

Peru Creek concentration data generally reveal that the water in the Pennsylvania Mine drainage channel is an important, but not exclusive, source of ARD. An approximately equal amount of water is known to flow in laterally upstream of PR2 and concentrations continue to increase downstream to Chihuahua Gulch. The dearth of sampling sites along this reach prevents the identification of more specific sources. Much of the ARD may be entering in the vicinity of the Pennsylvania Mine and Chihuahua Gulch or sources may occur along a broader stretch of reach.

The further identification of sources between sites PR2 and PR3 is crucial as the Snake River Task Force begins considering remediation alternatives. Currently, the Pennsylvania Mine drainage is the primary target of such efforts. The results of this study suggest that efforts must extend beyond this drainage or they may neglect much of the contamination which enters the stream.

Longitudinal mass-flow patterns varied somewhat from concentrations. On the Snake River, decreasing mass-flows for Fe, Al and Cu between sites SN1 and SN4 are evidence of oxide formation, co-precipitation and sorption along large stretches of reach. On Peru Creek mass-flow profiles differed from concentration profiles in that increases were seen down to site PR4, just below the Chihuahua Gulch confluence. This is interesting because the Chihuahua Gulch inflow has lower concentrations than Peru Creek (Table A.6). It may be that lateral inflows from the ARD source area continue to contribute metals. It would be interesting to collect several samples at varying distances both above and below this confluence to develop a better definition of stream and tributary waters. Al was the only solute which experienced a decrease in mass-flow between sites PR3 and PR4 due to the precipitation of large amounts of Al oxides.

It is also intriguing to consider the water lost in the Chihuahua Gulch confluence area in relation to the Peru Creek and Snake River confluence. If mass-flows at sites PR5 and SN4 (immediately upstream of the confluence) are summed, they are not sufficient to account for the large increase in metals that occurs at site SN5. However, mass-flows at site PR4 (the next upstream Peru Creek site, just below the Chihuahua Gulch confluence) and SN4 add up more closely to those at SN5. This suggests that some of the water lost in the vicinity of Chihuahua Gulch may be what is reentering the stream laterally at the confluence with the Snake River.

The calculation of lateral concentrations and mass-flows can identify regions of chemical reactivity. At the confluence of Peru Creek and the Pennsylvania Mine drainage, for example, all lateral mass-flows were negative. These negative values

are likely due to major losses in the formation of a massive amount of oxides as well as a lateral loss of metal-rich water from the drainage channel. Oxides coat the streambed at this confluence and, in the mine drainage channel, oxide deposition is over 10 cm deep in many places. This region also has many visible seeps so much of what was sampled at the top of the mine drainage ditch may flow out laterally before the drainage enters Peru Creek. Evidence of Fe and Al deposition is also present in the form of negative lateral mass-flows for these metals at the Deer Creek confluence. Fe loss is much less than Al and it can be inferred that waters began mixing and oxides forming upstream of the confluence. This is very possible as the region immediately upstream is a porous wetland. Al oxides began to precipitate just below the confluence.

Results also reveal the origin of lateral inflows. Assuming SO_4 is behaving conservatively, lateral concentrations and mass-flows at the Deer Creek confluence are estimated to be much greater than tributary inflows. Lateral inflows must be resurfacing acidic and metal rich Snake River waters rather than circumneutral Deer Creek inflows. At the confluence with Peru Creek, lateral and tributary SO_4 concentrations are estimated to be equal, supporting the hypothesis that lateral inflows have their origin in Peru Creek. Higher lateral discharge produced higher lateral mass-flow for conservative SO_4. This confluence did not appear to be very reactive as is supported by the similarity between lateral and tributary concentrations and mass-flows for the majority of metals. For many metals upstream Snake River and Peru Creek concentrations were very similar. The same was true for pH.

Lateral inflows for non-confluence zones revealed that Fe and Al continued to be removed from the stream column for many kilometers below the Deer Creek confluence. Minor positive mass-flows for other metals suggest that small point source mines, located along this segment of reach, may be a very limited source of ARD to the basin. On Peru Creek, substantial metal loading occurred below the Pennsylvania Mine, supporting earlier findings.

Oxide deposition results revealed that Fe and Al oxides were present to some extent at every stream site. Fe oxides began forming upstream of Al oxides, as would be expected according to their solubility products. Fe deposition above the Chihuahua Gulch confluence indicates a mixing of waters beginning above the actual confluence. The extent of deposition reveals the importance of this confluence in driving stream chemistry. More Fe and Al oxides were deposited in this region than anywhere else in the watershed. More neutral inflows and subsequent reactions greatly diminished downstream metal concentrations. Two other major areas of oxide deposition occurred. On the Snake River considerable oxide deposition was found at the Deer Creek confluence and, on Peru Creek, oxide deposition was substantial in the vicinity of the Pennsylvania Mine confluence. Results also show that the deposition of Al oxides was greater than that of Fe oxides. Rate results were interesting but would be more useful with additional data. Assuming conditions remained the same, it would take approximately two months to accumulate the mass of oxides found on the rocks in July. This leads to additional questions regarding oxide deposition such as "How often and to what extent are oxides scoured from rocks?", "Are there temporal variations in deposition rates?", and "Is there a

maximum amount of deposition that a flow regime will permit?" Oxides and

dissolved metals eventually end up in stream sediments and downstream in Lake

Dillon (Greve et al. 2001, Apodaca et al. 2000).

      Attempts were made to identify threshold levels of metal oxide deposition that

limit the growth of algae in stream reaches receiving acid mine drainage. It was also

hoped that a downstream recovery profile for algal communities could be developed.

Periphyton populations were severely impaired at every stream sampling site.

Chihuahua Gulch and Deer Creek had the most robust populations though these were

less abundant than periphyton typically found in other Rocky Mountain streams

(Niyogi, 1999). These populations were prevented from colonizing downstream due

to the same circumneutral waters that made their presence possible. As soon as

tributary waters mixed with ARD waters, considerable Fe and Al oxide deposition

produced inhabitable downstream reaches (Fig. 5.2). The extremely limited

periphyton populations that were present throughout the basin led to a lack of obvious

patterns and made it impractical to identify threshold levels of oxide deposition

impacting periphyton biomass.

FIGURE 5.2: Peru Creek immediately below the relatively pristine Chihuahua Gulch inflow. This mixing of waters with very different chemistries causes Al oxides to form, coating the streambed. (Fe oxides formed further upstream). This confluence has the greatest mass of Al and Fe oxide deposition of the 17 sites sampled.

A correlation between the percent of Al by mass in deposited oxides and chlorophyll *a* was identified and supports an earlier finding that Al oxides have an extremely detrimental effect on periphyton communities (Niyogi, 1999). The presence and extent of Al oxides throughout the basin has tremendous implications for the restoration of periphyton communities and the entire stream ecosystem. Improvements in water quality by increasing pH could, in effect, further impair aquatic habitats due to the formation of Fe and Al oxides. Also, the weathering of disseminated pyrite in the Upper Snake River is a natural source of Al. No attempts at manipulating the chemistry of these waters are likely to be made. Therefore, this source will continue to affect periphyton communities for large segments of stream reach. Though Peru Creek was a source of Al to the Snake River, much of this metal

had already been removed upstream at the Pennsylvania Mine and Chihuahua Gulch confluences.

Both oxide deposition and poor water quality have detrimental effects on aquatic organisms. Table 5.1 is a synthesis of the Snake River and Peru Creek synoptic data. The highest Snake River and Peru Creek concentrations are listed as well as the location and stream order of the most elevated concentrations. While the natural source in the upper Snake River and the anthropogenic source on Peru Creek differed in their maximum concentrations for many metals, they both served as important sources of ARD to the basin.

Table 5.1: August maximum sampled concentrations not including tributary data (Snake River Watershed synoptic study)

Metal	Snake River Maximum Concentration (mgL^{-1})	Peru Creek Maximum Concentration (mgL^{-1})	Stream Order Where Max Concentration Occurred	Location of Max Concentration
Fe	0.87	0.21	2nd	SN1
Al	5.49	2.50	2nd	SN1
Mg	5.41	4.01	2nd	SN1
Cu	0.02	0.10	2nd	PR2
Zn	0.85	1.45	2nd	PR3
Mn	1.23	1.25	3rd and 2nd	PR3 and SN1
Pb	0.03	0.03	4th and 3rd	SN6 and PR4

Metal concentration standards for aquatic toxicity vary by geographic location. Table 5.2 presents chronic and acute toxicity levels for Colorado aquatic life calculated for the Snake River according to methods described by the Colorado Department of Public Health and Environment (1999). These levels are determined by hardness (mg L^{-1} CaCO$_3$). Generally, higher concentrations of metals can be tolerated by stream biota as hardness is increased. Using the Snake River watershed

synoptic data, July and August values for hardness were calculated for each sampling

site. Values were similar throughout the basin and an average hardness of 41 mg L^{-1}

was determined. This is somewhat comparable to hardness data collected by

Clements (1995), who measured hardness ranging from 36 – 63 mg L^{-1} at various

points in the basin. Table 5.3 reveals that toxic aquatic life standards for many metals

were exceeded in both the Snake River and Peru Creek.

Table 5.2: State of Colorado Aquatic Life Standards applied to the Snake River (Colorado Department of Public Heath and Environment, 1999). Toxicity levels are based upon a hardness of 41.0 m L^{-1}.

Metal	Chronic Toxicity Level (µg L^{-1})	Acute Toxicity Level (µg L^{-1})
Al	87	750
Cu	5.5	7.67
Fe	1000	Not designated
Pb	1.1	22.7
Mn	900	1566
Zn	49.8	55.0

Table 5.3: Toxicity levels in the Snake River Watershed

Upper Snake River Diel Study	
Metal	*Toxicity Level*
Al	Acute levels at all sites
Cu	Acute levels at all sites during at least part of the day except at 0 m and 450 m where chronic levels were present during a portion of the day
Fe	Toxic levels at all sites except 0 m
Pb	Below detection
Mn	Ok
Zn	Acute levels at all sites except 0 m
Snake River Synoptic Study	
Al	Chronic levels at PR2, SN1, SN2; Acute levels at PR3, PR4, PR5, SN3 SN4, SN5
Cu	Acute levels at all Peru Creek sites and SN1, SN2, SN3, SN5; Chronic levels at SN6
Fe	Ok
Pb	Chronic levels at SN1, SN2, SN3, SN4, SN7, SN8, PR1 and PR2; Acute levels at SN5, SN6, PR4, PR5
Mn	Chronic levels at PR3, PR4, SN1
Zn	Acute levels at all sites

These aquatic life standards refer only to the impact of dissolved metal concentrations on stream biota and do not consider the combined effects of elevated concentrations and the presence of metal oxide deposition. In the Snake River watershed the impact of ARD on the aquatic ecosystem is extensive. The presence of Al and Fe oxides, as well as toxic levels of many metals, has severely limited periphyton populations throughout the basin. This has obvious implications for algal communities and at other trophic levels where organisms may be impacted by the negligible presence of primary producers as well as by ARD.

CHAPTER VI

CONCLUSIONS

Acid rock drainage is a significant problem throughout the western United

States and many parts of the world. This study examined the Snake River Watershed

in Summit County, Colorado, specifically, with the goal of identifying the sources

and effects of acidity and elevated metal concentrations resulting from both the

natural weathering of disseminated pyrite and the weathering of pyrite exposed in

abandoned mines. The results are important in understanding the environmental

impacts of ARD throughout the basin, in providing information for water resources

management decisions, and in developing future remediation alternatives.

6.1 - Findings

Upper Snake River results identified the principal source of ARD, the

importance of lateral inflows in transporting metals and acidity, and the extent of

environmental impact from the upper basin in the downstream reaches of the lower

basin. Elevated metal concentrations and low pH values were the result of the natural

weathering of pyrite disseminated throughout the eastern side of the upper Snake

River basin. Surface waters and lateral inflows were both significant sources of

ARD, with lateral flows providing the majority of mass loading at points along the

stream reach. Tributary waters often had very different chemistry from lateral

inflows as a result of varying exposure to rock, soils, organic matter and other solutes.

Confluences were critical to the transport of metals and acidity as tributary waters and

the majority of lateral inflows entered the stream in these regions.

Decreasing concentrations of Fe in the longitudinal direction suggests that Fe

oxides began to form along the study reach. Diel variations in Fe and Cu

concentrations were most likely the result of oxide formation, co-precipitation and

iron photochemistry. Toxic concentration levels were present for Fe and Cu during

only portions of the day.

The Snake River watershed synoptic study provided a great deal of

information regarding the sources, transport and effects of ARD throughout the entire

basin. Discharge data demonstrated the importance of lateral inflows along reaches

of stream and at several key confluences. Temporal variations were also apparent,

with increases in lateral flows in August resulting from a period of elevated

precipitation.

Both surface and subsurface waters played an important role in the transport

of ARD. In August, lateral inflows provided a continual, though smaller, source of

metals along the Snake River below Deer Creek. In this same month, lateral inflows

below the Pennsylvania Mine drainage provided more than half the total mass-flow of

most metals into Peru Creek. In August, the Peru Creek tributary was a less

significant source of metals to the Snake River than were lateral inflows. The

chemistry of tributary waters often differed from that of lateral inflows.

In August, the highest Snake River concentrations for most metals were seen at the uppermost Snake River site. Pb was the exception, with the highest concentrations found downstream of the Peru Creek inflow. In contrast, the highest Snake River mass-flows for the majority of metals were found below the confluence with Peru Creek. Al was the exception, showing the highest mass-flow at the uppermost Snake River site, a result of the disseminated nature of ARD and subsequent secondary weathering of country rock.

Metal oxides were present at all sampling sites in the synoptic study with the most significant deposition occurring in confluence zones. The greatest deposition occurred at the confluence of Peru Creek and Chihuahua Gulch. Other areas of considerable deposition were below the Pennsylvania Mine drainage and the confluence of the Snake River and Deer Creek. Oxide data and lateral inflow calculations suggested that mixing of tributary waters and formation of oxides began to occur in the hyporheic zones upstream of actual confluences.

Periphyton communities were shown to be severely stressed throughout the watershed with only minimal biomass present at all sampling sites. Concentration data along the Snake River and Peru Creek revealed that both natural and anthropogenic sources of ARD led to the presence of toxic levels of dissolved metals and metal oxide deposition. The presence of multiple and diverse sources in the basin prevents ecological recovery for many kilometers of stream and may limit remediation options.

6.2 - Implications

The findings of this research are both specific to the Snake River Watershed and have applications for the scientific community when studying other ARD affected ecosystems.

In the Snake River watershed the widespread presence of Al and Fe oxides from both natural and anthropogenic sources makes it difficult to develop an effective remediation plan. Though periphyton presence in the basin is minimal, in the upper Snake River algal species adapted to ARD are present. More Al appears to be mobilized as a result of the natural weathering of disseminated pyrite than is mobilized by the weathering of pyrite exposed by mining. This natural source of ARD may result in the deposition of Al oxides over a larger reach of stream and as a result may be more limiting to periphyton communities than the anthropogenic source. As the upper Snake River is a natural source of ARD, the question arises as to whether it is appropriate to manipulate this system to achieve the desired improvements in water quality necessary for downstream human use.

ARD resulting from the Pennsylvania Mine on Peru Creek has been and continues to be a target for remediation. Prior to the development of remediation plans, further investigation is necessary regarding the downstream effects of this point source. The natural ARD source in the upper Snake River necessitates additional research to determine if the effective remediation of the Pennsylvania Mine drainage would have a discernible impact on downstream water quality and stream biota. Furthermore, lateral inflows of ARD from the Pennsylvania Mine should be better documented before waters in the drainage canal are treated. A large percentage of

metals from the Pennsylvania Mine enter the stream laterally. Therefore, treatment of waters currently routed through the canal may not have much effect.

Lateral inflows in the Snake River basin vary in importance over time. At several key confluences, this study found waters being lost to the subsurface on the declining limb of the hydrograph with lateral inflows during a period of increased precipitation. Further studies of the timing and extent of subsurface and groundwater inflows are critical to understanding the transport and fate of ARD in the basin. More generally, the consideration of both surface and lateral inflows is necessary to identify the sources and extent of metal loading. This methodology has not commonly been utilized in the past and would be useful in future studies on ARD. Lateral inflows were important to the transport of metals not only in regions where disseminated pyrite was the source of ARD but also in the vicinity of point source mines. Calculations which overlook these inflows may overlook significant metal and acidity loads.

Confluence zones are extremely important, being the most chemically reactive regions as well as the location of the majority of lateral inflows. When examining confluences, it should be considered that waters may be entering the stream laterally as well as mixing and reacting in the hyporheic zone surrounding the confluence. The chemical makeup of tributary waters was found to vary from that of lateral waters emphasizing the importance of estimating not only lateral discharge but also lateral concentrations and mass-flows.

In ARD impacted systems, confluences have a tremendous effect on downstream concentrations. Most often, waters mixing in confluence zones have

very different chemistries, which in the case of ARD may lead to a rapid increase in stream pH and the subsequent formation of Fe and Al oxides and removal of metals from the stream column. While more neutral inflows may improve water quality, the formation of Fe and Al oxides creates an environment that is extremely detrimental to aquatic life.

Upper Snake River data revealed diel variations in Fe and Cu concentrations. Temporal variations may occur on a variety of scales and should be considered when developing a sampling plan and analyzing results. This study found that diel variations can be significant with Fe and Cu concentrations exceeding toxic levels at several sites during only a portion of the day. This has far reaching implications regarding sampling procedures as well as methods currently utilized to determine a stream's aquatic health.

This research has answered many questions regarding ARD in the Snake River watershed while raising others. It is hoped that the findings presented here, in conjunction with other studies, will assist the Snake River Task Force as they seek to develop realistic remediation options for the basin. Additionally, the methodologies presented here have more general applications for the research community regarding the study of ARD in other basins.

LITERATURE CITED

Apodaca LE, Driver NE, Bails JB (2001) Occurrence, transport, and fate of trace elements, Blue River Basin, Summit County, Colorado: an integrated approach. Environment Geology 39 (8): 901-913

Bencala KE (1984) Interactions of solutes and streambed sediment, 2. A dynamic analysis of the coupled hydrologic and chemical processes that determine solute transport. Water Resources Research 20(12) 1804-1814

Bencala KE, Kennedy VC, Zellweger GW, Jackman AP, Avanzino RJ (1984) Interactions of solutes and streambed sediment, 1. An experimental analysis of cation and anion transport in a mountain stream. Water Resources Research 20: 1797-1803

Bencala KE, McKnight DM (1987) Identifying in-stream variability: sampling iron in an acidic stream. In: Averett RC and McKnight DM (eds) Chemical Quality of Water and the Hydrologic Cycle. Lewis Publishers, Inc., Chelsea, Michigan, pp 255-265

Bencala KE, McKnight DM, Zellweger GW (1987) Evaluation of natural tracers in an acidic and metal-rich mountain stream. Water Resources Research 23: 827-836

Bencala KE, McKnight DM, Zellweger GW (1990) Characterization of transport in an acidic and metal-rich mountain stream based on a lithium tracer injection and simulations of transient storage. Water Resources Research 26: 989-1000

Bencala KE, Ortiz RF (1999) Theory and (or) reality: analysis of sulfate mass-balance at Summitville, Colorado poses process questions about the estimation of metal loadings. In: Morganwalp DW, Buxton HT (eds) Proceedings of the USGS Toxic Substances Hydrology Program - Contamination from Hardrock Mining: U.S.G.S. Water-Resources Investigations Report 99-4018A

Bove DJ, Mast MS, Wright WG, Verplank PL, Meeder GP, Yager DM (2000) Geologic Control on acidic and metal-rich waters in the southeastern Red Mountains area, near Silverton, Colorado. In: ICARD 2000: Proceedings from the fifth international conference on acid rock drainage: Littleton, Colorado, Society for Mining, Metallurgy, and Exploration, Inc., v.1, pp 523-534

Boyer, EW, McKnight DM, Bencala KE, Brooks PD, Anthony MW, Zellweger GW, Harnish RE (1999) Streamflow and Water Quality Characteristics for the Upper Snake River and Deer Creek Catchments in Summit County, Colorado: Water Years 1980 – 1990, Occasional Paper No 53, INSTAAR, University of Colorado

Brick CM, Moore JN (1996) Diel variations of trace metals in the Upper Clark Fork River, Montana. Environmental Science and Technology 30: 1953-1960

Brooks PD, McKnight DM and Bencala KE (2001) Annual maxima in Zn concentrations during spring snowmelt in streams impacted by mine drainage. Environmental Geology 40(11-12): 1447-1454

Broshears RE, Runkel RL, Kimball BA, McKnight DM, Bencala KE (1996) Reactive solute transport in an acidic stream: experimental pH increase and simulation of controls on pH, aluminum, and iron. Environmental Science & Technology 30: 3016-3024

Brown E, Skougstad MW, Fishman MJ (1970) In: Methods for collection and analysis of water samples for dissolved minerals and gases; Techniques for Water Resources Investigations of the United States Geological Survey, Book 5, Chapter A1, U.S. Government Printing Office: Washington DC. pp 101 – 105

Clements WH (1999) Metal tolerance and predator-prey interactions in benthic macroinvertebrate stream communities. Ecological Applications 9(3): 1073-1084

Clements WH (1995) Effects of heavy metals from mining on bethic communities in Peru Creek and French Gulch, Colorado: A final report submitted to the Northwest Colorado Council of Governments, Silverthorne, Colorado

Clements WH (1994) Benthic invertebrate community responses to heavy metals in the Upper Arkansas River Basin, Colorado. J. N. Benthol. Soc. 13: 30-44

Colorado Climate Center (2002) Summary precipitation data for the year 2000 for station 52281 Dillon 5E. http://ccc.atmos.colostate.edu/dly_form.html, last accessed March 4, 2002

Colorado Department of Public Health and Environment Water Quality Control Commission (1999) Water quality standards, regulation no. 31; the basic standards and methodologies for surface water (5 CCR 1002-31)

Colorado Mining Water Quality Task Force (1997) Report and recommendations regarding water quality impacts from abandoned or inactive mined lands, Department of Public Health and Environment. http://www.cdphe.state.co.us/op/wqcc/MWQTFreportword.PDF, last accessed February 14, 2001

Da Rosa CD, Lyon JS (1997) Golden dreams, poisoned streams: how reckless mining pollutes America's waters, and how we can stop it. Mineral Policy Center, Washington D.C.

Department of the Interior (1991) Noncoal Reclamation, Abandoned Mine Land Reclamation Program, Office of Surface Mining Reclamation and Enforcement. Office of Inspector General, Report No. 91-I-1248

Dillon Ranger District (1999) White River National Forest, Arapahoe Basin, Master Development Plan, Final Environmental Impact Statement, Silverthorne, Colorado

Elwood JW, Mulholland PJ (1989) Effects of acid precipitation on stream ecosystems. In: Adriano, Johnson (eds) Acid precipitation. v. 2: biological and ecological effects. Springer-Verlag, New York, pp 88-135

Environmental Protection Agency (2001) unpublished data from a site assessment and hydrological evaluation of the Snake River watershed, provided by Sabrina Forrest, EPA Region 8 (forrest.sabrina@epa.gov)

Gilliland ME (1999) Summit: a gold rush history of Summit County, Colorado. Alpenrose Press, Silverthorne, Colorado

Gray NF (1997) Environmental impact and remediation of acid mine drainage: a management problem. Environmental Geology 30(1/2): 62-71

Greve AJ, Spahr NE, Van Metre PC, Wilson JT (2001) Identification of water-quality trends using sediment cores from Dillon Reservoir, Summit County, Colorado: U.S. Geological Survey Water-Resources Investigations Report 01-4022. 33 p.

Harvey JW, Bencala KE (1993) The effects of streambed topography on surface-subsurface water exchange in catchments. Water Resources Research 29: 89-98

Johnson CA (1986) The regulation of trace element concentrations in river and estuarine waters contaminated with acid mine drainage: the adsorption of Cu and Zn on amorphous Fe oxyhydroxides. Geochim. Cosmochim. Acta 50: 2433-2438

Kimball BA, McKnight DM, Wetherbee GA, Harnish RA (1992). Mechanisms of
    iron photoreduction in a metal-rich, acidic stream (St. Kevin Gulch, Colorado,
    U.S.A.). Chemical Geology 96: 227-239

Kimball BA, Broshears RE, Bencala KE, McKnight DM (1994) Coupling of
    hydrologic transport and chemical reactions in a stream affected by acid mine
    drainage. Environmental Science and Technology 28: 2065-2073

Kimball BA, Bencala KE, Besser JM (1999) Synthesis of watershed characterization
    for making remediation decisions, Contamination from Hard-Rock Mining,
    U.S. Geological Survey Water Resources Investigations Report 99-4018A. pp
    3-7

Kimball BA, Runkel RL, Walton-Day K, Bencala KE (in press) Assessment of metal
    loads in watersheds affected by acid mine drainage by using tracer injection
    and synoptic sampling: Cement Creek, Colorado, USA. Applied
    Geochemistry

Lottermoser BG, Ashley PM, Lawie DC (1999) Environmental geochemistry of the
    Gulf Creek copper mine area, north-eastern New South Wales, Australia.
    Environmental Geology 39(1): 61-74

Lovering TS (1935) Geology and ore deposits of the Montezuma triangle. U.S.
    Geological Survey. pp 178

Lyon JS, et al. (1993) Burden of Gilt, Mineral Policy Center, Washington, D.C.

Makos JD, Hrncir DC (1995) Chemistry of Cr(VI) in a constructed wetland.
    Environmental Science and Technology 29(9): 2414-2419

McKnight DM, Feder GL (1984) The ecological effects of acid conditions and
    precipitation of hydrous metal oxides in a Rocky Mountain stream.
    Hydrobiologia 199:129-138

McKnight DM, Kimball BA, Bencala KE (1988) Iron photoreduction and oxidation
    in an acidic mountain stream. Science 240: 577-696

McKnight DM, Bencala KE (1989) Reactive iron transport in an acidic mountain
    stream in Summit County, Colorado: a hydrologic perspective. Geochemica et
    Cosmochimica Acta 53: 2225-2234

McKnight DM, Bencala KE (1990) The chemistry of iron, aluminum, and dissolved
    organic material in three acidic, metal-enriched mountain streams, as
    controlled by watershed and in-stream processes. Water Resources Research
    28:3087-3100

McKnight DM, Wershaw RL, Bencala KE, Zellweger GW, Feder GL (1992) Humic substances and trace metals associated with Fe and Al oxides deposited in an acidic mountain stream. The Science of the Total Environment 117/118: 485-498

McKnight DM, Kimball BA, Runkel RL (2001) pH dependence of iron photoreduction in a rocky mountain stream affected by acid mine drainage. Hydrological Processes 15: 1979 – 1992

Meyer JL (1997) Stream health: incorporating the human dimension to advance stream ecology. Journal of the North American Benthological Society 16(2): 439-447

Moran RE, Wentz DA (1974) Effects of metal-mine drainage on water quality in selected areas of Colorado, 1972-73. Colorado Water Resources Circular No. 25, Colorado Water Conservation Board, Denver

Morris DP, Lewis WM (1988) Phytoplankton nutrient limitation in Colorado mountain lakes. Freshwater Biology 20: 315-327

Mulholland PJ, Driscoll CT, Elwood JW, Osgood MP, Palumbo AV, Rosemond AD, Smith ME, Schofield C (1992) Relationships between stream acidity and bacteria, macroinvertebrates, and fish – a comparison of north temperate and south temperate mountain streams, USA. Hydrobiologia 239(1): 7-24

Munk L, Gunter F, Pride DE, Bigham JM (2002) Sorption of trace metals to an aluminum precipitate in a stream receiving acid rock-drainage: Snake River, Summit County, Colorado. Applied Geochemistry 17: 421-430

Neuerburg GJ, Botinelly T (1972) Map showing geologic and structural control of ore deposits, Montezuma District, Central Colorado. U.S. Geological Survey. Miscellaneous Geologic Investigations, Map I-750

Niyogi DK (1999) Effects of stress from mine drainage on ecosystem functions in Rocky Mountain streams. Ph.D. Dissertation, University of Colorado, Boulder, Colorado

Niyogi DK, Lewis WM, McKnight DM (2001) Litter breakdown in mountain streams affected by drainage: biotic mediation of abiotic controls. Ecological Applications 11(2): 506-516

Nordstrom DK, Southam, G (1997) Geomicrobiology of sulfide mineral oxidations, In: Banfield JR, Nealson KH (eds) Geomicrobiology: Interactions between Microbe and Minerals, v. 35, pp 361 – 390

Nordstrom DK, Alpers CN (1999) Geochemistry of Acid Mine Waters, Rev. Econ. Geol. 6A:133 – 160

Runkel RL, McKnight DM, Bencala KE, Chapra SC (1996) Reactive solute transport in streams 2. Simulation of a pH modification experiment. Water Resources Research 32: 419-430

Runkel RL, Kimball BA, McKnight DM, Bencala KE (1999) Reactive solute transport in streams. A surface complexation approach for trace metal sorption. Water Resources Research 35: 3829-3840

Singer PC, Stumm W (1970). Acidic mine drainage: the rate determining step. Science 167: 1121-1123

Snake River Watershed Task Force (1999) Mission Statement. Keystone Center, Keystone, Colorado

Steinman AD, Lamberti GA (1996) Biomass and pigments of benthic algae. In: Hauer FR, Lamberti GA (eds) Methods in stream ecology. Academic Press. pp 295-313

Sullivan AB, Drever JI, McKnight DM (1998) Diel variation in element concentration, Peru Creek, Summit, County, Colorado. Journal of Geochemical Exploration 64: 141-145

Sullivan AB, Drever JI (2001a) Spatiotemporal variability in stream chemistry in a high-elevation catchment affected by mine drainage. Journal of Hydrology 252: 237-250

Sullivan AB, Dever JI (2001b) Geochemistry of suspended particles in a mine-affected mountain stream. Applied Geochemisty 16: 1663-1676

Summit Country (2001), Summit County, Colorado Web Site, http://www.co.summit.co.us/statistics/population.htm, last accessed February 5, 2002

Theobald, Jr. PK, Lakin HW, Hawkins DB (1963) The precipitation of aluminum, iron and manganese at the junction of Deer Creek with the Snake River in Summit County, Colorado. Geochemica et Cosmochimica Acta 27: 121-132

United States Geological Survey (1997) A plan for the USGS, abandoned mine lands initiative, 1997 – 2001, U.S. Geological Survey, Reston, Virginia, 31 p.

United States Geological Survey (2001) unpublished sampling data, provided by David Fey, U.S. Geological Survey, Mineral Resources Team (dfey@usgs.gov)

Williams TM, Smith B (2000) Hydrochemical characterization of acute acid mine drainage at Iron Duke mine, Mazowe, Zimbabwe. Environmental Geology 39: 272-278

Wilson AB, LaRock EJ (1992) Map showing mineralized areas and principal lode mines in southern Summit County, Colorado. U.S. Geological Survey. Map MF-2163

Wilson MA, Carpenter SR (1999) Economic valuation of freshwater ecosystem services in the United States: 1971-1997. Ecological Applications 9: 772-783

APPENDIX A

TABLES

Table A.1: Sampling data, upper Snake River diel study

Site ID	Time	Temp °C	Discharge $m^3\ s^{-1}$	pH	Conductivity mS	DOC
2250m	930	—	0.240	3.95	—	1.02
2250m	1002	—	—	4.03	—	1.24
2250m	1100	—	—	4.06	—	1.04
2250m	1200	14.8	—	3.92	—	0.96
2250m	1318	—	—	3.86	—	2.09
2250m	1400	—	—	3.88	—	0.88
2250m	1500	—	—	3.83	—	1.17
2120m	930	—	0.224	3.94	—	3.01
2120m	1200	—	—	3.91	—	1.15
2120m	1503	14.8	—	3.88	—	0.89
2085m	930	—	0.172	4.11	—	—
2085m	1200	—	—	4.12	—	0.95
2085m	1457	11.9	—	4.00	—	1.45
1935m	941	—	0.176	4.17	0.081	1.11
1935m	1205	12.9	—	3.89	0.081	0.95
1935m	1508	12.2	—	4.01	0.081	0.74
1875m	930	—	0.195	4.16	0.085	—
1875m	1200	—	—	3.87	0.085	0.68
1875m	1500	12.0	—	3.97	0.085	0.56
940m	930	—	0.175	4.13	0.096	—
940m	1200	—	—	3.94	0.096	0.63
940m	1505	11.2	—	3.99	0.096	1.33
900m	937	—	0.098	4.08	0.107	—
900m	1205	—	—	3.90	0.107	1.51
900m	1500	14.3	—	3.95	0.107	1.24
700m	930	—	0.095	4.07	0.106	0.67
700m	1200	13.6	—	3.88	0.106	0.50
700m	1508	14.0	—	3.94	0.106	1.02
485m	934	—	0.104	4.07	0.11	0.62
485m	1204	13.3	—	3.88	0.11	0.78
485m	1504	13.2	—	3.93	0.11	0.76
450m	930	—	0.063	4.30	0.077	1.30
450m	1200	—	—	4.10	0.077	—
450m	1500	13.0	—	4.15	0.077	1.40
0m	915	—	0.039	5.06	0.046	1.34
0m	1000	—	—	5.11	0.046	—
0m	1100	—	—	5.13	0.046	1.32
0m	1200	—	—	4.85	0.046	1.29
0m	1300	—	—	4.82	0.046	—
0m	1400	13.3	—	4.97	0.046	0.62
0m	1500	12.7	—	4.91	0.046	1.32
Trib 2095m	932	—	0.031	3.74	—	0.49
Trib 2095m	1205	—	—	3.76	—	0.55
Trib 2095m	1500	10.3	—	3.55	—	2.24
Trib 915m	934	—	0.036	4.17	0.076	1.12
Trib 915m	1203	12.1	—	3.94	0.076	—
Trib 915m	1502	11.1	—	4.03	0.076	0.72
Trib 670m	933	—	0.008	5.80	0.042	1.34
Trib 670m	1203	—	—	5.46	0.042	0.89
Trib 670m	1506	12.4	—	5.83	0.042	1.92
Trib 460m	932	—	0.011	3.54	0.282	1.00
Trib 460m	1202	13.5	—	3.36	0.282	0.60
Trib 460m	1502	13.9	—	3.42	0.282	—

Table A.1: Sampling data, upper Snake River diel study

Site ID	Time	Fe²⁺ mg L⁻¹	Readily Soluble Fe mg L⁻¹	FeT mg L⁻¹	StdDev	Cu (FA) ug L⁻¹	StdDev
				Solute Concentrations			
2250m	930	0.693	0.943	1.266	0.004	19.548	0.992
2250m	1002	0.834	1.004	1.266	0.053	21.231	2.113
2250m	1100	0.888	1.045	1.266	0.033	20.726	1.244
2250m	1200	0.847	1.001	1.247	0.004	20.341	1.348
2250m	1318	1.021	1.062	1.207	0.031	18.971	1.565
2250m	1400	0.912	1.057	1.226	0.026	19.211	0.765
2250m	1500	0.913	0.978	1.160	0.009	22.073	1.448
2120m	930	1.003	0.919	1.227	0.014	22.914	0.873
2120m	1200	1.058	1.019	1.237	0.017	21.520	3.350
2120m	1503	0.791	0.945	1.137	0.023	19.957	1.767
2085m	930	—	—	1.369	0.005	13.272	2.243
2085m	1200	1.025	1.092	1.344	0.026	15.845	0.913
2085m	1457	0.872	1.016	1.254	—	14.451	0.167
1935m	941	0.526	0.493	1.348	0.013	15.148	1.127
1935m	1205	1.008	1.118	1.335	0.007	14.571	0.901
1935m	1508	0.900	1.003	1.219	0.038	14.980	0.292
1875m	930	0.998	1.201	1.457	0.043	14.499	0.954
1875m	1200	1.021	1.186	1.450	0.010	16.735	1.448
1875m	1500	0.916	1.115	1.353	0.016	16.254	1.587
940m	930	1.107	1.337	1.608	0.012	19.139	0.423
940m	1200	1.055	1.288	1.603	0.045	16.663	0.878
940m	1505	1.040	1.246	1.487	0.079	19.933	1.083
900m	937	0.846	1.150	1.855	0.005	8.464	0.613
900m	1205	1.148	1.500	1.756	0.011	8.680	0.804
900m	1500	1.262	1.482	1.775	0.028	7.911	1.921
700m	930	1.230	1.577	1.877	0.025	9.978	0.686
700m	1200	1.364	1.510	1.814	0.012	10.772	0.751
700m	1508	1.218	1.709	1.773	0.004	10.050	1.364
485m	934	1.268	1.567	2.093	0.001	9.473	1.481
485m	1204	1.289	1.698	2.014	0.036	9.257	0.522
485m	1504	1.366	1.675	1.997	0.041	9.401	0.861
450m	930	1.194	1.344	1.631	0.041	4.761	1.664
450m	1200	1.106	1.247	1.576	0.004	5.698	0.696
450m	1500	1.224	1.345	1.566	0.027	6.396	2.613
0m	915	0.842	0.854	1.036	0.029	5.097	1.445
0m	1000	0.860	0.868	1.042	0.037	6.829	0.666
0m	1100	0.878	0.921	1.029	0.019	5.867	0.723
0m	1200	0.809	0.827	0.961	0.029	5.025	0.902
0m	1300	0.808	0.812	0.964	0.019	3.462	0.450
0m	1400	0.854	0.821	1.413	0.039	4.737	0.952
0m	1500	0.824	0.853	1.024	—	7.213	1.582
Trib 2095m	932	0.357	0.618	0.770	0.012	55.326	0.721
Trib 2095m	1205	0.322	0.640	0.786	—	59.870	4.252
Trib 2095m	1500	0.470	0.663	0.764	0.001	54.244	1.023
Trib 915m	934	0.834	1.159	1.378	0.001	36.547	1.271
Trib 915m	1203	0.949	1.089	1.291	—	37.966	0.682
Trib 915m	1502	0.833	1.021	1.281	0.013	37.870	0.505
Trib 670m	933	0.049	0.047	0.078	0.001	3.727	1.589
Trib 670m	1203	0.069	0.013	0.060	0.001	4.977	0.216
Trib 670m	1506	0.035	0.024	0.089	0.001	3.318	0.563
Trib 460m	932	1.682	1.631	5.578	0.123	33.133	1.649
Trib 460m	1202	1.581	1.580	5.541	0.013	33.590	0.771
Trib 460m	1502	1.689	1.493	5.565	0.037	34.720	1.354

Table A.1: Sampling data, upper Snake River diel study

		Solute Concentrations					
		Cu(RA)		Mg		Zn	
Site ID	Time	ug L^{-1}	StdDev	mg L^{-1}	StdDev	mg L^{-1}	StdDev
2250m	930	19.380	1.301	2.428	0.001	0.138	0.001
2250m	1002	17.985	1.216	2.419	0.037	0.136	0.001
2250m	1100	21.904	0.737	2.392	0.030	0.133	0.001
2250m	1200	20.918	1.127	2.412	0.013	0.133	0.001
2250m	1318	20.606	0.341	2.417	0.037	0.134	0.001
2250m	1400	18.899	1.560	2.442	0.019	0.135	0.000
2250m	1500	18.057	0.896	2.386	0.018	0.134	0.000
2120m	930	20.510	1.195	2.404	0.011	0.134	0.000
2120m	1200	21.832	0.507	2.481	0.019	0.139	0.000
2120m	1503	20.125	1.161	2.428	0.002	0.135	0.000
2085m	930	13.345	0.382	2.101	0.017	0.110	0.000
2085m	1200	15.917	0.670	2.136	0.005	0.107	0.000
2085m	1457	11.974	0.753	2.098	—	0.107	0.001
1935m	941	17.047	0.795	2.047	0.028	0.102	0.001
1935m	1205	18.153	1.401	2.008	0.011	0.101	0.000
1935m	1508	14.523	0.541	2.019	0.008	0.102	0.000
1875m	930	13.633	1.421	2.061	0.057	0.107	0.000
1875m	1200	17.023	1.312	2.074	0.005	0.106	0.001
1875m	1500	14.643	0.573	2.081	0.005	0.107	0.001
940m	930	16.879	0.850	2.046	0.013	0.119	0.001
940m	1200	19.957	1.051	2.055	0.005	0.118	0.001
940m	1505	17.769	1.291	2.039	0.030	0.120	0.000
900m	937	8.127	0.356	2.440	0.025	0.105	0.000
900m	1205	7.574	0.450	2.433	0.019	0.104	0.000
900m	1500	7.382	0.927	2.405	0.009	0.106	0.000
700m	930	9.738	1.161	2.409	0.025	0.110	0.000
700m	1200	7.838	1.309	2.410	0.008	0.110	0.001
700m	1508	11.686	0.721	2.449	0.004	0.109	0.000
485m	934	10.219	0.927	2.515	0.001	0.114	0.000
485m	1204	6.901	1.515	2.515	0.003	0.116	0.000
485m	1504	8.247	1.922	2.509	0.019	0.116	0.000
450m	930	9.089	0.191	1.942	0.013	0.076	0.000
450m	1200	8.608	0.220	1.926	0.004	0.078	0.000
450m	1500	3.438	0.798	1.947	0.006	0.076	0.000
0m	915	5.434	0.842	1.768	0.023	0.052	0.000
0m	1000	4.208	0.730	1.806	0.008	0.052	0.000
0m	1100	3.198	0.341	1.764	0.008	0.055	0.000
0m	1200	6.780	0.641	1.705	0.023	0.051	0.000
0m	1300	5.097	1.227	1.717	0.024	0.050	0.000
0m	1400	4.809	0.974	1.805	0.008	0.053	0.000
0m	1500	3.030	0.439	1.816	1.238	0.056	0.000
Trib 2095m	932	49.411	3.648	4.189	0.029	0.304	0.002
Trib 2095m	1205	50.349	0.125	4.181		0.301	0.001
Trib 2095m	1500	55.061	0.890	4.255	0.016	0.307	0.002
Trib 915m	934	37.124	1.481	1.468	0.008	0.149	0.001
Trib 915m	1203	35.032	1.063	1.416		0.148	0.001
Trib 915m	1502	35.489	1.082	1.450	0.013	0.152	0.000
Trib 670m	933	3.246	0.250	1.249	0.016	0.019	0.000
Trib 670m	1203	2.188	0.182	1.206	0.014	0.018	0.000
Trib 670m	1506	3.823	0.500	1.239	0.005	0.021	0.000
Trib 460m	932	34.696	0.260	5.621	0.047	0.344	0.000
Trib 460m	1202	33.446	1.175	5.795	0.011	0.349	0.002
Trib 460m	1502	32.989	1.963	5.805	0.008	0.353	0.000

Table A.1: Sampling data, upper Snake River diel study

		Solute Concentrations				
		Al		SO$_4$	Ca	
Site ID	Time	mg L^{-1}	StdDev	mg L^{-1}	mg L^{-1}	StdDev
2250m	930	2.630	0.010	44.007	0.567	0.009
2250m	1002	2.649	0.060	43.757	0.572	0.012
2250m	1100	2.580	0.062	43.832	0.561	0.014
2250m	1200	2.590	0.055	44.031	0.562	0.008
2250m	1318	2.587	0.023	43.938	0.610	0.090
2250m	1400	2.575	0.026	43.732	0.560	0.003
2250m	1500	2.550	0.005	43.945	0.553	0.002
2120m	930	2.628	0.001	44.031	0.626	0.011
2120m	1200	2.751	0.022	43.730	0.543	0.008
2120m	1503	2.613	0.054	43.928	0.540	0.003
2085m	930	1.616	0.006	—	0.623	0.005
2085m	1200	1.619	0.019	43.734	0.636	0.010
2085m	1457	1.611	0.030	43.983	0.644	0.018
1935m	941	1.554	0.034	43.036	0.625	0.009
1935m	1205	1.492	0.024	42.435	0.626	0.005
1935m	1508	1.499	0.021	42.579	0.646	0.007
1875m	930	1.585	0.001	43.745	0.617	0.009
1875m	1200	1.567	0.024	43.843	0.606	0.008
1875m	1500	1.564	0.035	43.903	0.663	0.006
940m	930	1.692	0.008	44.031	0.622	0.008
940m	1200	1.666	0.024	44.030	0.620	0.006
940m	1505	1.671	0.024	43.861	0.619	0.007
900m	937	1.834	0.041	43.968	0.735	0.005
900m	1205	1.801	0.003	43.949	0.740	0.022
900m	1500	1.799	0.008	43.917	0.721	0.000
700m	930	1.894	0.021	43.741	0.795	0.014
700m	1200	1.885	0.040	44.008	0.721	0.013
700m	1508	1.838	0.017	43.774	0.739	0.007
485m	934	1.988	0.030	43.881	0.703	0.006
485m	1204	2.007	0.001	43.728	0.681	0.012
485m	1504	1.984	0.023	43.831	0.689	0.009
450m	930	1.210	0.014	38.857	0.765	0.006
450m	1200	1.190	0.005	38.726	0.747	0.005
450m	1500	1.179	0.011	38.758	0.749	0.004
0m	915	0.339	0.004	29.561	1.324	0.023
0m	1000	0.319	0.003	29.625	1.350	0.015
0m	1100	0.337	0.003	28.806	1.272	0.016
0m	1200	0.336	0.001	28.854	1.297	0.021
0m	1300	0.320	0.002	28.408	1.256	0.012
0m	1400	0.447	0.008	29.629	1.281	0.017
0m	1500	0.345	0.005	30.472	1.452	0.011
Trib 2095m	932	8.744	0.107	43.935	0.360	0.001
Trib 2095m	1205	8.580	0.118	44.015	0.379	0.004
Trib 2095m	1500	8.606	0.167	43.852	0.346	0.006
Trib 915m	934	1.570	0.003	34.809	0.445	0.002
Trib 915m	1203	1.528	0.025	33.712	0.425	0.005
Trib 915m	1502	1.543	0.004	33.663	0.417	0.004
Trib 670m	933	0.068	0.001	19.124	1.651	0.027
Trib 670m	1203	0.057	0.000	18.732	1.592	0.037
Trib 670m	1506	0.087	0.001	19.360	1.637	0.038
Trib 460m	932	6.449	0.005	44.032	0.483	0.006
Trib 460m	1202	6.484	0.103	44.035	0.506	0.007
Trib 460m	1502	6.487	0.039	43.750	0.506	0.007

Table A.1: Sampling data, upper Snake River diel study

		Solute Concentrations					
		Mn		Na		Pb	
Site ID	Time	mg L^{-1}	StdDev	mg L^{-1}	StdDev	mg L^{-1}	StdDev
2250m	930	0.321	0.010	1.615	0.003	0.001	0.001
2250m	1002	0.310	0.007	1.602	0.004	BD	?
2250m	1100	0.318	0.018	1.627	0.025	BD	?
2250m	1200	0.322	0.000	—	—	BD	?
2250m	1318	0.323	0.006	1.621	0.014	BD	?
2250m	1400	0.312	0.003	1.631	0.017	BD	?
2250m	1500	0.311	0.006	1.648	0.012	BD	?
2120m	930	0.316	0.005	—	—	0.002	0.002
2120m	1200	0.323	0.003	1.656	0.004	BD	?
2120m	1503	0.326	0.003	1.654	0.007	0.001	0.000
2085m	930	0.262	0.010	—	—	BD	?
2085m	1200	0.271	0.006	—	—	BD	?
2085m	1457	0.271	—	1.616	0.007	BD	?
1935m	941	0.246	0.002	1.547	0.005	BD	?
1935m	1205	0.245	0.006	1.563	0.030	BD	?
1935m	1508	0.246	0.002	1.570	0.016	BD	?
1875m	930	0.246	0.013	1.546	0.011	BD	?
1875m	1200	0.257	0.001	1.544	0.019	BD	?
1875m	1500	0.256	0.002	1.571	0.007	BD	?
940m	930	0.261	0.004	1.478	0.010	0.001	0.000
940m	1200	0.272	0.011	—	—	0.001	0.001
940m	1505	0.264	0.011	1.474	0.014	BD	?
900m	937	0.255	0.001	1.473	0.009	BD	?
900m	1205	0.254	0.001	1.481	0.014	BD	?
900m	1500	0.250	0.005	1.515	0.019	BD	?
700m	930	0.242	0.012	—	—	0.001	0.001
700m	1200	0.253	0.001	1.483	0.008	0.001	0.000
700m	1508	0.251	0.008	1.499	0.008	BD	?
485m	934	0.266	0.006	1.491	0.020	BD	?
485m	1204	0.268	0.006	—	—	BD	?
485m	1504	0.262	0.006	1.522	0.016	0.001	0.000
450m	930	0.172	0.004	—	—	0.001	0.001
450m	1200	0.173	0.002	1.389	0.021	0.001	0.000
450m	1500	0.174	0.000	1.418	0.014	BD	?
0m	915	0.143	0.002	—	—	0.001	0.001
0m	1000	0.145	0.005	—	—	BD	?
0m	1100	0.141	0.003	—	—	BD	?
0m	1200	0.138	0.001	—	—	0.001	0.000
0m	1300	0.140	0.001	1.198	0.007	BD	?
0m	1400	0.143	0.000	1.211	0.004	0.002	0.000
0m	1500	0.149		1.227	0.011	0.010	0.012
Trib 2095m	932	0.585	0.003	1.902	0.018	BD	?
Trib 2095m	1205	0.583		1.894	0.022	0.008	0.014
Trib 2095m	1500	0.591	0.003	1.937	0.001	BD	?
Trib 915m	934	0.292	0.006	—	—	0.001	0.001
Trib 915m	1203	0.278		—	—	0.011	0.015
Trib 915m	1502	0.280	0.008	1.467	0.010	BD	?
Trib 670m	933	0.016	0.001	—	—	BD	?
Trib 670m	1203	0.015	0.000	1.080	0.007	BD	?
Trib 670m	1506	0.018	0.000	1.102	0.023	BD	?
Trib 460m	932	0.757	0.009	—		BD	?
Trib 460m	1202	0.777	0.000	—	—	BD	?
Trib 460m	1502	0.783	0.021	2.145	0.017	BD	?

BD = *below detection limits*

Table A.2: Calculated instream mass-flows, upper Snake River diel study

Site ID	Time	Fe^{2+} (g s^{-1})	Readily Soluble Fe (g s^{-1})	FeT (g s^{-1})	Cu (FA) (mg s^{-1})	Cu (RA) (mg s^{-1})	Mn (g s^{-1})
				Mass-Flows			
2250m	930	0.166	0.227	0.304	4.694	4.654	0.077
2250m	1002	0.200	0.241	0.304	5.098	4.319	0.074
2250m	1100	0.213	0.251	0.304	4.977	5.260	0.076
2250m	1200	0.203	0.240	0.299	4.885	5.023	0.077
2250m	1318	0.245	0.255	0.290	4.555	4.948	0.078
2250m	1400	0.219	0.254	0.294	4.613	4.538	0.075
2250m	1500	0.219	0.235	0.278	5.300	4.336	0.075
2120m	930	0.225	0.206	0.275	5.139	4.600	0.071
2120m	1200	0.237	0.229	0.277	4.826	4.896	0.072
2120m	1503	0.177	0.212	0.255	4.476	4.513	0.073
2085m	930	—	—	0.235	2.281	2.294	0.045
2085m	1200	0.176	0.188	0.231	2.724	2.736	0.047
2085m	1457	0.150	0.175	0.215	2.484	2.058	0.047
1935m	941	0.093	0.087	0.237	2.668	3.003	0.043
1935m	1205	0.178	0.197	0.235	2.566	3.197	0.043
1935m	1508	0.159	0.177	0.215	2.638	2.558	0.043
1875m	930	0.195	0.234	0.284	2.829	2.660	0.048
1875m	1200	0.199	0.231	0.283	3.265	3.321	0.050
1875m	1500	0.179	0.217	0.264	3.171	2.857	0.050
940m	930	0.194	0.234	0.282	3.355	2.959	0.046
940m	1200	0.185	0.226	0.281	2.921	3.498	0.048
940m	1505	0.182	0.218	0.261	3.494	3.115	0.046
900m	937	0.083	0.113	0.182	0.832	0.799	0.025
900m	1205	0.113	0.147	0.173	0.853	0.744	0.025
900m	1500	0.124	0.146	0.174	0.777	0.725	0.025
700m	930	0.117	0.150	0.178	0.947	0.924	0.023
700m	1200	0.129	0.143	0.172	1.022	0.744	0.024
700m	1508	0.116	0.162	0.168	0.953	1.109	0.024
485m	934	0.132	0.163	0.218	0.987	1.065	0.028
485m	1204	0.134	0.177	0.210	0.965	0.719	0.028
485m	1504	0.142	0.175	0.208	0.980	0.859	0.027
450m	930	0.075	0.084	0.102	0.298	0.569	0.011
450m	1200	0.069	0.078	0.099	0.357	0.539	0.011
450m	1500	0.077	0.084	0.098	0.400	0.215	0.011
0m	915	0.033	0.033	0.040	0.199	0.212	0.006
0m	1000	0.034	0.034	0.041	0.267	0.164	0.006
0m	1100	0.034	0.036	0.040	0.229	0.125	0.005
0m	1200	0.032	0.032	0.038	0.196	0.265	0.005
0m	1300	0.032	0.032	0.038	0.135	0.199	0.005
0m	1400	0.033	0.032	0.055	0.185	0.188	0.006
0m	1500	0.032	0.033	0.040	0.282	0.118	0.006
Trib	932	0.011	0.019	0.024	1.692	1.511	0.018
Trib	1205	0.010	0.020	0.024	1.831	1.540	0.018
Trib	1500	0.014	0.020	0.023	1.659	1.684	0.018
Trib 915m	934	0.030	0.041	0.049	1.304	1.325	0.010
Trib 915m	1203	0.034	—	0.046	1.355	1.250	0.010
Trib 915m	1502	0.030	0.036	0.046	1.351	1.266	0.010
Trib 670m	933	0.000	0.000	0.001	0.029	0.026	0.000
Trib 670m	1203	0.001	0.000	0.000	0.039	0.017	0.000
Trib 670m	1506	0.000	0.000	0.001	0.026	0.030	0.000
Trib 460m	932	0.018	0.018	0.060	0.357	0.373	0.008
Trib 460m	1202	0.017	0.017	0.060	0.361	0.360	0.008
Trib 460m	1502	0.018	0.016	0.060	0.374	0.355	0.008

Table A.2: Calculated instream mass-flows, upper Snake River diel study

Site ID	Time	Zn (g s^{-1})	Al (g s^{-1})	Mg (g s^{-1})	SO$_4$ (g s^{-1})	Ca (g s^{-1})	Na (g s^{-1})
				Mass-Flows			
2250m	930	0.583	0.033	0.631	0.14	0.388	10.567
2250m	1002	0.581	0.033	0.636	0.14	0.385	10.507
2250m	1100	0.574	0.032	0.619	0.13	0.391	10.525
2250m	1200	0.579	0.032	0.622	0.13	—	10.573
2250m	1318	0.580	0.032	0.621	0.15	0.389	10.551
2250m	1400	0.586	0.032	0.618	0.13	0.392	10.501
2250m	1500	0.573	0.032	0.612	0.13	0.396	10.553
2120m	930	0.539	0.030	0.589	0.14	—	9.875
2120m	1200	0.556	0.031	0.617	0.12	0.371	9.807
2120m	1503	0.545	0.030	0.586	0.12	0.371	9.852
2085m	930	0.361	0.019	0.278	0.11	—	—
2085m	1200	0.367	0.018	0.278	0.11	—	7.517
2085m	1457	0.361	0.018	0.277	0.11	0.278	7.560
1935m	941	0.360	0.018	0.274	0.11	0.272	7.580
1935m	1205	0.354	0.018	0.263	0.11	0.275	7.474
1935m	1508	0.356	0.018	0.264	0.11	0.277	7.500
1875m	930	0.402	0.021	0.309	0.12	0.302	8.535
1875m	1200	0.405	0.021	0.306	0.12	0.301	8.554
1875m	1500	0.406	0.021	0.305	0.13	0.307	8.566
940m	930	0.359	0.021	0.297	0.11	0.259	7.718
940m	1200	0.360	0.021	0.292	0.11	—	7.718
940m	1505	0.357	0.021	0.293	0.11	0.258	7.688
900m	937	0.240	0.010	0.180	0.07	0.145	4.320
900m	1205	0.239	0.010	0.177	0.07	0.146	4.318
900m	1500	0.236	0.010	0.177	0.07	0.149	4.315
700m	930	0.229	0.010	0.180	0.08	—	4.149
700m	1200	0.229	0.010	0.179	0.07	0.141	4.175
700m	1508	0.232	0.010	0.174	0.07	0.142	4.152
485m	934	0.262	0.012	0.207	0.07	0.155	4.573
485m	1204	0.262	0.012	0.209	0.07	—	4.557
485m	1504	0.262	0.012	0.207	0.07	0.159	4.568
450m	930	0.122	0.005	0.076	0.05	—	2.432
450m	1200	0.121	0.005	0.074	0.05	0.087	2.423
450m	1500	0.122	0.005	0.074	0.05	0.089	2.425
0m	915	0.069	0.002	0.013	0.05	—	1.155
0m	1000	0.071	0.002	0.012	0.05	—	1.158
0m	1100	0.069	0.002	0.013	0.05	—	1.126
0m	1200	0.067	0.002	0.013	0.05	—	1.128
0m	1300	0.067	0.002	0.013	0.05	0.047	1.110
0m	1400	0.071	0.002	0.017	0.05	0.047	1.158
0m	1500	0.071	0.002	0.013	0.06	0.048	1.191
Trib 2095m	932	0.128	0.009	0.267	0.01	0.058	1.344
Trib 2095m	1205	0.128	0.009	0.262	0.01	0.058	1.346
Trib 2095m	1500	0.130	0.009	0.263	0.01	0.059	1.341
Trib 915m	934	0.052	0.005	0.056	0.02	—	1.242
Trib 915m	1203	0.051	0.005	0.055	0.02	—	1.203
Trib 915m	1502	0.052	0.005	0.055	0.01	0.052	1.201
Trib 670m	933	0.010	0.000	0.001	0.01	—	0.151
Trib 670m	1203	0.009	0.000	0.000	0.01	0.009	0.147
Trib 670m	1506	0.010	0.000	0.001	0.01	0.009	0.152
Trib 460m	932	0.060	0.004	0.069	0.01	—	0.474
Trib 460m	1202	0.062	0.004	0.070	0.01	—	0.474
Trib 460m	1502	0.062	0.004	0.070	0.01	0.023	0.471

Table A.3: Confluence inflows, upper Snake River diel study

Discharge		
	Measured Tributary Inflow	**Calculated Lateral Inflow**
	$m^3\ s^{-1}$	$m^3\ s^{-1}$
0-450 m	—	0.024
450-485 m (trib 460 m)	0.011	0.031
485 -700 m (trib 670 m)	0.008	-0.017
700-900m	—	0.003
900-940 m (trib 915 m)	0.036	0.041
940-1875 m	—	0.020
1875-1935 m	—	-0.004
1935-2085 m	—	-0.019
2085-2120 m (trib 2095 m)	0.031	0.022
2120-2250 m	—	0.016

Table A.4: Inflow concentrations, upper Snake River diel study

Between Sites:		Confluence Zones							
		450 and 485 m		**485 and 700 m**		**900 and 940 m**		**2085 and 2120 m**	
		sampled tributary (460 m)	calculated lateral	sampled tributary (670 m)	calculated lateral*	sampled tributary (915 m)	calculated lateral	sampled tributary (2095 m)	calculated lateral
Readily Soluble									
Fe	$(mg\,L^{-1})$	1.568	2.353	0.028	—	1.090	1.256	0.640	0.678
Fe^{2+}	$(mg\,L^{-1})$	1.651	1.457	0.051	—	0.872	1.193	0.383	1.765
FeT	$(mg\,L^{-1})$	5.561	1.705	0.076	—	1.317	1.237	0.773	0.833
Zn	$(mg\,L^{-1})$	0.349	0.112	0.019	—	0.150	0.127	0.304	0.122
Al	$(mg\,L^{-1})$	6.474	2.053	0.071	—	1.547	1.469	8.643	2.546
Mn	$(mg\,L^{-1})$	0.773	0.276	0.016	—	0.283	0.280	0.587	0.368
Mg	$(mg\,L^{-1})$	5.741	2.552	1.231	—	1.445	1.666	4.208	2.527
Na	$(mg\,L^{-1})$	2.145	1.492	1.091	—	1.467	1.451	1.911	1.602
Ca	$(mg\,L^{-1})$	0.498	0.631	1.627	—	0.429	0.521	0.362	0.349
SO$_4$	$(mg\,L^{-1})$	43.939	53.975	19.072	—	34.061	52.599	43.934	44.144
Cu(FA)	$(\mu g\,L^{-1})$	33.814	8.479	4.007	—	37.461	26.588	56.480	27.064

= losing reach

Between Sites:		Stream Reaches			
		0 and 450 m	700 and 900 m	940 and 1875 m	2120 and 2250 m
Readily Soluble					
Fe	$(mg\,L^{-1})$	0.059	SL	0.002	0.049
Fe^{2+}	$(mg\,L^{-1})$	0.049	SL	0.005	SL
FeT	$(mg\,L^{-1})$	0.070	0.031	0.004	0.049
Zn	$(mg\,L^{-1})$	0.003	SL	0.000	0.003
Mg	$(mg\,L^{-1})$	0.063	0.071	0.065	0.059
Na	$(mg\,L^{-1})$	0.049	0.041	0.063	0.034
Ca	$(mg\,L^{-1})$	SL	0.006	0.020	0.016
Al	$(mg\,L^{-1})$	0.074	0.003	0.018	0.045
Mn	$(mg\,L^{-1})$	0.006	0.011	0.004	0.007
SO$_4$	$(mg\,L^{-1})$	1.543	1.326	1.205	1.241
Cu(RA)	$(\mu g\,L^{-1})$	0.312	SL	SL	0.099
Cu(FA)	$(\mu g\,L^{-1})$	0.166	SL	SL	0.109

SL = solute loss occurred between sites

Table A.5: Inflow mass-flows, upper Snake River diel study

Between Sites:	Confluence Zones							
	450 and 485m		485 and 700 m		900 and 940m		2085 and 2120m	
	sampled tributary (460m)	calculated lateral	sampled tributary (670 m)	calculated lateral*	sampled tributary (915m)	calculated lateral	sampled tributary (2095m)	calculated lateral
Readily Soluble								
Fe $(g\,s^{-1})$	0.017	0.073	0.000	—	0.039	0.052	0.020	0.015
Fe^{2+} $(g\,s^{-1})$	0.018	0.045	0.000	—	0.031	0.049	0.012	0.038
FeT $(g\,s^{-1})$	0.060	0.053	0.001	—	0.047	0.051	0.024	0.018
Zn $(g\,s^{-1})$	0.004	0.003	0.000	—	0.005	0.005	0.009	0.003
Al $(g\,s^{-1})$	0.070	0.063	0.001	—	0.055	0.061	0.264	0.056
Mn $(g\,s^{-1})$	0.008	0.009	0.000	—	0.010	0.012	0.018	0.008
Mg $(g\,s^{-1})$	0.062	0.079	0.010	—	0.052	0.069	0.129	0.055
Na $(g\,s^{-1})$	0.023	0.046	0.009	—	0.052	0.060	0.058	0.035
Ca $(g\,s^{-1})$	0.005	0.019	0.013	—	0.015	0.022	0.011	0.008
SO$_4$ $(g\,s^{-1})$	0.473	1.666	0.150	—	1.215	2.175	1.344	0.963
Cu(FA) $(mg\,s^{-1})$	0.364	0.262	0.032	—	1.337	1.099	1.727	0.590

= losing reach

Between Sites:	Stream Reaches			
	0-450m	700-900m	940-1875m	2120-2250m
Readily Soluble				
Fe $(g\,s^{-1})$	0.049	-0.016	0.002	0.028
Fe^{2+} $(g\,s^{-1})$	0.041	-0.014	0.004	-0.004
FeT $(g\,s^{-1})$	0.058	0.004	0.003	0.027
Zn $(g\,s^{-1})$	0.003	0.000	0.000	0.002
Mg $(g\,s^{-1})$	0.052	0.009	0.045	0.033
Na $(g\,s^{-1})$	0.040	0.005	0.044	0.019
Ca $(g\,s^{-1})$	-0.004	0.001	0.014	0.009
Al $(g\,s^{-1})$	0.061	0.000	0.013	0.025
Mn $(g\,s^{-1})$	0.005	0.001	0.003	0.004
SO$_4$ $(g\,s^{-1})$	1.280	0.159	0.844	0.695
Cu(RA) $(mg\,s^{-1})$	0.259	-0.169	-0.244	0.056
Cu(FA) $(mg\,s^{-1})$	0.138	-0.153	-0.168	0.061

Table A.6: Sampling data, Snake River Watershed synoptic study

July Data					
Site	**Data**	**Time**	**pH**	**Discharge** $m^3\ s^{-1}$	**DOC** *NPOC mg L^{-1}*
SN1	7/28/00	10:45	4.1	0.12	—
SN2	7/28/00	10:15	5.6	0.25	—
SN3	7/28/00	13:10	6.5	0.35	—
SN4	7/27/00	17:30	7.0	0.80	—
SN5	7/27/00	17:30	6.4	1.35	—
SN6	7/28/00	15:00	6.3	1.35	—
SN7	7/28/00	16:50	6.8	1.01	—
SN8	7/28/00	16:45	7.0	1.44	—
PR1	7/26/00	13:00	6.7	—	—
PR2	7/26/00	16:00	5.2	—	—
PR3	7/27/00	14:00	4.3	—	—
PR4	7/27/00	14:30	5.1	—	—
PR5	7/27/00	17:30	5.9	0.83	—
DC1	7/28/00	10:30	7.3	0.16	—
PN1	7/27/00	10:15	3.2	—	—
CH1	7/27/00	13:45	7.3	—	—
NF1	7/28/00	16:30	7.5	0.40	—

August Data					
Site	**Data**	**Time**	**pH**	**Discharge** $m^3\ s^{-1}$	**DOC** *NPOC mg L^{-1}*
SN1	8/24/00	10:50	4.1	0.12	0.92
SN2	8/24/00	11:10	5.4	0.25	0.91
SN3	8/24/00	13:15	6.2	0.28	0.71
SN4	8/24/00	14:00	6.9	0.44	1.03
SN5	8/24/00	14:00	6.4	1.35	0.62
SN6	8/24/00	17:45	6.6	1.10	0.73
SN7	8/25/00	15:30	7.0	0.90	1.67
SN8	8/25/00	15:30	7.1	1.42	1.63
PR1	8/25/00	11:30	6.2	0.13	0.49
PR2	8/25/00	11:40	5.9	0.17	0.67
PR3	8/25/00	13:20	4.7	0.33	—
PR4	8/25/00	13:35	5.3	0.57	0.74
PR5	8/24/00	14:00	6.3	0.42	0.48
DC1	8/24/00	10:50	6.6	0.11	1.83
PN1	8/25/00	10:45	3.6	0.02	0.89
CH1	8/25/00	13:30	6.5	0.39	1.46
NF1	8/25/00	15:50	7.1	0.44	—

Table A.6: Sampling data, Snake River Watershed synoptic study

	July Solute Concentrations

Site	Fe		SO$_4$	Cu		Zn		Pb	
	mg L^{-1}	StdDev	mg L^{-1}	µg L^{-1}	StdDev	mg L^{-1}	StdDev	mg L^{-1}	StdDev
SN1	0.783	0.001	77.73	18.70	0.344	0.661	0.002	0.016	0.001
SN2	0.232	0.006	42.86	7.48	0.482	0.354	0.007	0.013	0.000
SN3	0.122	0.000	43.50	1.92	0.255	0.268	0.012	0.021	0.001
SN4	0.086	0.001	44.58	2.04	0.040	0.211	0.006	0.017	0.001
SN5	0.027	0.001	46.80	8.63	0.230	0.530	0.006	0.010	0.001
SN6	0.049	0.000	44.07	8.01	0.181	0.470	0.002	0.013	0.001
SN7	0.010	0.014	41.95	3.98	3.267	0.388	0.001	0.019	0.005
SN8	0.039	0.001	30.88	5.26	0.043	0.199	0.001	0.014	0.000
PR1	0.012	0.001	35.80	16.29	0.128	0.432	0.011	0.016	0.000
PR2	0.375	0.003	53.51	175.65	2.968	1.617	0.006	0.020	0.000
PR3	0.293	0.006	72.57	105.25	1.680	1.558	0.011	0.020	0.001
PR4	0.211	0.002	55.77	78.55	0.312	1.265	0.046	0.021	0.000
PR5	0.089	0.003	47.19	45.51	0.147	1.043	0.019	0.022	0.001
DC1	0.098	0.006	8.39	1.56	0.383	0.029	0.002	0.014	0.000
PN1	40.363	0.733	691.00	5779.0	34.635	36.571	0.050	0.033	0.001
CH1	0.077	0.001	16.36	0.50	0.312	0.166	0.005	0.020	0.002
NF1	0.053	0.002	5.42	1.01	0.207	0.018	0.003	0.013	0.001

	August Solute Concentrations

Site	Fe		SO$_4$	Cu		Zn		Pb	
	mg L^{-1}	StdDev	mg L^{-1}	µg L^{-1}	StdDev	mg L^{-1}	StdDev	mg L^{-1}	StdDev
SN1	0.873	0.004	86.89	22.44	0.047	0.845	0.006	0.012	0.000
SN2	0.392	0.006	60.91	11.25	0.039	0.471	0.003	0.018	0.003
SN3	0.251	0.000	57.22	7.73	0.253	0.417	0.002	0.016	0.000
SN4	0.035	0.000	54.77	3.46	0.079	0.386	0.010	0.014	0.001
SN5	0.090	0.002	55.00	19.21	0.075	0.730	0.004	0.025	0.002
SN6	0.032	0.000	52.42	6.70	0.033	0.580	0.001	0.033	0.001
SN7	0.016	0.000	47.00	5.10	0.048	0.395	0.002	0.014	0.000
SN8	0.058	0.000	28.48	3.62	0.030	0.187	0.004	0.014	0.000
PR1	0.014	0.000	45.16	13.67	0.059	0.347	0.005	0.013	0.001
PR2	0.155	0.003	57.27	96.89	0.089	1.100	0.006	0.017	0.002
PR3	0.212	0.001	82.52	89.92	0.540	1.454	0.021	0.025	0.001
PR4	0.150	0.002	65.20	62.27	0.003	1.072	0.000	0.031	0.001
PR5	0.117	0.001	55.06	43.26	0.018	0.989	0.006	0.024	0.001
DC1	0.135	0.003	11.92	1.83	0.311	0.051	0.001	0.026	0.001
PN1	27.332	0.584	602.00	4269.4	16.029	29.433	0.122	0.033	0.001
CH1	0.093	0.001	20.75	1.88	1.327	0.015	0.002	0.020	0.003
NF1	0.107	0.001	6.88	1.76	0.035	0.038	0.002	0.024	0.001

Table A.6: Sampling data, Snake River Watershed synoptic study

Site	July Solute Concentrations								
	Mn		**Al**		**Ca**		**Mg**		**Cl**
	$mg\ L^{-1}$	StdDev	$mg\ L^{-1}$	StdDev	$mg\ L^{-1}$	StdDev	$mg\ L^{-1}$	StdDev	$mg\ L^{-1}$
SN1	0.878	0.008	3.663	0.015	7.830	0.009	4.271	0.042	0.18
SN2	0.441	0.003	0.581	0.005	8.571	0.336	2.922	0.020	0.22
SN3	0.339	0.000	0.029	0.007	9.927	0.198	2.911	0.025	0.85
SN4	0.335	0.019	0.183	0.000	12.403	0.525	2.984	0.029	0.71
SN5	0.521	0.008	0.051	0.001	11.747	0.060	2.802	0.007	0.81
SN6	0.417	0.009	0.136	0.002	11.909	0.306	2.744	0.034	0.60
SN7	0.166	0.234	0.051	0.000	6.362	8.304	1.374	1.857	1.02
SN8	0.203	0.006	0.057	0.000	11.087	0.267	2.281	0.001	3.63
PR1	0.229	0.005	0.062	0.001	8.157	0.153	2.364	0.011	1.62
PR2	0.986	0.003	0.559	0.021	10.479	0.068	3.071	0.057	2.02
PR3	1.159	0.013	2.505	0.069	11.653	0.261	3.536	0.033	1.19
PR4	0.895	0.013	1.742	0.038	10.908	0.383	3.008	0.011	0.92
PR5	0.634	0.017	0.134	0.001	10.824	0.758	2.559	0.015	0.89
DC1	0.016	0.001	0.021	0.000	8.414	0.102	1.493	0.007	1.93
PN1	21.579	0.179	18.839	0.602	81.720	2.752	23.217	0.288	0.63
CH1	0.004	0.000	0.056	0.002	8.427	0.097	1.436	0.002	1.05
NF1	0.007	0.000	0.024	0.000	8.540	0.640	1.592	0.036	3.84

Site	August Solute Concentrations								
	Mn		**Al**		**Ca**		**Mg**		**Cl**
	$mg\ L^{-1}$	StdDev	$mg\ L^{-1}$	StdDev	$mg\ L^{-1}$	StdDev	$mg\ L^{-1}$	StdDev	$mg\ L^{-1}$
SN1	1.234	0.007	5.493	0.025	9.336	0.157	5.407	0.032	1.50
SN2	0.697	0.011	2.040	0.039	9.430	0.371	3.806	0.044	1.05
SN3	0.528	0.003	0.471	0.007	11.073	0.295	3.612	0.011	0.48
SN4	0.489	0.002	0.114	0.002	14.784	0.462	3.724	0.006	1.21
SN5	0.638	0.006	0.157	0.003	13.353	0.186	3.210	0.010	2.14
SN6	0.522	0.002	0.050	0.002	13.502	0.213	3.206	0.017	2.14
SN7	0.381	0.001	0.046	0.000	13.035	0.316	2.965	0.001	1.85
SN8	0.221	0.000	0.057	0.001	12.201	0.139	2.507	0.006	2.65
PR1	0.251	0.000	0.032	0.001	10.797	0.148	3.124	0.020	2.38
PR2	0.795	0.002	0.094	0.002	12.686	0.015	3.653	0.033	1.39
PR3	1.252	0.016	2.498	0.061	13.622	0.177	4.013	0.012	1.43
PR4	0.901	0.009	1.272	0.020	12.846	0.317	3.378	0.012	0.88
PR5	0.725	0.001	0.093	0.002	12.378	0.123	2.959	0.030	1.23
DC1	0.037	0.000	0.027	0.001	10.004	0.490	1.846	0.008	1.96
PN1	20.878	0.324	15.140	0.466	78.371	0.163	22.695	0.168	0.86
CH1	0.007	0.000	0.025	0.001	9.628	0.117	1.634	0.015	0.57
NF1	0.015	0.000	0.065	0.003	9.998	0.012	1.904	0.005	8.94

Table A.7: Calculated instream mass-flows, Snake River Watershed synoptic study

	July Solute Mass-Flows									
	Fe	**SO4**	**Cu**	**Zn**	**Pb**	**Mn**	**Al**	**Ca**	**Mg**	**Cl**
Site	$g\,s^{-1}$	$g\,s^{-1}$	$mg\,s^{-1}$	$g\,s^{-1}$	$g\,s^{-1}$	$g\,s^{-1}$	$g\,s^{-1}$	$g\,s^{-1}$	$g\,s^{-1}$	$g\,s^{-1}$
SN1	0.097	9.62	2.314	0.082	0.002	0.109	0.453	0.969	0.529	0.023
SN2	0.058	10.78	1.881	0.089	0.003	0.111	—	2.155	0.735	0.057
SN3	0.043	15.29	0.676	0.094	0.007	0.119	0.010	3.489	1.023	0.297
SN4	0.069	35.85	1.640	0.170	0.014	0.269	—	9.974	2.399	0.567
SN5	0.036	63.07	11.632	0.714	0.014	0.702	0.069	15.830	3.776	1.093
SN6	0.066	59.35	10.787	0.634	0.017	0.562	0.183	16.038	3.695	0.808
SN7	0.011	42.26	4.009	0.390	0.019	0.167	0.051	6.408	1.384	1.031
SN8	0.057	44.60	7.600	0.288	0.021	0.293	0.082	16.011	3.293	5.239
PR1	—	—	—	—	—	—	—	—	—	—
PR2	—	—	—	—	—	—	—	—	—	—
PR3	—	—	—	—	—	—	—	—	—	—
PR4	—	—	—	—	—	—	—	—	—	—
PR5	0.073	39.06	37.672	0.863	0.019	0.525	NA	8.959	2.118	0.738
DC1	0.016	1.36	0.253	0.005	0.002	0.003	0.003	1.365	0.242	0.314
PN1	—	—	—	—	—	—	—	—	—	—
CH1	—	—	—	—	—	—	—	—	—	—
NF1	0.021	2.19	0.407	0.007	0.005	0.003	0.010	3.451	0.643	1.551

	August Solute Mass-Flows									
	Fe	**SO4**	**Cu**	**Zn**	**Pb**	**Mn**	**Al**	**Ca**	**Mg**	**Cl**
Site	$g\,s^{-1}$	$g\,s^{-1}$	$mg\,s^{-1}$	$g\,s^{-1}$	$g\,s^{-1}$	$g\,s^{-1}$	$g\,s^{-1}$	$g\,s^{-1}$	$g\,s^{-1}$	$g\,s^{-1}$
SN1	0.104	10.33	2.669	0.101	0.001	0.147	0.653	1.110	0.643	0.178
SN2	0.097	15.06	2.781	0.116	0.005	0.172	0.504	2.331	0.941	0.260
SN3	0.070	15.86	2.142	0.116	0.004	0.146	0.130	3.070	1.001	0.134
SN4	0.016	24.05	1.520	0.170	0.006	0.215	0.050	6.493	1.635	0.531
SN5	0.121	74.18	25.916	0.984	0.034	0.860	0.212	18.010	4.330	2.883
SN6	0.035	57.59	7.363	0.637	0.036	0.573	0.055	14.835	3.522	2.356
SN7	0.014	42.52	4.613	0.358	0.012	0.345	0.041	11.793	2.683	1.675
SN8	0.081	40.32	5.121	0.265	0.020	0.313	0.080	17.275	3.549	3.747
PR1	0.002	5.96	1.804	0.046	0.002	0.033	0.004	1.425	0.412	0.313
PR2	0.026	9.52	16.106	0.183	0.003	0.132	0.016	2.109	0.607	0.231
PR3	0.070	27.29	29.742	0.481	0.008	0.414	0.826	4.505	1.327	0.472
PR4	0.085	37.15	35.476	0.611	0.018	0.514	0.725	7.319	1.924	0.503
PR5	0.049	23.11	18.156	0.415	0.010	0.304	0.039	5.195	1.242	0.516
DC1	0.014	1.26	0.193	0.005	0.003	0.004	0.003	1.057	0.195	0.207
PN1	0.495	10.91	77.373	0.533	0.001	0.378	0.274	1.420	0.411	0.016
CH1	—	—	—	—	—	—	—	—	—	—
NF1	0.047	3.01	0.771	0.017	0.010	0.006	0.028	4.380	0.834	3.918

Table A.8: Metal oxide deposition data, Snake River Watershed synoptic study

July Oxide Data

Site	Oxide Mass	Metal Oxide Deposition						Percent of Total Oxide Deposition					
		Fe		Al		Zn		Fe		Al		Zn	
	g	$mg\ m^{-2}$	StdDev	$mg\ m^{-2}$	StdDev	$mg\ m^{-2}$	StdDev	% by mass	StdDev	% by mass	StdDev	% by mass	StdDev
SN1	0.050	96.52	17.64	7.86	0.72	0.41	0.26	6.10	0.84	0.497	0.022	0.03	0.02
SN2	0.255	123.71	37.09	1471.97	739.82	2.14	1.06	1.56	0.35	18.372	7.959	0.03	0.01
SN3	0.022	561.04	223.14	410.25	10.50	6.61	1.44	11.34	6.62	7.937	1.470	0.13	0.05
SN4	0.047	419.07	255.93	181.52	196.72	18.31	18.60	3.57	2.00	1.022	0.189	0.11	0.00
SN5	0.068	220.83	34.76	251.90	72.26	5.00	0.99	5.32	0.11	6.019	0.925	0.12	0.01
SN6	0.067	667.69	475.70	728.15	585.75	47.25	36.89	8.59	0.25	8.943	0.898	0.59	0.04
SN7	0.048	93.74	13.26	112.00	32.30	13.35	3.24	2.67	0.23	3.181	0.744	0.38	0.07
SN8	0.084	87.76	—	95.66	—	51.93	—	0.38	—	0.417	—	0.23	—
PR1	0.191	126.29	108.52	956.03	1.21	8.00	2.90	1.61	1.27	12.781	1.354	0.10	0.03
PR2	0.243	763.01	15.65	2030.36	458.22	5.94	2.08	6.14	1.12	15.993	0.369	0.05	0.01
PR3	0.153	1421.51	277.72	186.93	26.93	1.79	0.09	23.81	1.54	3.201	0.874	0.03	0.01
PR4	0.697	262.67	96.84	2879.25	390.45	1.94	0.53	1.56	0.33	17.414	0.502	0.01	0.00
PR5	0.062	51.49	7.13	72.81	0.94	1.54	0.14	3.20	0.35	3.806	1.205	0.10	0.01
DC1	0.023	150.70	109.68	18.10	7.63	8.12	2.66	4.70	2.74	0.582	0.143	0.28	0.14
PN1	3.177	18278.2	456.49	394.59	52.79	8.91	1.61	16.85	0.42	0.364	0.049	0.01	0.00
CH1	0.155	50.91	17.64	30.19	12.67	1.35	0.10	1.20	0.21	0.704	0.179	0.03	0.01
NF1	0.012	47.80	—	13.22	—	0.56	—	2.44	—	1.023	—	0.03	—

August Oxide Data

Site	Oxide Mass	Metal Oxide Deposition						Percent of Total Oxide Deposition					
		Fe		Al		Zn		Fe		Al		Zn	
	g	$mg\ m^{-2}$	StdDev	$mg\ m^{-2}$	StdDev	$mg\ m^{-2}$	StdDev	% by mass	StdDev	% by mass	StdDev	% by mass	StdDev
SN1	0.063	164.80	174.40	28.99	27.34	0.52	0.09	9.92	2.75	1.924	0.094	0.06	0.05
SN2	0.300	162.81	33.64	1334.86	62.07	1.37	0.24	2.08	0.48	16.972	0.370	0.02	0.00
SN3	0.222	44.39	37.50	75.65	10.53	1.64	0.89	3.53	0.49	8.350	5.385	0.15	0.04
SN4	0.570	59.95	12.25	62.85	27.23	8.68	4.23	3.79	0.91	3.766	0.004	0.51	0.03
SN5	0.156	68.62	38.67	207.29	58.23	4.19	2.04	4.03	0.74	12.965	1.662	0.25	0.02
SN6	0.229	146.85	177.44	183.51	206.09	14.25	16.83	5.17	0.11	7.675	1.878	0.53	0.04
SN7	0.086	46.88	42.94	72.06	55.53	7.12	5.49	3.38	0.56	5.904	2.259	0.58	0.22
SN8	0.552	32.22	22.18	36.25	19.87	4.03	2.50	2.18	2.01	2.811	2.853	0.29	0.28
PR1	0.254	74.46	10.28	340.80	161.37	6.64	0.23	2.32	0.65	10.141	3.437	0.21	0.04
PR2	0.564	304.47	7.64	578.28	164.50	7.89	8.08	6.30	1.88	12.396	6.662	0.14	0.12
PR3	0.255	809.34	620.85	113.82	60.84	1.26	0.36	20.26	5.55	3.081	0.060	0.04	0.01
PR4	0.671	402.86	394.08	1638.08	276.21	4.41	0.56	2.59	1.92	13.329	7.029	0.04	0.02
PR5	0.072	80.03	—	217.36	—	2.67	—	2.73	—	7.412	—	0.09	—
DC1	0.079	21.69	3.66	9.10	1.04	1.60	0.34	2.96	0.43	1.243	0.115	0.22	0.05
PN1	3.834	16375.3	59.70	125.97	27.21	8.73	0.92	24.58	3.09	0.187	0.016	0.01	0.00
CH1	0.155	—	—	—	—	—	—	—	—	—	—	—	—
NF1	0.066	3.75	0.85	2.51	0.02	0.23	0.10	1.64	0.28	1.148	0.456	0.10	0.00

Table A.9: Periphyton data, Snake River Watershed synoptic study

Site	July Periphyton Data		
	Mean Chl *a*	Mean AFDM	AFDM Deposition Rate
	$mg\ m^{-2}$	$mg\ m^{-2}$	$mg\ m^{-2}\ d^{-1}$
SN1	BD	813.92	—
SN2	0.033	3375.67	—
SN3	BD	2280.16	—
SN4	BD	474.36	—
SN5	BD	924.52	—
SN6	0.330	3908.98	—
SN7	0.359	1252.88	—
SN8	0.078	772.53	—
PR1	0.184	2246.56	—
PR2	0.070	7380.87	—
PR3	0.245	2501.67	—
PR4	0.013	7809.45	—
PR5	0.217	1045.47	—
DC1	0.309	972.02	—
PN1	0.107	44753.34	—
CH1	0.559	678.71	—
NF1	0.108	387.01	—

Site	August Periphyton Data		
	Mean Chl *a*	Mean AFDM	AFDM Deposition Rate
	$mg\ m^{-2}$	$mg\ m^{-2}$	$mg\ m^{-2}\ d^{-1}$
SN1	0.160	501.19	18.56
SN2	0.022	3971.07	147.08
SN3	0.033	1397.41	51.76
SN4	0.194	1449.20	51.76
SN5	BD	1144.17	40.86
SN6	BD	652.95	24.18
SN7	0.249	1523.73	54.42
SN8	0.157	673.18	24.04
PR1	0.020	1019.30	33.98
PR2	BD	—	0.00
PR3	0.237	1849.63	63.78
PR4	0.064	5666.24	195.39
PR5	BD	959.21	34.26
DC1	0.300	218.41	8.09
PN1	0.098	15681.74	540.75
CH1	0.495	592.52	20.43
NF1	0.083	630.13	22.50

BD = *below detection limits*

Table A.10: Confluence inflows, Snake River Watershed synoptic study

July		Measured Tributary $m^3\ s^{-1}$	Calculated Lateral $m^3\ s^{-1}$
Between Sites:	**Tributary**		
SN1 and SN2	DC1	0.16	-0.03
SN2 and SN3		—	0.10
SN3 and SN4		—	0.45
SN4 and SN5	PR5	0.83	-0.28
SN5 and SN6		—	0.00
SN6 and SN7		—	-0.34
SN7 and SN8	NF1	0.40	0.03
PR1 and PR2[‡]	PN1	—	—
PR2 and PR3[‡]		—	—
PR3 and PR4[‡]	CH1	—	—
PR4 and PR5[‡]		—	—

[‡] *= flow data not collected so mass-flow calculations could not be made*

August		Measured Tributary $m^3\ s^{-1}$	Calculated Lateral $m^3\ s^{-1}$
Between Sites:	**Tributary**		
SN1 and SN2	DC1	0.11	0.02
SN2 and SN3		—	0.03
SN3 and SN4		—	0.16
SN4 and SN5	PR5	0.42	0.49
SN5 and SN6		—	-0.25
SN6 and SN7		—	-0.19
SN7 and SN8	NF1	0.44	0.07
PR1 and PR2	PN1	0.02	0.02
PR2 and PR3		—	0.16
PR3 and PR4	CH1	0.39	-0.15
PR4 and PR5		—	-0.15

Table A.11: Inflow concentrations, Snake River Watershed synoptic study

		July: Confluence Zones									
	Between Sites:	SN1 and SN2[†]		SN4 and SN5[†]		SN7 and SN8		PR1 and PR2[*]		PR3 and PR4[*]	
		sampled tributary (DC1)	calculated lateral	sampled tributary (PR5)	calculated lateral	sampled tributary (NF1)	calculated lateral	sampled tributary (PN1)	calculated lateral	sampled tributary (CH1)	calculated lateral
Fe	$(mg\,L^{-1})$	0.10	—	0.09	—	0.05	0.76	40.36	—	0.08	—
SO$_4$	$(mg\,L^{-1})$	8.39	—	47.19	—	5.42	4.55	691.00	—	16.36	—
Mn	$(mg\,L^{-1})$	0.02	—	0.63	—	0.01	3.73	21.58	—	0.00	—
Pb	$(mg\,L^{-1})$	0.01	—	0.02	—	0.01	SL	0.03	—	0.02	—
Cu	$(\mu g\,L^{-1})$	1.56	—	45.51	—	0.00	0.10	5779.00	—	0.50	—
Zn	$(mg\,L^{-1})$	0.03	—	1.04	—	0.02	SL	36.57	—	0.17	—
Al	$(mg\,L^{-1})$	0.02	—	0.13	—	0.02	0.64	18.84	—	0.06	—
Mg	$(mg\,L^{-1})$	1.49	—	2.56	—	1.59	38.54	23.22	—	1.44	—
Ca	$(mg\,L^{-1})$	8.41	—	10.82	—	8.54	187.29	81.72	—	8.43	—
Cl	$(mg\,L^{-1})$	1.93	—	0.89	—	3.84	80.88	0.63	—	1.05	—

		August: Confluence Zones									
	Between Sites:	SN1 and SN2		SN4 and SN5		SN7 and SN8		PR1 and PR2		PR3 and PR4[†]	
		sampled tributary (DC1)	calculated lateral	sampled tributary (PR5)	calculated lateral	sampled tributary (NF1)	calculated lateral	sampled tributary (PN1)	calculated lateral	sampled tributary (CH1)	calculated lateral
Fe	$(mg\,L^{-1})$	0.14	SL	0.12	0.12	0.11	0.28	27.33	SL	0.09	—
SO$_4$	$(mg\,L^{-1})$	11.92	152.93	55.06	55.15	6.88	SL	602.00	SL	20.75	—
Mn	$(mg\,L^{-1})$	0.04	0.96	0.73	0.70	0.01	SL	20.88	SL	0.01	—
Pb	$(mg\,L^{-1})$	0.03	0.02	0.02	0.04	0.02	SL	0.03	0.03	0.02	—
Cu	$(\mu g\,L^{-1})$	1.83	0.00	43.26	12.74	1.76	0.00	4269.4	SL	1.88	—
Zn	$(mg\,L^{-1})$	0.05	0.46	0.99	0.82	0.04	SL	29.43	SL	0.01	—
Al	$(mg\,L^{-1})$	0.03	SL	0.09	0.25	0.06	0.15	15.14	SL	0.02	—
Mg	$(mg\,L^{-1})$	1.85	4.54	2.96	2.97	1.90	0.44	22.70	SL	1.63	—
Ca	$(mg\,L^{-1})$	10.00	7.25	12.38	12.91	10.00	15.08	78.37	SL	9.63	—
Cl	$(mg\,L^{-1})$	1.96	0.00	1.23	3.75	8.94	SL	0.86	SL	0.57	—

[*] = flow data not collected so lateral calculations could not be made

[†] = negative lateral inflows calculated

SL = solute loss occurred between upstream and downstream sampling sites

Table A.11: Inflow concentrations, Snake River Watershed synoptic study

July: Stream Reaches							
Between Sites:	**SN2 and SN3**	**SN3 and SN4**	**SN5 and SN6***	**SN6 and SN7**[†]	**PR2 and PR3**[‡]	**PR4 and PR5**[‡]
Fe $(mg\,L^{-1})$	SL	0.002	—	—	—	—
SO$_4$ $(mg\,L^{-1})$	1.277	1.286	—	—	—	—
Mn $(mg\,L^{-1})$	0.002	0.009	—	—	—	—
Pb $(mg\,L^{-1})$	0.001	0.000	—	—	—	—
Cu $(\mu g\,L^{-1})$	0.000	0.060	—	—	—	—
Zn $(mg\,L^{-1})$	0.001	0.005	—	—	—	—
Al $(mg\,L^{-1})$	0.003	SL	—	—	—	—
Mg $(mg\,L^{-1})$	0.082	0.086	—	—	—	—
Ca $(mg\,L^{-1})$	0.378	0.406	—	—	—	—
Cl $(mg\,L^{-1})$	0.068	0.017	—	—	—	—

August: Stream Reaches							
Between Sites:	**SN2 and SN3**	**SN3 and SN4**	**SN5 and SN6**[†]	**SN6 and SN7**[†]	**PR2 and PR3**	**PR4 and PR5**[†]
Fe $(mg\,L^{-1})$	SL	SL	—	—	0.008	—
SO$_4$ $(mg\,L^{-1})$	0.760	1.432	—	—	3.059	—
Mn $(mg\,L^{-1})$	SL	0.012	—	—	0.049	—
Pb $(mg\,L^{-1})$	0.000	0.000	—	—	0.001	—
Cu $(\mu g\,L^{-1})$	SL	0.000	—	—	0.002	—
Zn $(mg\,L^{-1})$	SL	0.009	—	—	0.051	—
Al $(mg\,L^{-1})$	SL	SL	—	—	0.139	—
Mg $(mg\,L^{-1})$	0.057	0.111	—	—	0.124	—
Ca $(mg\,L^{-1})$	0.697	0.598	—	—	0.412	—
Cl $(mg\,L^{-1})$	SL	0.069	—	—	0.041	—

[‡] *= flow data not collected so mass-flow calculations could not be made*

[†] *= losing reaches*

* = no lateral gains or losses

SL *= solute loss occurred between upstream and downstream sampling sites*

Table A.12: Inflow mass-flows, Snake River Watershed synoptic study

July: Confluence Zones

Between Sites:		SN1 and SN2[†]		SN4 and SN5[†]		SN7 and SN8		PR1 and PR2[‡]		PR3 and PR4[‡]	
		sampled tributary (DC1)	calculated lateral	sampled tributary (PR5)	calculated lateral	sampled tributary (NF1)	calculated lateral	sampled tributary (PN1)	calculated lateral	sampled tributary (CH1)	calculated lateral
Fe	$(g\ s^{-1})$	0.016	—	0.073	—	0.021	0.025	—	—	—	—
SO_4	$(g\ s^{-1})$	1.362	—	39.056	—	2.192	0.149	—	—	—	—
Mn	$(g\ s^{-1})$	0.003	—	0.525	—	0.003	0.122	—	—	—	—
Pb	$(g\ s^{-1})$	0.002	—	0.019	—	0.005	-0.004	—	—	—	—
Cu	$(mg\ s^{-1})$	0.253	—	37.672	—	0.407	3.185	—	—	—	—
Zn	$(g\ s^{-1})$	0.005	—	0.863	—	0.007	-0.110	—	—	—	—
Al	$(g\ s^{-1})$	0.003	—	0.111	—	0.010	0.021	—	—	—	—
Mg	$(g\ s^{-1})$	0.643	—	2.118	—	0.643	1.266	—	—	—	—
Ca	$(g\ s^{-1})$	1.365	—	8.959	—	3.451	6.152	—	—	—	—
Cl	$(g\ s^{-1})$	0.314	—	0.738	—	1.551	2.657	—	—	—	—

August: Confluence Zones

Between Sites:		SN1 and SN2		SN4 and SN5		SN7 and SN8		PR1 and PR2		PR3 and PR4[†]	
		sampled tributary (DC1)	calculated lateral	sampled tributary (PR5)	calculated lateral	sampled tributary (NF1)	calculated lateral	sampled tributary (PN1)	calculated lateral	sampled tributary (CH1)	calculated lateral
Fe	$(g\ s^{-1})$	0.014	-0.021	0.049	0.056	0.047	0.020	0.495	-0.471	0.036	—
SO_4	$(g\ s^{-1})$	1.259	3.464	23.106	27.019	3.014	—	10.910	-7.350	8.079	—
Mn	$(g\ s^{-1})$	0.004	0.022	0.304	0.341	0.006	-0.039	0.378	-0.279	0.003	—
Pb	$(g\ s^{-1})$	0.003	0.000	0.010	0.017	0.010	-0.003	0.001	0.000	0.008	—
Cu	$(mg\ s^{-1})$	0.193	-0.081	18.156	6.240	0.771	-0.263	77.373	-63.072	0.732	—
Zn	$(g\ s^{-1})$	0.005	0.011	0.415	0.399	0.017	-0.109	0.533	-0.396	0.006	—
Al	$(g\ s^{-1})$	0.003	-0.152	0.039	0.123	0.028	0.011	0.274	-0.263	0.010	—
Mg	$(g\ s^{-1})$	0.195	0.103	1.242	1.453	0.834	0.032	0.411	-0.216	0.636	—
Ca	$(g\ s^{-1})$	1.057	0.164	5.195	6.323	4.380	1.102	1.420	-0.736	3.749	—
Cl	$(g\ s^{-1})$	0.207	-0.126	0.516	1.837	3.918	—	0.016	-0.098	0.223	—

[†] = negative lateral inflows calculated

[‡] = flow data not collected so mass-flow calculations could not be made

Note: negative lateral mass-flows signal a loss of solutes in the confluence zones

Table A.12: Inflow mass-flows, Snake River Watershed synoptic study

	July: Stream Reach						
Between Sites:	**SN2 and SN3**	**SN3 and SN4**	**SN5 and SN6***	**SN6 and SN7[†]**	**PR2 and PR3[‡]**	**PR4 and PR**
Fe $(g\ s^{-1})$	-0.015	0.026	—	—	—	—
SO$_4$ $(g\ s^{-1})$	4.508	20.563	—	—	—	—
Mn $(g\ s^{-1})$	0.008	0.150	—	—	—	—
Pb $(g\ s^{-1})$	0.004	0.006	—	—	—	—
Cu $(mg\ s^{-1})$	-1.205	0.964	—	—	—	—
Zn $(g\ s^{-1})$	0.005	0.076	—	—	—	—
Al $(g\ s^{-1})$	0.010	-0.010	—	—	—	—
Mg $(g\ s^{-1})$	0.288	1.377	—	—	—	—
Ca $(g\ s^{-1})$	1.334	6.486	—	—	—	—
Cl $(g\ s^{-1})$	0.241	0.270	—	—	—	—

	August: Stream Reach						
Between Sites:	**SN2 and SN3**	**SN3 and SN4**	**SN5 and SN6[†]**	**SN6 and SN7[†]**	**PR2 and PR3**	**PR4 and PR**
Fe $(g\ s^{-1})$	-0.027	-0.054	—	—	0.044	—
SO$_4$ $(g\ s^{-1})$	0.805	8.192	—	—	17.773	—
Mn $(g\ s^{-1})$	-0.026	0.068	—	—	0.282	—
Pb $(g\ s^{-1})$	0.000	0.002	—	—	0.005	—
Cu $(mg\ s^{-1})$	-0.639	-0.622	—	—	0.014	—
Zn $(g\ s^{-1})$	-0.001	0.054	—	—	0.298	—
Al $(g\ s^{-1})$	-0.374	-0.080	—	—	0.810	—
Mg $(g\ s^{-1})$	0.060	0.634	—	—	0.720	—
Ca $(g\ s^{-1})$	0.739	3.423	—	—	2.397	—
Cl $(g\ s^{-1})$	-0.126	0.396	—	—	0.241	—

[†] = losing reaches

[‡] = flow data not collected so mass-flow calculations could not be made

* = no lateral inflows or outflows

Note: negative lateral mass-flows signal a loss of solutes in the confluence zones

Table A.13: Snake River Watershed Task Force Members (*as of 3/28/2002*)

Joel Bitler
Citizen

David Bucknam
Colorado Division of Minerals & Geology

John Cathrall
Citizen

Stan Church
U.S. Geological Survey

Jamie Connell
U.S. Forest Service

Robert Craig
The Keystone Center

Thomas Davidson
Keystone Real Estate Developments

Dale Fields
Summit Guides

Greg Finch
Dundee Realty USA

Sarah Fowler
U.S. Environmental Protection Agency

Jim Gentling
Arapahoe Basin

Chad Guinn
Snake River Planning Commission

Taylor Hawes
Northwest Colorado Council of Governments
(NWCCOG)

James Herron
Colorado Department of Natural Resources

Paul Hinkley
Town of Montezuma

Deborah Lebow
U.S. Environmental Protection
Agency

Gary Lindstrom
Summit County Board of County
Commissioners

Steve Lohman
Denver Water Board
Tom Long
Summit County Board of County
Commissioners

Brian Lorch
Summit County Government

Justin McCarthy
Summit County Democrats

Bill McKee
Colorado Department of Public
Health and Environment

Diane McKnight
INSTARR

J. Boyd Mitchell
Keystone Resort

Scott Peckham
University of Colorado at
Boulder

Jim Rada
Summit County Environmental
Health

Robert Ray
Northwest Colorado Council of
Governments (NWCCOG)

Carol Russell
U.S. Environmental Protection
Agency

Table A.13: Snake River Watershed Task Force Members

Steven Smith
U.S. Geological Survey

Norm Spahr
USGS

Phil Strobel
U.S. Environmental Protection Agency

Steve Swanson
Vidler Water Company

Delbert Tolen
St. John Mine

Kenneth Wiggins
Keystone Citizens League

Lane Wyatt
Northwest Colorado Council of Governments (NWCCOG)

Kirby Wynn
U.S. Geological Survey

Table A.14: Snake River Watershed Task Force Interested Parties (*as of 3/28/2002)*

Heide Andersen
Town of Breckenridge

Bud Anderson
Transpacific Tourism

Jerry Anton
Citizen

Robert Barber
Citizen

Richard Bateman
Citizen

Laura Belanger
University of Colorado

Bob Berwyn
Ten Mile Times

Tracy Bouvette
Camp Dresser & McKee Inc.

Frank Burcik
Water Treatment and Decontamination
International

Kyle Burris
Citizen

Rafer Chambers
Colorado School of Mines

Jan Christiansen
Citizen

Lou and Sue Clinton
Citizen

Mark Cowan
U.S. Army Corps of Engineers

Robert Cronkright
Citizen

Max & Edna Dercum
Citizen

Rolf & Judy Dercum
Citizen

Douglas Druliner
U.S. Geological Survey
Sabre Duren
University of Colorado

John Emerick
Colorado School of Mines

Halle Enyedy
The Keystone Center

Jack and Donna Euler
Citizen

Lauren Evans
Pinyon Environmental Engineering Resources

Allan and Maureen Fazendin
Citizen

Roger Flynn
Western Mining Action Project

Dave Folkes
Enviro Group Limited

Nicol Gagstetter
Citizen

Bert Garcia
U.S. Environmental Protection Agency

Colleen Gillespie
U.S. Environmental Protection Agency

John Gitchell
Vail Resorts, Inc.

Jack Goralnik
Citizen

Table A.14: Snake River Watershed Task Force Interested Parties (*as of 3/28/2002)*

Adrienne Greve
U.S. Geological Survey

Bill Griffith
Citizen

Leo Harris
Citizen

Philip Hegeman
Colorado Department of Public Health and Environment

Alan Henceroth
Arapahoe Basin Ski Area
Bob and Sue Herbst
Current Water Technology

David Holm
Colorado Department of Public Health and Environment

Sonja Jackson
Citizen

Joy Jenkins
Citizen

Curtis Johnson
Citizen

Ted Kowalski
Colorado Water Conservation Board

David Kurz
Enviro Group Limited

Ron Lamutt
Lamar Industires

Don Leonard
Chihuahua Mining and Milling Co.

Steve Lipsher
The Denver Post

John Loughlin
Loughlin Law Firm

Judy Lozano
The Keystone Center

Zach Margolis
Town of Silverthorne

Janet Martin
Citizen

Jim Martin
Citizen

Sandy McClure
The Keystone Center

Gordon McEvoy
Citizen

Christina McGrath
Town of Silverthorne

Terry McGrath-Craig
Citizen

Chris McKinnon
Western Governor's Association

Lane Middleton
The Keystone Center

Gary & Kikken Miller
Citizen

Sean Moran
Colorado School of Mines

Ted Mueser
Citizen

John Neiley
Trout Unlimited

Rosalie O'Donoghue
Citizen

Joe O'Malley
Snake River Planning Commission

Brad Piehl
Foster Wheeler Environmental Corporation

Tom Pike
U.S. Environmental Protection Agency

Table A.14: Snake River Watershed Task Force Interested Parties (*as of 3/28/2002)*

Hollis Pirkey
Citizen

Jennifer Pratt Miles
Shaping Our Summit

Robert Reisinger
Knight Piesold Consulting
Beth Riley
Citizen

Todd Robertson
Summit County Government

Kevin Rogers
Colorado Division of Wildlife

Larry Sandoval
U.S. Forest Service

John Schaecher
Citizen

Marjorie Schell
Citizen

Ronald Schmiermund
Knight Piesold Consulting

William Schroeder
U.S. Environmental Protection Agency

Paul Semmer
U.S. Forest Service

Harris Sherman
Arnold & Porter

David Sloan
Marsh USA Inc.

Leann Small
Colorado State University

Rocky Smith
Colorado Wild!

Mark Stacell
Marsh USA Inc.

Dorothy Sumner
Citizen

David Thompson
David A. Thompson, M.D., Inc.

David Thompson, M.D.
Citizen

Alf & Sunni Tieze
Citizen

Andrew Todd
University of Colorado

Samantha Tokash
Colorado School of Mines

Reid Turnquist
Citizen

James Tyler
Citizen

Guff Van Vooren
The Keystone Center

Peter VanMetre
U.S. Geological Survey

Mauha Voelter
Citizen

Jim and Polly Weigel
Citizen

Mark Weinhold
U.S. Forest Service

Sharon Westmoreland
University of Denver

Paul Wexler
Citizen

Len & Katie Wheeler
Citizen

Harold Wiles
Citizen

Patrick Willits
Trust for Land Restoration